Renal proximal tubular reabsorption of sodium, water and calcium are interconnected

by

Devishree Krishnan

A thesis submitted in partial fulfillment of the requirements for the degree of

Doctor of Philosophy

Department of Physiology
University of Alberta

Abstract

Intravascular volume is maintained by complex interplay between organ systems with a main role for renal sodium, and water handling. The glomerulus filters a large quantity of water and salt daily with the majority of sodium, water and calcium being reabsorbed from the proximal tubule (PT). The renal reabsorption of sodium, water and calcium are interconnected. Apical influx of sodium from the PT occurs via NHE3 in exchange for a cytosolic proton. Cytosolic sodium is excreted back into the blood via either the sodium potassium ATPase or a sodium dependent bicarbonate transporter. The rate-limiting step for NHE3 activity is the presence of a cytosolic proton. This is generated by cytosolic carbonic anhydrase II (CAII), an enzyme mediating the catalysis of CO_2 and H_2O to form HCO_3^- and H^+. CO_2 and H_2O enter the PT epithelial cell through the water channel aquaporin-1 (AQP1). Osmotically driven water flux across the PT also drives calcium reabsorption from this segment, a process linked by NHE3. CAII interacts with many membrane transporters including NHE1, AE1, MCT1 and NBCe1. We identified potential CAII binding sites in both NHE3 and AQP1. A primary hypothesis of this thesis is that CAII physically and functionally interacts with both NHE3 and AQP1.

CAII and NHE3 were closely associated in a renal proximal tubular cell culture model as revealed by a proximity ligation assay. Direct physical interaction was confirmed in solid-phase binding assays with immobilized CAII and C-terminal NHE3 glutathione-*S*-transferase fusion constructs. To assess the effect of CAII on NHE3 function, we expressed NHE3 in a proximal tubule cell line and measured

NHE3 activity. NHE3-expressing cells had a significantly greater rate of intracellular pH recovery than controls. Inhibition of endogenous CAII activity with acetazolamide significantly decreased NHE3 activity, indicating that CAII activates NHE3. To ascertain whether CAII binding *per se* activates NHE3, we expressed NHE3 with wild-type CAII, a catalytically inactive CAII mutant (CAII-V143Y), or a mutant unable to bind other transporters (CAII-HEX). NHE3 activity increased upon wild-type CAII coexpression, but not in the presence of the CAII-V143Y or HEX mutant. These studies support an association between CAII and NHE3 that increases the transporter's activity.

CAII colocalizes with AQP1 in the renal proximal tubule. Expression of AQP1 with CAII increased water flux relative to AQP1 expression alone. Expression of catalytically inactive CAII failed to increase water flux through AQP1. Proximity ligation assays revealed close association of CAII and AQP1, an effect requiring an acidic cluster of amino acids in the cytosolic tail of AQP1. This motif was also necessary for CAII to increase AQP1-mediated water flux. Red blood cell ghosts resealed with CAII demonstrated increased osmotic water permeability compared with ghosts resealed with albumin. Renal cortical membrane vesicles isolated from CAII-deficient mice has reduced water flux, which is measured by stopped-flow light scattering. Water flux across renal cortical membrane vesicles, measured by stopped-flow light scattering, was reduced in CAII-deficient mice compared with wild-type mice. These data are consistent with CAII increasing water conductance through AQP1 by a physical interaction between the two proteins.

Evaluation of urinary calcium excretion from humans and mice fed altered sodium containing diets revealed that urinary calcium excretion is proportionate to sodium intake. We hypothesized that angiotensin II mediated regulation of NHE3 activity is central to alterations in urinary calcium excretion in response to altered salt intake. To assess this possibility we performed mRNA and protein expression studies on sodium transporters and tight junction proteins along the nephron involved in sodium and calcium reabsorption. We did not find a significant decrease in the expression of these transporters when animals were fed high salt diets. This diet did however decrease renal renin mRNA expression. Previous studies found that the angiotensin I receptor (AT1R) and NHE3 are expressed in the proximal tubule. Using a cell culture model we demonstrate that angiotensin II increases NHE3 membrane localization and enhances its activity. Thus we postulate that increased sodium intake decreases renin production, and AngII levels that in turn translocate NHE3 from the brush border to an endomembrane compartment. This would decrease both sodium reabsorption from the proximal tubule and consequently increase calcium excretion in the urine. Together these studies highlight an interconnection between sodium, water and calcium reabsorption from the renal proximal tubule.

Preface

Chapter 2: Carbonic anhydrase II binds to and increases the activity of the epithelial sodium-proton exchanger, NHE3

(Much of this paper has been published as: *Krishnan D, Liu L, Wiebe SA, Casey JR, Cordat E, Alexander RT,* Carbonic anhydrase II binds to and increases the activity of the epithelial sodium proton exchanger, NHE3. Am J Physiol Renal Physiol. 2015 Jun 3:ajprenal.00464.2014. doi: 10.1152/ajprenal.00464.2014. [Epub ahead of print] Devishree Krishnan completed all the experiments. Lei Liu generated the CAII Myc cDNA. Shane Wiebe completed some experimental revisions, which are not presented in the figures.

Chapter 3: Increased Water Flux Induced by an Aquaporin-1/Carbonic Anhydrase II interaction

Parts of this chapter have been published in: *Vilas G*, Krishnan D*, Loganathan SK*, Malhotra D, Liu L, Beggs MR, Gena P, Calamita G, Jung M, Zimmermann R, Tamma G, Casey JR, Alexander RT.* Mol Biol Cell. 2015 Mar 15;26(6):1106-18. doi: 10.1091/mbc.E14-03-0812. Epub 2015 Jan 21 *represents equal contribution to the work Devishree Krishnan completed all the experiments in Figures 3-2, 3-3, 3-4, 3-13, 3-14,3-15, 3-16, 3-17, Table 3-I, 3-II, 3-III. The experiments in Figures 3-5, 3-6, 3-7, 3-8, 3-9, 3-10, 3-11, 3-12 were completed by Loganathan SK. They have been included for the completeness of the story. The light scattering experiments were performed by G. Calamita and the peptide blot was generated by Martin Jung and Richard Zimmermann.

Chapter 4: Effect of sodium intake on urinary calcium excretion.

Mice fed different sodium containing diets was performed by Dr. Henrik Dimke, analysis of this experiment, including immunoblotting and quantitative real-time PCR was performed by Devishree Krishnan, the human experiment was carried out by Dr. Bramm, however urinary analysis of calcium, creatinine and sodium was completed by Devishree Krishnan.

Acknowledgements

Firstly, I wish to thank my sister Dr. Kavithaa Loganathan and my brother-in-law Loganathan Krishnaswamy who were truly inspirational, and motivated me to pursue a career in research. I appreciate their support both before and after choosing this career path.

I would like to express my special appreciation and thanks to my professor Dr. Todd Alexander for giving me the wonderful opportunity to work in his lab. I would like to thank him for being an amazing mentor through out this journey. I appreciate all his time, ideas, funding and especially patience to make my Ph.D. experience productive and successful. The joy and enthusiasm he has for his research was truly inspirational and motivational for me, even during tough times in the Ph.D. journey. I could not have imagined having a better advisor and mentor for my Ph.D. study.

I have developed so many close friendships during my time in the lab. Wanling Pan has been there for my entire journey. I will be forever thankful for her help around the lab, and will always treasure our friendship.

I would like to thank professor Dr. Emmanuelle Cordat and her lab members for their valuable friendship, enjoyable moments, brilliant comments and suggestions on my projects during our lab meetings. Also I would like to thank my committee members Dr. Joseph R Casey and Dr. Larry Fliegel for their valuable ideas and suggestions regarding my project during my committee meetings. Also I would like to express my appreciation to former Dr. Casey's lab members Dr. Danielle Johnson and Dr. Sampath Kumar Loganathan for their support while

writing my thesis. I would like to acknowledge funding from the Women and Children Health Research Institute (WCHRI).

My friends in Edmonton will always mean a lot to me (Prajakta, Prarthna, Deeptha, Sushmitha, Indrani, Dipen, Nikhil, Mudit, Santhosh, Pinak, Pritam, Saket, Rajpreet and Shyam). Prajakta Desai has been a great friend from the very beginning, and I have valued knowing her and sharing this journey of friendship and science with her. Prarthna Nagar is a great friend, and my experience would not have been the same without her.

Words cannot express my love and gratitude to my family. I could not have done this without the support of my parents, Krishnan and Radhamani, and my husband Rajiv. They have always encouraged me through out this journey.

Table of Contents

Chapter 1: General introduction **1**

1.1 Thesis overview **2**

1.2 Na^+/H^+ exchangers (NHE's) **3**

1.2.1 NHE's isoforms **3**

1.2.2 NHE3 structure and localization **5**

1.2.3 Function of NHE3 ..... **8**

1.2.4 Hormonal regulation **8**

1.2.5 NHE3 phosphorylation **9**

1.2.6 Regulatory domains **11**

1.2.7 Similarities between the NHE-CAII binding site and the NHE3 C-terminus **13**

1.3 Carbonic anhydrase (CA) enzyme **13**

1.3.1 CA isoforms and distribution **13**

1.3.2 CAII function **14**

1.3.2.1 CAII deficiency in human and mouse 14

1.3.3 CAII mutants **15**

1.3.4 Metabolon **15**

1.3.4.1 AE/CAII/CAIV interaction 16

1.3.4.2 NBC/CAII interaction 16

1.3.4.3 SLC26/CAII interaction 17

1.3.4.4 MCT/ CAII interaction 17

1.3.4.5 N-type sodium-dependent neutral amino acid transporter isoform 3 (SNAT3) and CAII 18

1.3.4.6 NHE1/CAII interaction 19

1.3.4.7 NHE3 homologous binding site for CAII 19

1.4 Aquaporins (AQP's) **21**

1.4.1 AQP isoform and distributions **21**

1.4.2 AQP1 structure and function **22**

1.4.2.1 AQP1 deficiency in mice and human 23

1.4.2.2 AQP1 binding sites for CAII 23

1.5 Volume homeostasis **25**

1.5.1 Brief overview **25**

1.5.2 Paracellular reabsorption **25**

1.5.3 Claudins **26**

1.5.4 Transcellular reabsorption 27
1.5.5 Sodium reabsorption along the nephron 27
1.5.6 Regulation of volume homeostasis by hormones 35
1.6 Calcium homeostasis 36
1.6.1 Calcium reabsorption along the nephron 37
1.6.2 Link between sodium and calcium reabsorption 40
1.7 Hypothesis 41
1.8 Thesis objectives 41
References 42
CHAPTER 2 59
Carbonic anhydrase II binds to and increases the activity of the epithelial sodium-proton exchanger, NHE3 59
2.1 Introduction 60
2.2 Materials and methods 62
2.2.1. Materials 62
2.2.2. Cell culture 62
2.2.3. Immunoblotting 63
2.2.4. Measurement of Na^+/H^+ exchange activity in the presence of CO_2 ... 64
2.2.5. Measurement of Na^+/H^+ exchanger activity in the absence of CO_2 ... 65
2.2.6. Generation of glutathione-S-transferase constructs and CAII-myc .. 66
2.2.7. Purification of glutathione-S-transferase fusion proteins 67
2.2.8. Microtiter plate binding assay 68
2.2.9. Proximity ligation assay (PLA) 69
2.2.10. Coimmunoprecipitation 70
2.2.11. Statistical analysis 71
2.3. Results 72
2.3.1. Acetazolamide inhibits NHE3 activity in the presence of CO_2 and HCO_3^-. 72
2.3.2. Acetazolamide does not inhibit NHE3 activity in the absence of CO_2 . 78
2.3.3. NHE3 and CAII associate closely 81
2.3.4. CAII binds the C terminus of NHE3 83
2.4. Discussion 87
References 91
CHAPTER 3 97

Increased Water Flux Induced by an Aquaporin-1/Carbonic Anhydrase II interaction 97

3.1. Introduction 98

3.2. Materials and methods 101

3.2.1. Animal studies 101

3.2.2. Preparation of mammalian expression constructs 102

3.2.3. Preparation of ΔCABI and ΔCABII AQP1 mutants 103

3.2.4. Protein expression 104

3.2.5. Membrane water permeability measurements 104

3.2.6. Immunoblotting 105

3.2.7. Peptide spot assay 106

3.2.8. Proximity ligation assay 106

3.2.9. Preparation of red blood cell ghosts and renal cortical membrane vesicles, and stopped-flow light scattering measurement of water permeability 108

3.2.10. Statistical analysis 110

3.3 Results 111

3.3.1. The cytosolic C-terminus of AQP1 contains two potential CAII binding sites 111

3.3.2. AQP1 is coexpressed in proximal tubular brush border membranes with CAII 113

3.3.3. CAII binds to the acidic motifs in the tail of AQP1 116

3.3.4. CAII increases water flux through AQP1 in kidney cells 118

3.3.5. AQP1 and CAII associate in mammalian cells 125

3.3.6. CABI and CABII are required to increase the water conductance of AQP1 129

3.3.7. CAII increases water permeability of red blood cell ghosts 131

3.3.8. CAII-deficient mice are polydipsic, polyuric and have dilute urine .. 133

3.3.9. AQP1 expression is increased in CAII-deficient mice 135

3.3.10. Water flux across renal cortical membranes isolated from CAII-deficient mice is increased despite decreased AQP1 expression..... 139

3.4. Discussion 141

References 146

CHAPTER 4 153

Effect of dietary sodium on urinary calcium secretion 153

4.1. Introduction 154

4.2. Materials and Methods 158

4.2.1. Cell culture studies **158**
4.2.2. Animal experiment **158**
4.2.3. Urinary calcium **159**
4.2.4. Urinary creatinine **159**
4.2.5. RNA isolation **159**
4.2.6. Quantitative PCR **160**
4.2.7. Protein extraction **163**
4.2.8. Immunoblotting **163**
4.2.9. Cell surface expression of NHE3 ..... **164**
4.2.10. Measurement of Na^+/H^+ exchanger activity in the absence of CO_2 . **164**
4.2.11. Human diets **165**
4.2.12. Statistical analysis **166**
4.3 Results **167**
4.3.1. In humans, increased sodium ingestion increases urinary calcium excretion **167**
4.3.2. In mice, a high sodium diet increases calcium excretion in urine **169**
4.3.3. RNA expression in whole kidney **171**
4.3.4. Protein expression in whole kidney **173**
4.3.5. Renin mRNA expression in whole kidney **175**
4.3.6. Cell surface expression of NHE3 in the presence of AngII **177**
4.3.7. AngII increased Na^+/H^+ exchanger activity **179**
4.4. Discussion **181**
References **184**
Chapter 5: Discussion **188**
5.1 Summary **189**
5.1.1 CAII physically and functionally interacts with NHE3 and enhances its activity **189**
5.1.2 CAII physically and functionally interacts with AQP1 enhancing its activity **191**
5.1.3 The role of angiotensin II in altering urinary calcium excretion in response to altered sodium ingestion **193**
5.2 Future directions **195**
References **199**
Bibliography **201**

List of Tables

Table 3.1 Blood gas analysis of wild type and CAII deficient mice 134
Table 3.2 Metabolic cage data from wild type and CAII deficient mice 134
Table 3.3 Urine analysis of wild type and CAII deficient mice 134
Table 4.1 Real time PCR primers and probes 162
Table 4.2 WT: Blood gas analysis 170
Table 4.3 WT: Metabolic cage data 170
Table 4.4 WT: Serum electrolytes 170
Table 4.5 WT: Urine electrolytes 170

List of Figures

Figure 1.1 NHE3 topology model 7

Figure 1.2 NHE3 topology model and C-terminus highlighting the putative CAII binding site..... 20

Figure 1.3 AQP1 topology model and C-terminus showing the CAII binding site..... 24

Figure 1.4 Schematic representation of sodium reabsorption along the nephron 28

Figure 1.5 Schematic representation of sodium reabsorption from the renal Proximal tubule (PT)..... 30

Figure 1.6 Schematic representation of sodium reabsorption from the renal Thick ascending limb (TAL)..... 32

Figure 1.7 Schematic representation of sodium reabsorption from the renal Distal convoluted tubule (DCT)..... 34

Figure 1.8 Schematic representation of calcium reabsorption along the nephron 39

Figure 2.1 Opossum kidney (OK) cells overexpressing sodium/proton exchanger isoform3 (NHE3) demonstrate increased sodium-dependent recovery of pH..... 74

Figure 2.2 The carbonic anhydrase inhibitor acetazolamide (ATZ) inhibits NHE3 76

Figure 2.3 ATZ does not inhibit NHE3 activity in the absence of CO_2 77

Figure 2.4 CAII activity and binding are required to enhance NHE3 activity 80

Figure 2.5 CAII associates closely with NHE3..... 82

Figure 2.6 CAII binds the C-terminus of NHE3..... 85

Figure 2.7 CAII binding to C-terminus of NHE3 is NaCl concentration and pH sensitive 86

Figure 3.1 The cytosolic C-terminus of AQP1 has two CAII binding motifs 112

Figure 3.2 CAII and AQP1 colocalize in mouse proximal tubular brush border membrane 114

Figure 3.3 Negative control for CAII staining in Car2 deficient mice..... 115

Figure 3.4 Increased water flux induced by an aquaporin-1/carbonic anhydrase II interaction 117

Figure 3.5 CAII expression increases water flux through AQP1 expressed in HEK293 cells 120

Figure 3.6 The amount of aquaporin-1 expression correlates with water permeability of HEK293 cells, as measured by the dilution of fluorescence 121

Figure 3.7 CAII expression increases water flux through AQP1 expressed in HEK293 cells 122

Figure 3.8 Cell surface biotinylation data used to normalize water permeability studies performed in HEK293 cells 123

Figure 3.9 CAII expression does not increase water flux through AQP2 expressed in HEK293 cells 124

Figure 3.10 AQP1 and CAII are in close proximity 127

Figure 3.11 hCNT3 is expressed at the cell surface despite the absence of a PLA signal..... 128

Figure 3.12 CABII is necessary to mediate increased water flux through AQP1 by CAII 130

Figure 3.13 CAII increases the water permeability of red blood cell ghosts 132

Figure 3.14 Renal AQP1 expression is increased in CAII-deficient mice.. 136

Figure 3.15 AQP1 mRNA expression increases in CAII-deficient mice.... 137

Figure 3.16 No change in AQP2 mRNA expression in CAII-deficient mice 138

Figure 3.17 CAII deficient cortical kidney membrane vesicles have reduced water permeability 140

Figure 4.1 Schematic representation of calcium reabsorption along the nephron 156

Figure 4.2 In humans, sodium ingestion mirrors urinary calcium excretion 168

Figure 4.3 mRNA expression in whole kidney from WT mice fed either a normal or high salt diet 172

Figure 4.4 Protein expression in whole kidney from WT mice fed either a normal or high salt diet 174

Figure 4.5 mRNA expreseion of renin in whole kidney from mice fed either a normal or high salt diet 176

Figure 4.6 Cell surface expression of NHE3 in the presence and absence of AngII 178

Figure 4.7 AngII increases NHE3 activity, in the absence of CO_2 181

Figure 5.1 Potential CAII and CAIV binding sites in NHE3..... 196

List of Symbols, Nomenclature, Abbreviations

β_{CO_2}	CO_2-dependent buffer capacity
$\beta_{intrinsic}$	intrinsic buffer capacity
β_{total}	total buffer capacity
l_{em}	emission wavelength
l_{ex}	excitation wavelength
µm	micrometer
µM	micro Molar
nm	nanometer
A1/A2/A3	Adenosine receptors
AE1	Cl^-/HCO_3^- anion exchanger isoform 1
AE1-LDAAA	a human AE1 mutant unable to bind CAII
AE1/2/3	isoform 1,2,3
Akt2	RAC-beta serine/threonine-protein kinase
cAMP	cyclic adenosine monophosphate
AngII	Angiotensin II
ANP	atrial natriuretic peptide
AQP	aquaporin isoforms 1-9
AT1R	Angiotensin 1 receptor
ATZ	Acetazolamide
ATP	adenosine triphosphate
A.U.	arbitrary units
AVP	arginine vasopressin

A_v	vesicle surface area
BCA	bicinchoninic acid
BCECF-AM	2′,7′-Bis(2-carboxyethyl)-5(6)-carboxyfluorescein acetoxymethyl ester
BSA	bovine serum albumin
ΔC	osmotic gradient
CA	carbonic anhydrase
CAII, IV	carbonic anhydrase isoform II, IV
CAII-HEX	an N-terminal CAII mutant unable to bind AE1
CAII-V143Y	a catalytically inactive CAII mutant
CAII-WT	wild type carbonic anhydrase isoform II (also referred to as CAII)
CAB	carbonic anhydrase binding site
CaM	calmodulin
Car2	carbonic anhydrase II
cAMP	cyclic adenosine monophosphate
cDNA	complementary deoxyribonucleic acid
CD	collecting duct
CFP	cyan fluorescent protein
ChCl	choline chloride
CHP	calcineurin homologous protein 1,2,3 isoform

CHIP28	Aquaporin isoform 1
CIP	calf intestinal alkaline phosphatase
CK2	Casein kinase II
Cldn	Claudin
Calb28K	Calbindin 28 K
CLCkb	voltage gated chloride channel
CNT	connecting tubule
C-terminal	carboxy terminus
Co-IP	coimmunoprecipitation
CO_2	carbon dioxide
pCO_2	partial pressure of carbon dioxide
DCT	distal convoluted tubule
deGFP4	dual emission green fluorescent protein 4
DAPI	Diamidino-2-phenylindole
DMEM	Dulbecco's modified Eagle media
DNA	deoxyribonucleic acid
DTT	dithiothreitol
EDTA	ethylenediaminetetraacetic acid
EGTA	ethyleneglycoltetraacetic acid
eGFP	enhanced GFP
EIPA	5-(N-ethyl-N-isopropyl)-amiloride

ELISA	enzyme-linked immunosorbent assay
em.	emission
ENaC	epithelial sodium channel
ex.	excitation
ERM	ezrin/radixin/moesin
FBS	fetal bovine serum
G418	geneticin
GAPDH	glyceraldehyde 3-phosphate dehydrogenase
GFP	green fluorescent protein
GFR	glomerular filtration rate
GkII	guanosine kinase II
cGMP	cyclic guanosine monophosphate
GPI	glycosylphosphatidyl inositol
GST	glutathione S-transferase
GTP	guanosine triphosphate
h	hour
HA	hemagglutinin
Hb	hemoglobin
HCT	hematocrit
hCNT3	human concentrative nucleoside transporter isoform 3
HEK293 cells	human embryonic kidney 293 cells

HEPES	4-(2-hydroxyethyl)-1-piperazineethanesulfonic acid
His	histidine
HRP	horseradish peroxidase
I_{max}	highest fluorescence intensity at a given pH
I_{pH}	fluorescence intensity at any pH
IgG	immunoglobin G
IPTG	isopropyl beta D-1- thioglactopyranoside
IRBIT	inositol 1,4,5, triphosphate-binding protein
JAM	junctional adhesion molecule
kAE1	kidney AE1
LB-AMP	Luria-Bertani medium supplemented with 0.1 mg/ml ampicillin and 0.02% w/v L-arabinose
M	molar
MAP	p38 mitogen-activated protein
MAPKPK2	p38 mitogen-activated protein kinase activate kinase 2
MCT1	monocarboxylate transporter isoform 1
min	minute
mM	milli Molar
NaAc	sodium acetate
NaCl	sodium chloride
NBC	Na^+/HCO_3^- co-transporter
NCC	Na^+/Cl^- co-transporter
NCX	Na^+/Ca^{2+} exchanger

NHE	Na^+/H^+ exchanger isoform 1-9
NHE3 Tail 1	NHE3 carboxy terminus tail amino acids between 630-730
NHE3 Tail 2	NHE3 carboxy terminus tail amino acids between 730-831
NHERF	Na^+/H^+ exchanger regulating factor
NKCC	Na^+-K^+-$2Cl^-$ co-transporter
nM	nanomolar
NP-40	igepal-40
NT	nucleoside transport protein
N-terminus	amino terminus
OK cells	opossum kidney cells
PBS	phosphate-buffered saline
PCR	polymerase chain reaction
PDZ	post synaptic density protein, drosophila disc large tumor suppressor, zonula occluden-1 protein
pH_i	intracellular pH
pH_o	extracellular pH
PI3K	phosphatidyl inositol 3-kinase
PI3K-SGK1	phosphatidyl inositol 3-kinase and serum glucocorticoid dependent kinase 1
PIP2	phosphatidylinositol bisphosphate
PKA	protein kinase A
PKC	protein kinase C
PKG	protein kinase G
pK_a	logarithmic measure of acid dissociation constant

2.5

PLA	proximity ligation assay
PM	plasma membrane
PMCA1b	plasma membrane calcium ATP-ase
PMSF	phenylmethanesulfonylfluoride
PP2A	protein phosphatase 2A
PSG	penicillin-streptomycin-glutamine
PT	proximal tubule
PTH	parathyroid hormone
PVDF	polyvinylidine fluoride membrane
QPCR	quantitative polymerase chain reaction
RAAS	renin-angiotensin-aldosterone system
RBC	red blood cell
ROI	region of interest
ROMK	renal outer medullary potassium channel
s	second
SDS	sodium dodecyl sulfate
SDS-PAGE	sodium dodecyl sulfate polyacrylamide gel electrophoresis
SGK	serum glucocorticoid kinase
SGLT1	Na^+/glucose cotransporter isoform 1
SLC	solute carrier
SNAT3	N-type sodium-dependent neutral amino acid transporter isoform 3
t	time

2.5

T	total
TAL	thick ascending limb
TDL	thin descending limb
TER	transepithelial resistance
TGF	tubular glomerular filtration rate
TJ	tight junction
TMD	transmembrane domain
TRPV5	transient receptor potential cation channel subfamily V
TX100	Triton X 100
V	velocity
VDR	1,25 dihydroxyvitamin D3 receptor
V_{max}	velocity at maximal substrate concentration
Vo	vesicle volume
Vol	volume
Vw	molar volume of water
Wk	week
WT	wild type
wt	weight
ºC	degrees Celsius

Chapter 1: General introduction

1.1 Thesis overview

The objective of thesis is to determine whether CAII physically and functionally interacts with NHE3 and AQP1 in the proximal tubule (PT). A third objective is to delineate how sodium intake alters urinary calcium excretion. We therefore examined the functional and physical interaction of CAII with both NHE3 and AQP1. The majority of sodium, water and calcium are reabsorbed from the renal proximal tubule. Main players in sodium and water reabsorption are NHE3 and AQP1. NHE3 is expressed in human gut and kidney, but also in heart, brain, thymus, prostate, ovary, testis and lungs at lower levels. AQP1 is expressed in kidney, choroid plexus, the ciliary body, alveolar microvessels, gallbladder, placenta and various other epithelia and endothelia. CAII is expressed in bone, intestine, kidney, RBC, brain, eye, stomach, liver, pancreas, salivary glands and uterus. The focus of the thesis is on human renal proximal tubule. The introduction begins with a brief description of NHE3, distribution, function and regulation, then is followed by a brief discussion about AQP1 and CAII. Schematic diagrams describe the topology model of NHE3 and AQP1 and potential CAII binding site.

This thesis follows a paper-based format, where the second, third and fourth chapters are the main contributions. Each chapter has a specific introduction, materials and methods, results and discussion. The second chapter is about how carbonic anhydrase II binds to and increases the activity of the epithelial sodium-proton exchanger, NHE3. The third chapter is about increased water flux induced by an Aquaporin-1/Carbonic Anhydrase II interaction. Both of these chapters have

been published and I am the first or joint first author of both papers. The fourth chapter examines the effect of sodium intake on urinary calcium excretion and the fifth chapter is a general discussion of the main finding and proposes future experimental directions.

1.2 Na^+/H^+ exchangers (NHE's)

1.2.1 NHE's isoforms

The sodium proton exchanger (NHE) family of proteins plays an important role in maintaining cytosolic pH, cellular volume and systemic acid-base balance (2, 4). The family contains nine isoforms (38, 73), which can be generally divided based on their subcellular localization. Whereas NHEs 1-5 reside and function predominantly at the plasma membrane, NHEs 6-9 localize to endomembrane organelles (31, 38). NHEs function to antiport intracellular protons for extracellular sodium. Kinetic modeling supports a single binding site alternatively occupied by sodium or a proton (20). Because of its single binding site, NHEs alternate between an open conformation facing either the cytoplasm or the extracellular space (lumen of endomembrane compartment for NHE6-9). All NHEs studied to date demonstrate pH dependence, via specific regions that sense pH. This region is called the pH sensor (20). NHEs contain approximately 800 amino acids and two general domains that can be differentiated into an integral membrane domain and a cytosolic domain (35). The degree of homology for NHE1 to the other eight isoforms varies from 25-70%. NHEs are also sensitive to amiloride inhibition (35).

General structure: The N-terminal domain is responsible for cation movement. This domain has 12 transmembrane regions. In NHE1, the transmembrane (TM) IV amino acid residues Phe161, Phe162, Leu163 and Gly173 mediate the affinity for sodium and/or inhibitors (35). A point mutation in Phe165 of TM-IV provides resistance to inhibitors. Therefore the affinity binding site for the inhibitor is present in that domain (25). In TM-VII Glu262 and Asp267 are critical for exchanger activity. They are involved in the coordination of sodium to the protein. TM-IX His349 mediates sensitivity to amiloride compounds. TM-XI residues Tyr454 and Arg458 are essential for membrane trafficking of NHE1 (35).

NHEs 1-5: NHE1 is expressed ubiquitously. In epithelial cells, NHE1 is present in the basolateral membrane (73). It plays an important role in regulating cell volume, pH and cell proliferation (60). Given its ubiquitous nature, NHE1 has been referred to as a "house keeping gene" (38). NHE2 is expressed in the gut, skeletal muscle, kidney, brain, uterus, testis, heart and lung (38). NHE3 expression is observed predominantly in the gut and kidney, but also in heart, brain, thymus, prostate, ovary, testis and lungs at lower expression levels (4, 38, 73). It localizes to the apical membrane predominantly and a fraction is also seen in sub-apical vesicles (2, 23). It plays a central role in maintaining the systemic electrolyte, fluid and acid base balance (88). NHE4 is expressed in gut, kidney, brain, uterus and skeletal muscles (38). It is located in the basolateral membrane of epithelial cells (38, 73). NHE5 expression is high in the central nervous system (73), but it is also present in testis, spleen and skeletal muscles (38). It is located in both plasma membrane and

endomembrane compartments (38, 73). NHE5 maintains endosomal pH and may be involved in neuron cell differentiation (38).

NHEs 6-9: NHE 6-9 localize to endomembrane organelles. Specifically, NHE6 is located in recycling endosomes. NHE7 localizes to the trans-Golgi compartment. NHE8 is present in mid to trans-Golgi complex as well as the brush border of some epithelia. NHE9 is found in late and recycling endosome and lysosomes (31, 38, 73). The luminal pH of the secretory and endocytic pathway of organelles decreases towards the trafficking destination from endoplasmic reticulum (pH ~7.1) to Golgi (pH ~6.2-7.0), trans-Golgi network (pH~6.0) and secretory granules (pH ~5.0). Similarly pH changes from early and late endosomes (pH ~6.5) to lysosomes (pH ~4.5) (70). Cellular events such as post-translational modification, sorting of newly synthesized proteins into the secretory pathway and degradation or recycling of internalized ligand-receptor complexes and fluid-phase solutes from the endocytic pathway is permitted by this progressive acidification. Membrane ion carriers such as pumps, channels and transporters maintain this gradient via acidification of different organelles. NHEs localized to various organelles mediate electroneutral exchange of protons for sodium and/or potassium thereby participating in the maintenance of luminal pH (70).

1.2.2 NHE3 structure and localization

Topology model: NHE3 is made up of 834 amino acids. It consists of two domains roughly split into a N-terminal and a C-terminal domain. The N-terminal domain is composed of 12 transmembrane domains (TMD) (~ amino acids 1-454). It is

followed by the cytosolic C-terminal tail (~ amino acids 455-834) (4, 32). Based on comparison with NHE1, it is proposed that the TMD mediates ion exchange, whereas the C-terminus regulates exchange activity (4).

Localization of NHE3 along the nephron

NHE3 is localized in the epithelial brush border of proximal tubule, the apical membrane of the thick ascending limb, as well as a sub-apical endomembrane compartment (32). Importantly NHE3 in the endomembrane compartment traffics into the plasma membrane, thereby altering NHE3 activity (4).

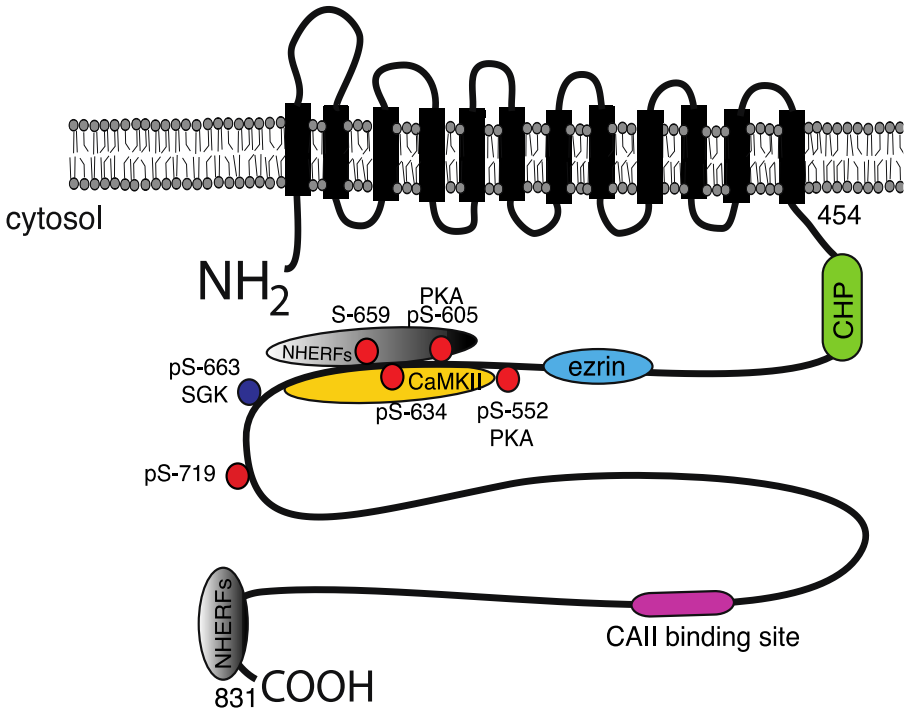

Figure 1.1: NHE3 topology model. A NHE3 topology model showing 12 transmembrane domains with an amino and carboxy terminus. In the carboxy terminus NHE3 regulating sites are highlighted.

1.2.3 Function of NHE3

The major function of NHE3 in the kidney is to reabsorb sodium (and therefore subsequently chloride) as well as bicarbonate from the proximal portion of the nephron thereby helping in the maintenance of intravascular volume and pH homeostasis (4, 31). Water reabsorption from the proximal nephron is also mediated by the movement of sodium across the apical membrane, which creates the osmotic driving force for its reabsorption (4). Given this role in the kidney, NHE3 also likely contributes to calcium and magnesium reabsorption via passive paracellular convection via an analogous process to the intestine (4, 74). Also NHE3 has a physical interaction with megalin a process that implicated NHE3 in the reabsorption of filtered protein from the lumen of the proximal tubule (4). NHE3 also plays an important role in ammonia metabolism. NHE3 in the proximal tubule has affinity for NH_4^+ in addition to Na^+/H^+ exchange system (54, 103). It can substitute NH_4^+ for H^+. Consistent with this in micro perfusion studies, the NHE3 inhibitor EIPA, decreases ammonia secretion by ~50% (89). During metabolic acidosis, angiotensin II acts on AT_1 receptor and increases NHE3 expression and ammonia secretion from the proximal tubule (69). Taken together, all these studies support a role for NHE3 mediating NH_4^+ secretion from the proximal tubule.

1.2.4 Hormonal regulation

NHE3 is a heavily regulated protein. Hormones which regulate NHE3 include the calciotropic hormones, 1,25-dihydroxy vitamin D_3 and PTH (74). Renal brush border NHE3 is stimulated by endothelin-1, angiotensin and exposure

to acidosis (32). Endothelin-1 stimulates NHE3 via the Ca^{2+}-CaMK dependent pathway (24, 30). Angiotensin II interacts with the AT1 receptor in the brush border membrane of the proximal tubule to increase intracellular calcium, thereby stimulating CaMKII. This induces the interaction of inositol 1,4,5, triphosphate binding protein (IRBIT) with NHE3 and the translocation of NHE3 to the plasma membrane thereby increasing the surface expression and activity of NHE3 (46). Parathyroid hormone (PTH) inhibits NHE3 by activating the PKA/PKC signaling pathway via cAMP generation from adenylate cyclase activation (8, 30). Further, when 1,25- dihydroxy vitamin D_3 is present along with PTH, it inhibits cAMP accumulation (stimulated by PTH) and increases NHE3 activity (14). The serum glucocorticoid kinase (SGK) phosphorylates NHE3 on serine 663 causing redistribution of endomembrane NHE3 to the apical membrane (4, 76). In proximal tubule, volume and acid base regulation are regulated by insulin through stimulation of NHE3. Chronic insulin administration (24 h) stimulates NHE3 via phosphatidylinositol 3-kinase and a serum glucocorticoid dependent kinase 1 (PI3K-SGK1) pathway (39). NHE3 is also activated by beta-adrenergic stimulation (via epinephrine or norepinephrine) (4).

1.2.5 NHE3 phosphorylation

Phosphorylation of the cytosolic C-terminus of NHE3 functions to regulate the exchanger. NHE3 can be phosphorylated on both serine and threonine residues in this domain. In total there are 19 C-terminal serine/threonine phosphorylation sites of rabbit NHE3 that have been identified (30). The molecules mediating these events and how they do so are discussed below.

SGLT1 (sodium glucose transporter protein 1): NHE3 activity is stimulated by activation of a signaling pathway that is regulated by SGLT1 and includes P38 mitogen-activated protein (MAP) kinase, MAP Kinase activate kinase 2 (MAPKAPK2), phosphatidylinositol 3-kinase (PI3K), Akt2 and ezrin. These signaling events stimulate the trafficking of NHE3 to the apical membrane thereby increasing transporter activity (30).

cAMP: The NHE3 C-terminus contains cAMP-dependent protein kinase A phosphorylation sites. Ser^{605} and Ser^{634} are necessary for cAMP-mediated inhibition of NHE3 activity. Although interestingly in this process Ser^{605} is phosphorylated while Ser^{634} is not phosphorylated, regardless both residues are necessary for cAMP mediated NHE3 regulation (30, 57).

cGMP: cGMP/cGKII inhibits NHE3 by reducing surface expression of the protein. This inhibition occurs via phosphorylation of three serine residues (Rabbit Serine 554, 607, 663 and Mouse serine 552, 605, 659 of NHE3) (22).

Elevated cytosolic calcium levels: Increased cytosolic calcium levels inhibit NHE3 by a PKC □-dependent process (30, 106). Elevated intracellular calcium inhibits NHE3 by decreasing trafficking to the plasma membrane, via forming a complex with NHE3, NHERF2, actin-4 and □PKC in an endomembrane compartment (59).

Other Kinases: Calmodulin kinase II (CaMKII) binds directly to and regulates NHE3. This is in contrast to other kinases such as PKA, PKG, PKC that associate with NHE3 via a signaling complex or intermediates in a signaling network which

are necessary for the acute regulation of NHE3 either by regulating surface expression or trafficking to the membrane (30).

Protein phosphatase (PP): PP2A interacts with NHE3 and dephosphorylates NHE3 in response to dopamine D2-like receptor signaling. Dephosphorylation of NHE3 is a reversible post translation modification, which reduces the surface expression of NHE3 thereby reducing NHE3 activity (15). Immunoprecipitation studies revealed that the regulatory domain, B56δ of PP2A interacts with the C-terminus of NHE3 (~557-794 amino acids) (15).

1.2.6 Regulatory domains

The COOH terminal tail of NHE3, from amino acids 455-844, serves as a regulatory domain. There are many complexes that bind to the C-terminus and regulate NHE3 activity directly or via trafficking. Below is a description of some of the complexes that are involved in NHE3 regulation.

a) CHP: Calcineurin homologous protein (CHP) is a calcium binding protein. There are three CHP isoforms CHP1, CHP2 and CHP3. CHP1 is ubiquitously expressed while CHP2 is expressed tremendously in intestine with minimal expression in the kidney (75, 110). CHP3 is also called tescalin, because it was originally isolated from mouse testis. It is also predominantly expressed in mouse heart, brain and stomach. Expression of CHP3 is restricted to heart tissue in adult humans (107). In Opossum kidney cells, CHP1 enhances NHE3 transport activity by increasing surface abundance and this is dependent on NHE3 phosphorylation by ezrin (27). The CHP binding region is present in the C-terminus of NHE3 between amino acids 462-552 (30).

b) Adenosine receptor: Sodium homeostasis is controlled via adenosine. It does so by regulating various agents including renal haemodynamics, glomerular filtration rate (GFR), tubuloglomerular feedback (TGF), renin release and tubular sodium and water transport. The adenosine receptor is of four types that are called A1, A2A, A2B and A3. The basolateral membrane adenosine receptor (A2) is activated and involved in acute inhibition of apical membrane NHE3. This inhibition occurs via a PKA dependent mechanism and is dependent on amino acids serine 552 and 605 of rat NHE3 (28).

c) ERM: Ezrin, radixin and moesin are linker molecules that together are often referred to as ERM proteins. ERM protein N-terminal domains allow binding with an integral membrane protein. The N-terminus of the ERM is followed by an alpha helical domain and charged C-terminal domain that interacts with F- actin. Ezrin binds NHE3 both directly and indirectly via either NHERF or 2 linker proteins. The binding occurs between amino acids 515 and 595 of the NHE3 carboxy terminus (30). Ezrin binds directly to NHE3 C-terminus. Point mutations at K516, R520, R527 of NHE3 prevent ezrin binding. Ezrin traffics newly synthesized NHE3 to the plasma membrane and also helps limit NHE3 brush border lateral mobility (21).

d) Phosphatidylinositol-4,5- bisphosphate (PIP2): PIP2 binding activates ezrin by phosphorylating ezrin at threonine 567. Expression of ezrin lacking a PIP2 binding site results in the inhibition of NHE3 actitivy (~40%), suggesting that ezrin is required to maintain NHE3 activity (9). Whether a direct interaction between NHE3 and PIP2 modulates NHE3 activity however remains to be determined.

e) CaM and CaM kinase II (CaMKII): CaMKII is a multifunctional kinase. There are four CaMKII isoforms □, □, □ and □. This kinase is expressed ubiquitously. CaMKII binds to the NHE3 C-terminus directly between amino acids 586-660. This binding is necessary to inhibit NHE3 activity (111).

f) NHERF family: NHERF (Na/H exchanger regulating factor -1) interacts with the NHE3 C-terminus via its PDZ domain. This interaction is necessary to inhibit NHE3 activity via the cAMP pathway (104). The Predicted NHERF1-PDZ domain is ^{829}STHM^{832}. However, NHERF2 binds to a PDZ domain II between 585-660 amino acid (104).

g) Casein kinase II: CK2 binds to the NHE3 C-terminus between 590-667. It stimulates NHE3 by phosphorylating a single amino acid serine 719 at the NHE3 C-terminus. It regulates NHE3 activity via increased trafficking of the transporter to the plasma membrane (86).

1.2.7 Similarities between the NHE-CAII binding site and the NHE3 C-terminus:

CAII regulates NHE1 by direct binding to the C-terminus of NHE1 at the ^{790}RIQRCL**SD**PGPHP^{802} motif (60). Examination of the cytosolic C-terminus of NHE3 revealed a potential CAII binding site, ^{710}IKEKDLEL**SD**TEE^{722}, consistent with the motif established for NHE1 (60, 61).

1.3 Carbonic anhydrase (CA) enzyme

1.3.1 CA isoforms and distribution

Carbonic anhydrase (CA) enzymes catalyze the reaction $CO_2 + H_2O$ -> H_2CO_3 -> $HCO_3^- + H^+$. To-date, 16 isoforms of carbonic anhydrase have been identified. Out of these, 12 isoforms are catalytically active (82, 91). CA's have been classified into three major groups according to their subcellular localization: - CA – I, II, III, VII and XIII are present in the cytosol, CA – IV, IX, XII, XIV and XV are membrane associated, among these IV and XV are tethered to the outer leaflet of the plasma membrane via a glycosylphosphatidyl inositol lipid anchor (66, 82). CAV and VI are endomembrane/secreted while CAV is located in the mitochondria and CAVI is secreted into saliva and milk (91).

1.3.2 CAII function

CAII is expressed as a 29-kDa monomeric protein in the cytosol. It is found in bone, intestine, kidney, RBC, brain, eye, stomach, liver, pancreas, salivary glands and uterus (82). CAII is expressed very highly in the RBC where it binds to the Cl^-/HCO_3^- exchanger and enhances transport activity by the formation of a transport metabolon (83, 92). CAII expression is low in the proximal small intestine and very high in colon (26, 101). CAII and IV are the predominant isoforms present in human and rabbit kidneys (82). Previous studies have shown CAII expression in the proximal tubule, thin descending limb, thick ascending limb and cortical collecting duct of the nephron. CAII expression in the nephron accounts for 95% of total CA activity in the kidney (82).

1.3.2.1 CAII deficiency in human and mouse

In humans, CAII deficiency is associated with the autosomal recessive syndrome of osteopetrosis with renal tubular acidosis and cerebral calcification

(60, 64, 90). Further some patients have medullary nephrocalcinosis and urolithiasis (51). Although, CAII deficiency in mice is associated with renal tubular acidosis, stunted growth and cerebral calcification, these animals lack severe osteopetrosis (64).

1.3.3 CAII mutants

CAII HEX mutant (binding mutant): Binding of CAII with transporters is pH dependent (56,100). The histidine rich amino terminus of CAII is responsible for binding of CAII to transporters (99). The amino terminal sequence of human CAII is M^{1}SHHWGYGKHNGPEHWHKDFPIAKGERQSP (83, 99, 100). Truncation or mutating the histidines to basic residues in the amino terminus prevents binding with transporters (99, 100). This mutant is named the CAII-HEX mutant (M^{1}**S**P**D**WGY**DDK**NGPE**Q**W**S**KLYPIANGN). Importantly even though binding is lost, this mutant enzyme is catalytically active (56).

CAII V143Y mutant (inactive mutant): Valine 143 of the CAII enzyme is important for catalytic activity and structure of the protein. Valine 143 is present in the hydrophobic pocket where it is important for substrate association with the CAII enzyme. The V143Y mutant of CAII has catalytic activity that is approximately 3000 fold lower than the wild type CAII enzyme (1, 34).

1.3.4 Metabolon

A metabolon is a physical complex of two enzymes with sequential functions that increase the flux of substrate (67). The transfer of substrate occurs between the active sites of the two enzymes that catalyze the sequential reactions. This reaction transfers the intermediate molecules directly and thereby the loss of

substrate via diffusion is controlled (66). Metabolons exist that regulate and increase the efficiency of the glycolytic chain, the citric acid cycle and the urea cycle (83).

1.3.4.1 AE/CAII/CAIV interaction

The interaction between CAII and AE1 was initially observed in the erythrocyte (100). A number of studies in erythrocytes showed that CAII and AE1 interact in the erythrocyte membrane with high affinity (66, 83). The interaction between CAII and AE1 is based on a pH dependent electrostatic interaction (101). CAII binds directly to an acidic motif in the C-terminal domain of AE1, LDADD. When the acidic motif D887ADD was truncated, the binding of CAII to AE1 was lost (66, 101). Similarly, AE2 and AE3 isoforms also bind to CAII via a homologous acidic motif that is present in the C-terminus of AE2 and AE3 isoforms (92, 101). Further studies found that both the catalytic activity of CAII and direct physical interaction with the transporter is necessary to enhance bicarbonate flux mediated by AE1 (93).

CAIV is an extracellular carbonic anhydrase isoform that binds to the extracellular surface of the cell via a GPI linkage. This enzyme interacts via the fourth extracellular loop of AE1 (92). CAIV increases bicarbonate transporter activity when there is overexpression of the CAII-V143Y (inactive CAII), thereby inferring the need for a physical interaction with CAIV to mediate the increased activity of AE1 (92). CAIV physically interacts with all three AE isoform as does CAII (66, 92).

1.3.4.2 NBC/CAII interaction

NBC is an electrogenic sodium bicarbonate cotransporter. Similar to the AE1 C-terminal tail, NBC1 C-terminus contains a D^{986}NDD acidic motif (45). CAII binds to the C-terminus of NBC1 and regulates transport activity of NBC1. Also the CAIV enzyme binds to the G767 amino acid of the extracellular loop 4 of NBC1 thereby increasing transporter activity even in the presence of overexpressed CAII-V143Y, catalytically inactive mutant of CAII (6). Similarly a CAII physical and functional interaction is necessary to augment NBC3 transport activity (62).

1.3.4.3 SLC26/CAII interaction

The SLC26s are a family of plasma membrane chloride/bicarbonate exchangers. Among the SLC26A family, SLC26A6 is the first protein found to interact with CAII. The CAII binding site is present in ^{546}DVDF^{549} of the C-terminus. When this site is mutated, transport activity is reduced. This infers that CAII physically and functionally interacts with the SLC26A protein (7). The SLC26A7 isoform is expressed in alpha intercalated cells and it colocalize with the AE1 protein. Pendrin (SLC26A4) mediates chloride/bicarbonate exchange in beta-intercalated cells and is also present in non-alpha/non-beta intercalated cells. Intercalated cells are rich in cytosolic CAII. In CAII deficient mice, both SLC26A7 and Pendrin expression are significantly reduced when compared to wild type mice (94).

1.3.4.4 MCT/ CAII interaction

Monocarboxylate transporters (MCT) belong to the SLC16 family, which comprises four isoforms. These proteins are expressed at high levels in brain and muscle (10-13). CAII increases MCT1 activity. However, when oocytes

overexpress the CAII-HEX mutant (binding mutant) with MCT1, the activity is not increased. This suggests that a CAII physical interaction is necessary to increase the activity of MCT1 (12), whereas inactive CAII (CAII-V143Y), when overexpressed with MCT1, also increases activity (11). Therefore for this metabolon only the CAII interaction is necessary to enhance MCT1 activity but not the catalytic property of CAII (11, 12). Studies suggest that CAII accumulates near the plasmamembrane, and may accelerate the removal of protons from the MCT1 inner face. This stimulates MCT1 activity (13). In a similar way, MCT4 transport activity is also induced by an interaction with CAII, and this does not depend on catalytic property (10). MCT2 coexpression with CAII does not alter MCT2 activity, an extracellular interaction of CAIV with MCT2 in a non catalytic manner does augment transporter activity (55).

1.3.4.5 N-type sodium-dependent neutral amino acid transporter isoform 3 (SNAT3) and CAII

SNAT3 is a glutamine/neutral amino acid transporter (SLC38A3). The transfer of glutamine plays a vital role in amino acid and nitrogen metabolism in liver, muscle, kidney and brain (105). Like other acid/base transporters, a potential interaction between CAII and SNAT3 has been examined. CAII WT or CAII-HEX mutant coexpressed with SNAT3 have no effect on transporter activity but unexpectedly they suppresses SNAT3's membrane association and conductance. Whereas when SNAT3 is coexpressed with CAII-V143Y mutant this does not affect membrane conductance. This suggests that SNAT3 associated membrane conductance is suppressed by the enzymatic activity of CAII (105).

1.3.4.6 NHE1/CAII interaction

The Na^+/H^+ exchanger isoform 1 (NHE1) is expressed ubiquitously. Like NHE3, the NHE1 C-terminus regulates the activity of the transporter. Many proteins interact with this domain including calcineurin homologous protein (CHP), calmodulin (CaM) and heat shock protein. In addition, phosphorylation sites also present in the C-terminus regulate transporter activity (60, 61). When CAII is overexpressed with NHE1, it increases transporter activity by two fold. Further, a microtitre plate assay and affinity blotting of NHE1 against CAII suggest that there is a physical interaction between NHE1 and CAII. These studies found that CAII binds to NHE1 and stimulates NHE1 activity. Other studies have shown that a phosphorylation site near to the CAII binding site regulates CAII binding with NHE1 (60). NHE1 also has a similar acidic motif mediating the CAII interaction, like bicarbonate transporters. However, CAII does not bind to NHE1 at that motif. Instead CAII binds to NHE1 within the ^{790}RIQRCL**SD**PGPHP^{802} motif (61). When the residues at S796 and D797 are mutated by site directed mutagenesis, CAII binding was prevented. Further phosphorylation of the serine residue increases the binding of CAII protein to the C-terminus of NHE1 (61).

1.3.4.7 NHE3 homologous binding site for CAII

When we examined the C-terminus of NHE3 we observed a potential CAII binding site ^{710}IKEKDLEL**SD**TEE^{722}, homologous to the NHE1 C-terminal motif. We speculate that CAII may therefore physically and functionally interact with NHE3.

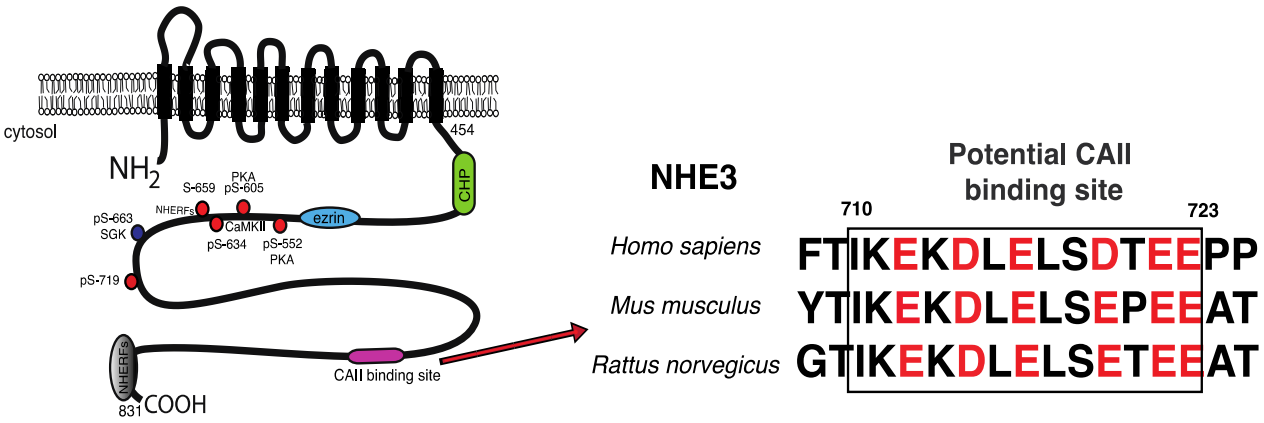

Figure 1.2: NHE3 topology model with C-terminus highlighting the putative CAII binding site. Left panel shows a topology model of NHE3 with 12 transmembrane domains, N-terminus and C-terminus in the cytosol. Right panel represents the conserved putative CAII binding site and its conservation across different species.

1.4 Aquaporins (AQPs)

1.4.1 AQP isoform and distributions

Water is filtered through the glomerulus in large quantities, and the majority is reabsorbed via the proximal tubule. The rate of water reabsorption by diffusion through the lipid layer is significantly lower than the rate that this occurs. This observation led to the discovery of a water channel in red blood cells and ultimately in the proximal tubule (97). The Nobel Prize winning work of Peter Agre was the identification of aquaporin-1 (AQP1) from red blood cells (80, 81). Initially it was named as Channel forming integral protein of 28 kDa (CHIP28). CHIP28 is abundant in mammalian RBC's and renal proximal tubules (81). Localization studies found that AQP1 is expressed in the proximal tubule, ascending thin and thick limbs of Henle, and erythrocytes, but is not present in the collecting duct (85, 108). In humans, 11 isoforms have been identified so far (AQP0-AQP10) (109). AQP's were categorized into two groups (AQP and aquaglyceroporins) 1) AQP 0, 1, 2, 4, 5, 6 and 8 are classified as orthodox aquaporins that conduct water, 2) AQP 3, 7, 9 and 10 isoforms are categorized as the aquaglyceroporins group. In addition to conducting water, they also conduct urea and glycerol (40).

AQP0 participates in CO_2 permeability in monkey lens fibers. Apart from transporting water and CO_2, AQP1 in RBCs contributes to the transfer of NH_3 from various tissues to the liver where it undergoes a detoxification process. AQP2 in the apical collecting duct reabsorbs water under the influence of arginine vasopressin (40). The AQP3 isoform is present in the basolateral membrane of the

collecting duct. It likely contributes to the transport of NH_3 from the interstitium to the tubule lumen for excretion of NH_4^+ into the urine. AQP4 in rat consists of two isoforms M1 and M23. M1 acts as a water channel, whereas M23 is involved in water and carbon dioxide transport. rM23 is present in astrocyte end feet at the blood brain barrier (40). AQP5 is expressed in alveolar type 1 pneumocytes. It conducts water and carbon dioxide. AQP6 colocalizes with the H^+-ATPase in the renal collecting duct. It may serve to extrude carbon dioxide from intracellular vesicles in renal collecting duct (40). AQP7 facilitates water, glycerol, urea, ammonia and arsenite transport. It is present in adipose tissue and the straight proximal tubule. In proximal tubule it promotes glycerol reabsorption, and may contribute to water uptake and NH_3 secretion (40). AQP8 transports water and ammonia. It is present in the inner mitochondrial membrane of hepatocytes and the renal proximal tubule. It helps in regulating NH_3 secretion from proximal tubule and plays a role in maintaining acid-base metabolism. AQP9 is expressed in the sinusoidal plasma membrane of hepatocytes. It effluxes carbon dioxide from the mitochondrial matrix. It is also permeable to carbamides, polyols, purines and pyrimidines (40).

1.4.2 AQP1 structure and function

AQP1 has six transmembrane domains and forms a tetramer (87). Each monomer of aquaporin-1 contains an individual channel pore (95). In kidney, AQP1 expression is observed in apical and basolateral plasma membranes of epithelial cells of the proximal tubule and thin descending limb of Henle's loop and in endothelial cells of the descending vasa recta (87, 95). Also AQP1 is present

in choroid plexus, ciliary body, alveolar microvessels, gallbladder, placenta and various other epithelia and endothelia (63). Protein kinase C positively regulates AQP1 channel function(109).

1.4.2.1 AQP1 deficiency in mice and human

AQP1 null mice have impairment in urinary concentrating ability. The mice appear normal but compared to wildtype mice they have mild growth retardation. When they are water deprived for 1-2 days, they are unable to concentrate their urine and display marked dehydration and serum hyperosmolality (63). AQP1 knockout mice have decreased osmotic water permeability across the proximal tubule by ~78% and reduced net fluid reabsorption, ~50%. These data support that the majority of water reabsorption from the proximal tubule is via transcellular transport (87). In humans, mutations in AQP1 prevent the expression of functionally active water channels. These patients who are deficient in AQP1, do not have polyuria but they fail to concentrate their urine when they are deprived of water (53, 79).

1.4.2.2 AQP1 binding sites for CAII

As previously stated, many acid/base transporters interact with CAII. CAII regulates transporters activity. When we examined the C-terminus of AQP1 we observed an LDADD motif, the exact sequence that binds CAII in AE1 (99, 101). We speculated therefore that there might be an interaction of CAII with AQP1 in its C-terminus and like other acid/base transporters AQP1 activity may also regulate CAII.

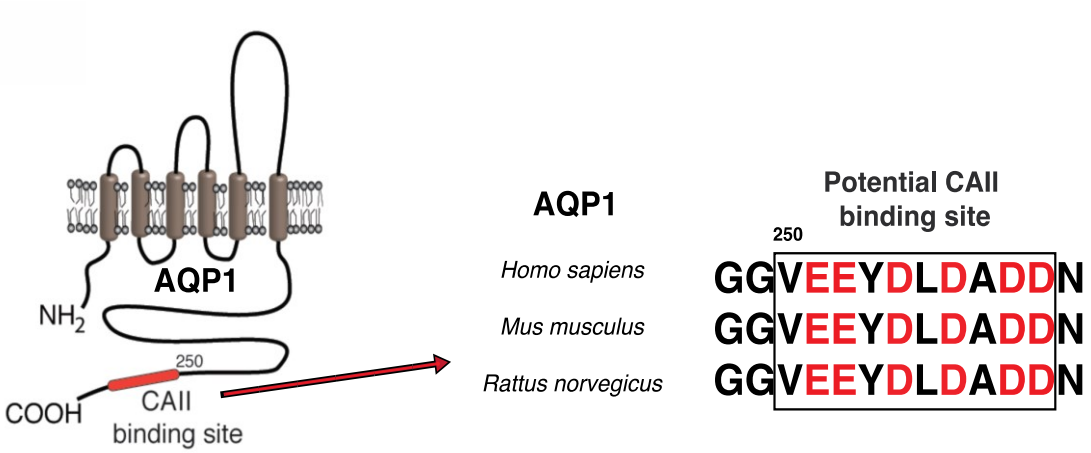

Figure 1.3: AQP1 topology model and C-terminus showing the CAII binding site. Left panel displays an AQP1 topology model with 6 transmembrane domains, amino and carboxy terminus. Right panel represents the conserved potential CAII binding site, and its conservation across different species.

1.5 Volume homeostasis

1.5.1 Brief overview

Two-thirds of the glomerular filtrate is reabsorbed by the proximal tubule. Sodium transport from the proximal tubule regulates blood pressure, extracellular fluid volume, the renin-angiotensin system, sympathetic nervous system and intrarenal dopamine natriuretic system (65). NHE3 mediates the reabsorption of sodium and water from the filtrate into the cell. This stimulates the Na^+/K^+ ATPase and NBC1 at the basolateral membrane. These membrane transporters transfer sodium back into the interstitium. This serves to drive water flux, intravascular volume and therefore also blood pressure (3). Consistent with this, *NHE3* knockout mice demonstrate intravascular volume contraction, when compared to wild type mice (88).

1.5.2 Paracellular reabsorption

The main role of epithelia is to separate two different compartments and regulate the transfer of molecules between these two compartments (47). The intercellular space between epithelial cells in some cases permits the diffusion of small molecules and ions. This form of reabsorption is called paracellular transport (47). In this pathway molecules are selectively permeable. Tight junction's (TJs) serve as a barrier to the passage of ions through this pathway (43, 47). The study of paracellular transport of molecules was given importance only after inherited diseases such as familial hypomagnesemia, hypertension, autosomal recessive deafness (47).

The TJs are present in the apical region of polarized epithelial cells. TJs contains three different types of proteins including membrane proteins, cytoplasmic scaffolding proteins and signaling proteins (49). The membrane proteins play an important role in selective permeability. TJ proteins are of three types: occludin, claudins and junctional adhesion molecules (JAM) (43).

1.5.3 Claudins

The claudin family of proteins consists of 26 isoforms in mammals. They are composed of four transmembrane domains, two extracellular loops and both an N- and C-terminus present in the cytosol (49). Claudins are approximately 21-28 kDa proteins. The first extracellular loop of each claudin is composed of positive and negative charged amino acids. These charged residues are involved in paracellular ion selectivity (49). Extracellular loop 2 is predicted to be involved in mediating trans-claudin interactions (77). The C-termini of claudins have a PDZ domain, that interacts with ZO-1, 2, 3 and multi PDZ domain protein 1 (52). The C-terminal domain is also post translationally modified such with palmitoylation and phosphorylation. These posttranslational modifications contribute to claudin ion selectivity (49).

Claudins are classified into two groups 1) barrier and 2) pore forming. Based on this classification, claudins regulate the transepithelial resistance (TER) (49). In the proximal tubule, claudin -2, -10a, -12, and -17 are present. Claudin-2 acts as a cation pore (68). It is involved in calcium reabsorption and may also be involved in water reabsorption. Claudin -10a and -17 form anion selective pores (49). Claudin-12 in the intestine mediates calcium absorption,

consequently we speculate it may be present in the proximal tubule to reabsorb calcium (36).

1.5.4 Transcellular reabsorption

The transcellular pathway is the transfer of substances through the cell. This occurs through active transport processes. The energy for this process is provided by ATP hydrolysis. Transcellular reabsorption is a chain process where molecules are generally reabsorbed by a luminal transmembrane transporter, then are shuttled to the basolateral side of a polarized cell, at times by a cytosolic protein and finally get transported to the interstitium by a basolateral membrane transporter (29). Note that this process and paracellular transport can also occur in a basolateral to apical fashion so as to secrete an ion or molecule.

1.5.5 Sodium reabsorption along the nephron

Sodium from the glomerular filtrate is reabsorbed from different parts of the nephron. The majority of sodium ~65% is reabsorbed from the proximal tubule (56), ~20% from the thick ascending limb, ~10% from the distal convoluted tubule and ~<5% from the collecting duct. The remainder is excreted into the urine.

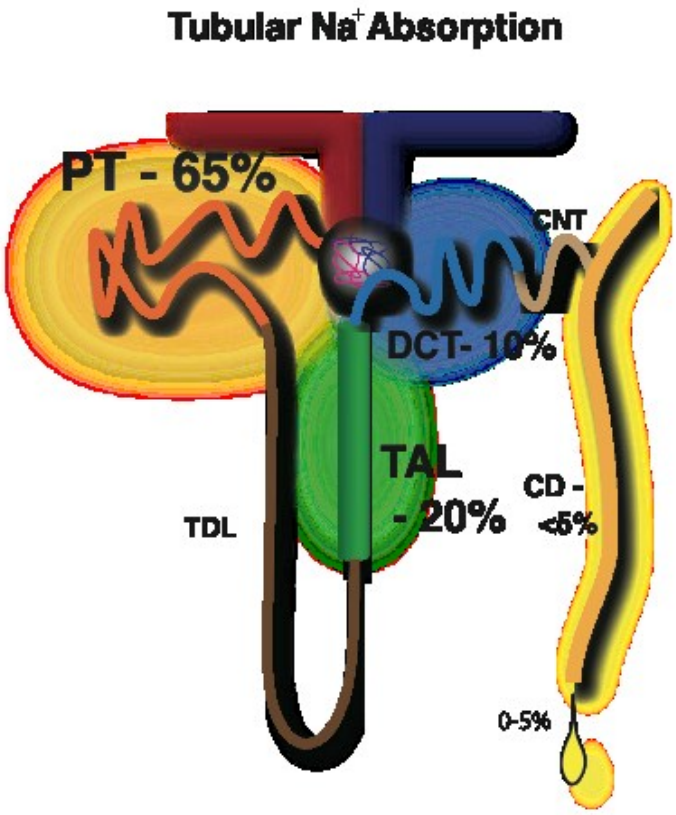

Figure 1.4: Schematic representation of sodium reabsorption along the nephron. Representation of the fraction of sodium reabsorption along different nephron segments including the proximal tubule (PT), thick ascending limb (TAL), distal convoluted tubule (DCT) and collecting duct (CD).

Proximal tubule sodium reabsorption

In the proximal tubule, sodium is reabsorbed by a transcellular mechanism and paracellularly. Many membrane transporters are involved in this sodium transport mechanism. The majority of sodium is reabsorbed from the apical membrane via the NHE3 protein which antiports sodium into the cell in exchange for the extrusion of a proton (4, 56, 88). This stimulates the transporters in the basolateral membrane such as the Na^+/K^+ ATPase, Na^+/HCO_3^- transporter 1 and NHE1. These in turn mediate the efflux of sodium from inside the cell into the intersitium. Also other sodium transporters present in the proximal tubule such as SGLT1, SGLT2, NaPi, and sodium amino acid transporters, mediate a smaller amount of apical sodium influx. Also a small amount of sodium gets reabsorbed through passive paracellular mechanism via TJ protein (Claudin) followed by water reabsorption (68).

In the proximal tubule, the majority of sodium reabsorption occurs via NHE3, whose activity depends on the presence of cytosolic protons. H^+ is generated by metabolic work but also by the cytosolic CAII, an enzyme mediating the catalysis of CO_2 and H_2O into HCO_3^- and a H^+. H_2O and CO_2 enter the cell from the tubular lumen (60), at least in part through the water channel aquaporin-1 (AQP1) (16, 78, 87). This process also drives HCO_3^- reabsorption, as GPI linked extracellular carbonic anhydrase IV (CAIV) mediates catalysis of effluxed H^+ to convert HCO_3^- into H_2O and CO_2 (102).

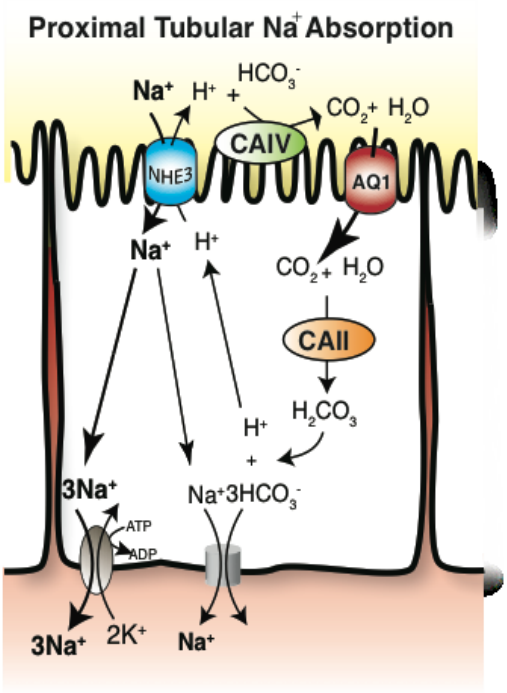

Figure 1.5: Schematic representation of sodium reabsorption from the renal proximal tubule (PT). Transcellular proximal tubular sodium reabsorption occurs via apical NHE3 in exchange for a proton. Cytosolic sodium is excreted into the blood via the Na^+/K^+ATPase or NBCe1 in the basolateral membrane. AQP1 transports CO_2 and H_2O into the cytosol. Cytosolic CAII catalyzes the CO_2 and H_2O reaction thereby providing substrate for NHE3. Extracellular CAIV catalyzes the effluxed H^+ and filtered HCO_3^- into CO_2 and H_2O.

Thick ascending limb (TAL) sodium reabsorption

In the TAL sodium reabsorption occurs by a transcellular pathway. The majority of sodium is reabsorbed by the sodium potassium chloride cotransporter 2 (NKCC2) (19). The driving force for NKCC2 is created by the basolateral Na^+/K^+ ATPase, CLCkb channel and apical ROMK channel, which recycle K^+ back to the lumen (44). A smaller amount of sodium is reabsorbed through NHE3 which is present in the apical membrane of the TAL (42).

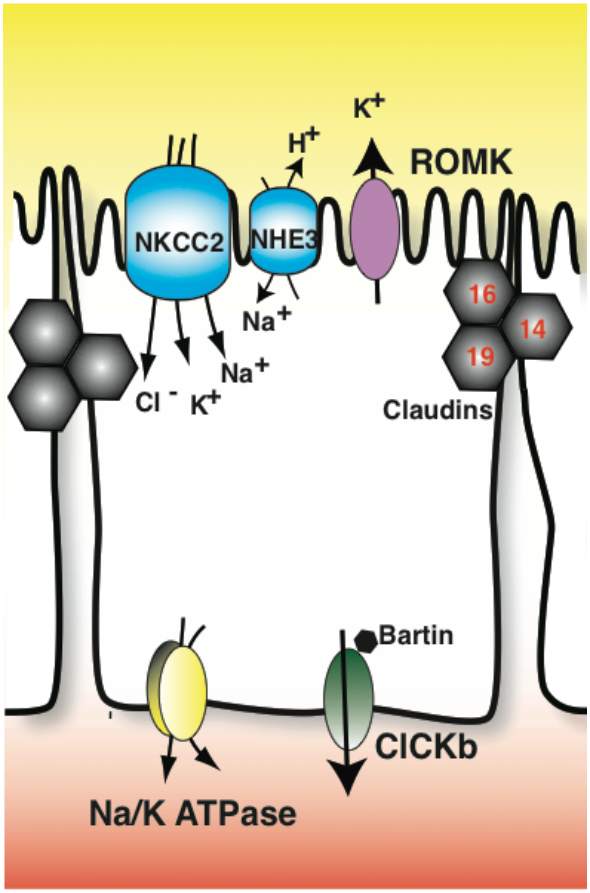

Figure 1.6: Schematic representation of sodium reabsorption from the renal thick ascending limb (TAL). Transcellular sodium reabsorption occurred via apical NHE3 and NKCC2. ROMK mediates excretion of K^+. Cytosolic sodium moves into the blood via the Na^+/K^+ ATPase. Claudin -14, -16 and -19 are present in the TAL and facilitate divalent cation transport.

Distal convoluted tubule (DCT) sodium reabsorption

The sodium chloride cotransporter (NCC) in the apical membrane of the DCT is involved in NaCl reabsorption. NCC is thiazide sensitive and regulated by aldosterone, arginine vasopressin (AVP) and angiotensin II (33). Sodium efflux is mediated by the Na^+/K^+-ATPase.

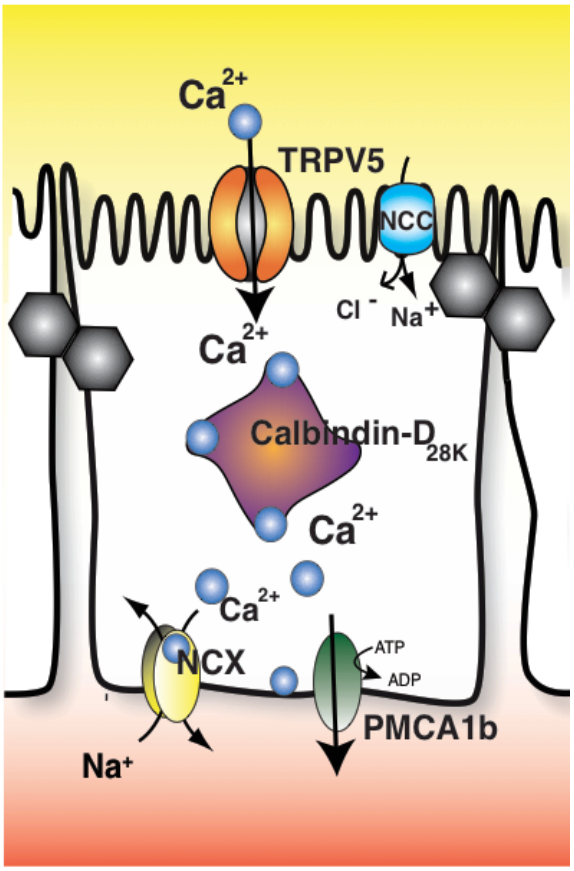

Figure 1.7: Schematic representation of sodium reabsorption from the distal convoluted tubule (DCT). Transcellular sodium reabsorption occurs via apical Na^+-Cl^- cotransporter. Further transcellular calcium reabsorption in the DCT via TRPV5, calbindin-D28K, NCX and PMCA1b are depicted.

Collecting duct sodium reabsorption

Transepithelial sodium transport in the collecting duct is mediated by the amiloride sensitive epithelial sodium channel (ENaC) (71). This channel is only expressed in the apical membrane of the principal cell. Efflux is via the sodium potassium ATPase. Importantly, sodium influx via ENaC is not limited by cell depolarization as ROMK is also expressed in this membrane and mediates potassium efflux.

1.5.6 Regulation of volume homeostasis by hormones

Renin-Angiotensin-aldosterone system (RAAS)

RAAS is a hormone system that regulates blood pressure and fluid balance. The juxta glomerular cells of the nephron converts pro-renin into renin and then secrete it into the blood stream again (18). Renin catalyzes the reaction converting angiotensinogen to angiotensin I (AngI), a molecule that is released by the liver. Angiotensin converting enzyme (ACE) converts AngI into AngII, the latter which activates the angiotensin receptors (AT1R and AT2R) (18). AngII stimulates aldosterone secretion from the adrenal cortex. Aldosterone stimulates sodium and water reabsorption into the blood and excretion of potassium.

ANP

Atrial natriuretic peptide (ANP) is produced in the kidney by proteolytic cleavage of pro-ANP by corin. ANP binds to guanylyl cyclase receptor such as NPR-A/NPR-B, leading to the conversion of guanosine triphosphate (GTP) to cGMP. cGMP binds to different proteins and regulates their activity. ANP

mediates natriuresis, by inhibiting sodium reabsorption from PT and TAL through the regulation of NHE's and NKCC2 (96).

Arginine vasopressin (AVP)

AVP is synthesized in the central nervous system and secreted from terminal axons of the pituitary gland into the blood stream. AVP receptors are subdivided into the V1a, V1b and V2 receptor (37). AVP stimulates both PKA and the cAMP pathways. Vasopressin binds to the V2 receptor in the collecting duct, connecting tubule, distal convoluted tubule and thick ascending limb. It regulates phosphorylation, protein trafficking and protein-protein binding (37). It plays an important role in urine concentration through stimulating the translocation of AQP2 from a subcellular compartment to the apical membrane of the collecting duct principal cells (37).

1.6 Calcium homeostasis

Calcium plays an important role in various physiological functions, such as bone mineralization, blood coagulation, neuromuscular transmission, muscle contraction, cell-cell adhesion and intracellular signaling (36, 48, 84). Calcium homeostasis is maintained by intestinal, bone and renal physiology (5, 47, 74). Ingested calcium is absorbed into the blood through the intestine via two distinct pathways: transcellular and paracellular (36). TRPV6, Calbindin-D_{9k} and PMCa1b have been implicated in transcellular reabsorption in DCT. Luminal calcium in the distal part of the nephron gets reabsorbed by TRPV6 and transferred into cytoplasm. Calcium in cytosol binds to the Calbindin-D_{9k}. This cytosolic protein shuttles calcium from the apical membrane to the basolateral membrane and the

basolateral membrane proteins PMCa1b and NCX1 transport calcium back into blood (47). Claudin-2 and -12 are involved in paracellular absorption in the intestine (36). 1,25 dihydroxyvitamin D3 increases the expression of claudin -2 and -12 in the intestinal TJ and stimulates calcium absorption by creating a permeation pores for cations (5). This type of calcium reabsorption depends on the solvent drag mechanism. Absorbed calcium can be deposited into bone or filtered by the glomerulus and either reabsorbed along the nephron or excreted into the urine. The excretion of urine with more/less calcium is referred to as hyper or hypocalciuria, respectively (5).

1.6.1 Calcium reabsorption along the nephron

In the nephron, 65% of calcium is reabsorbed from the PT, 20% by the TAL, 10% by DCT and connecting tubules and much less from the collecting ducts (47, 84). The remainder is excreted in the urine. In the proximal tubule, calcium reabsorption occurs paracellularly through the TJ (72). The TJ proteins involved in this reabsorption are claudins. Claudin-2 has been implicated in this process (68). Other claudins expressed here include claudin -10a, -17 although their role in calcium reabsorption is unknown. In the TAL, claudin -16, and -19 reabsorb calcium paracellularly by forming a cation pore (50). Increased claudin-14 expression in the TAL occurs in response to calcium sensing receptor (CaSR) signaling (41). It acts as a cation blocker to increase urinary calcium excretion thereby maintaining the blood calcium level. In the DCT, calcium transport is by active transcellular transport. TRPV5, Calbindin D_{28K} and NCX are the proteins involved

in this process (47). PTH and the active form of vitamin D upregulate these proteins and induce calcium reabsorption from the DCT/CNT (58).

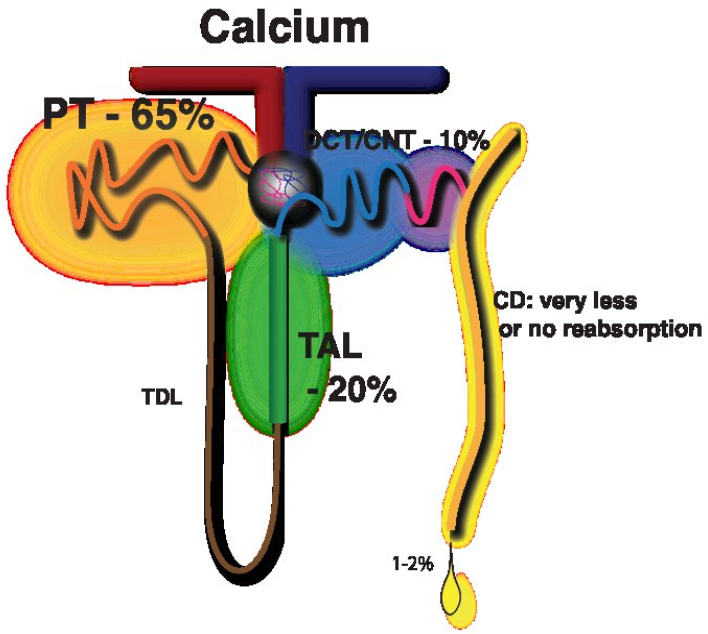

Figure 1.8: Schematic representation of calcium reabsorption along the nephron. Representation of the fraction of calcium reabsorption along different nephron segments including the proximal tubule (PT), thick ascending limb (TAL), distal convoluted tubule (DCT) and collecting duct (CD).

1.6.2 Link between sodium and calcium reabsorption

Previous studies with NHE3 KO mice showed that there is a link between sodium and calcium homeostasis that is regulated by NHE3. The absence of NHE3 in the apical membrane reduces sodium reabsorption, which in turn decreases water and consequently calcium reabsorption via the paracellular pathway (74). This leads to loss of calcium in the urine. Also clinical findings show that a high salt diet induces hypercalciuria and reduced salt intake is a treatment for kidney stones and hypercalciuria. This strongly infers that there is a link between salt intake, volume expansion, hypertension and hypercalciuria (17). The majority of sodium, calcium and water that is filtered through the glomerulus, is reabsorbed from the proximal tubule. Sodium, water and calcium reabsorption are linked procesess. NHE3 reabsorbs the majority of sodium from the PT. The transporter is present in the apical membrane of the proximal tubule. We speculate that this creates the water flux across the tubule. This either moves calcium with it by convection or after water is reabsorbed from lumen, it creates a concentration gradient for calcium, which creates a flux for calcium through the paracellular pathway.

1.7 Hypothesis

We hypothesize that carbonic anhydrase II (CAII) physically and functionally interacts with NHE3 and AQP1 apical membrane proteins mediating sodium, water and calcium reabsorption across the proximal tubule epithelial cells.

1.8 Thesis objectives

a) To determine whether the sodium proton exchanger isoform 3 (NHE3) activity is enhanced by a physical and functional interaction with carbonic anhydrase II (CAII)

b) To identify whether carbonic anhydrase II (CAII) enhances aquaporin I (AQP1) activity by a physical and functional interaction

c) To identify whether NHE3 is the link between altered dietary sodium intake and altered urinary calcium excretion

References

1. **Alexander RS, Nair SK, and Christianson DW**. Engineering the hydrophobic pocket of carbonic anhydrase II. *Biochemistry* 30: 11064-11072, 1991.

2. **Alexander RT, Furuya W, Szaszi K, Orlowski J, and Grinstein S**. Rho GTPases dictate the mobility of the Na/H exchanger NHE3 in epithelia: Role in apical retention and targeting. *Proceedings of the National Academy of Sciences of the United States of America* 102: 12253-12258, 2005.

3. **Alexander RT, and Grinstein S**. Na^+/H^+ exchangers and the regulation of volume. *Acta Physiologica* 187: 159-167, 2006.

4. **Alexander RT, and Grinstein S**. Tethering, recycling and activation of the epithelial sodium-proton exchanger, NHE3. *Journal of Experimental Biology* 212: 1630-1637, 2009.

5. **Alexander RT, Rievaj J, and Dimke H**. Paracellular calcium transport across renal and intestinal epithelia. *Biochemistry and Cell Biology* 92: 467-480, 2014.

6. **Alvarez BV, Loiselle FB, Supuran CT, Schwartz GJ, and Casey JR**. Direct Extracellular Interaction between Carbonic Anhydrase IV and the Human NBC1 Sodium/Bicarbonate Co-Transporter,. *Biochemistry* 42: 12321-12329, 2003.

7. **Alvarez BV, Vilas GL, and Casey JR**. Metabolon disruption: a mechanism that regulates bicarbonate transport. *EMBO J*, 24: p. 2499-25112005.

8. **Azarani A, Goltzman D, and Orlowski J**. Structurally Diverse N-terminal Peptides of Parathyroid Hormone (PTH) and PTH-related Peptide (PTHRP) Inhibit

the Na^+/H^+ Exchanger NHE3 isoform by binding to the PTH/PTHRP receptor type I and activating distinct signaling pathways. *Journal of Biological Chemistry* 271: 14931-14936, 1996.

9. **Babich V, and Di Sole F**. The Na^+/H^+ Exchanger-3 (NHE3) Activity Requires Ezrin Binding to Phosphoinositide and Its Phosphorylation. *PLoS ONE* 10: e0129306, 2015.

10. **Becker H, Klier M, and Deitmer J**. Nonenzymatic augmentation of lactate transport via monocarboxylate transporter isoform 4 by carbonic anhydrase II. *J Membrane Biol* 234: 125-135, 2010.

11. **Becker HM, and Deitmer JW**. Nonenzymatic proton handling by carbonic anhydrase II during H^+-Lactate cotransport via monocarboxylate transporter 1. *Journal of Biological Chemistry* 283: 21655-21667, 2008.

12. **Becker HM, Hirnet D, Fecher-Trost C, Sultemeyer D, and Deitmer JW**. Transport activity of MCT1 expressed in xenopus oocytes is increased by interaction with carbonic anhydrase. *Journal of Biological Chemistry* 280: 39882-39889, 2005.

13. **Becker HM, Klier M, Schuler C, McKenna R, and Deitmer JW**. Intramolecular proton shuttle supports not only catalytic but also noncatalytic function of carbonic anhydrase II. *Proceedings of the National Academy of Sciences* 108: 3071-3076, 2011.

14. **Binswanger U, Helmle-Kolb C, Forgo J, Mrkic B, and Murer H**. Rapid stimulation of Na^+/H^+ exchange by 1,25-dihydroxyvitamin D3; interaction with parathyroid-hormone-dependent inhibition. *Pflugers Arch* 424: 391-397, 1993.

15. **Bobulescu IA, Quinones H, Gisler SM, Di Sole F, Hu M-C, Shi M, Zhang J, Fuster DG, Wright N, Mumby M, and Moe OW**. Acute regulation of renal Na^+/H^+ exchanger NHE3 by dopamine: role of protein phosphatase 2A. *American journal of physiology:*298(5), p. F1205-F1213,2010.

16. **Bondy C, Chin E, Smith BL, Preston GM, and Agre P**. Developmental gene expression and tissue distribution of the CHIP28 water-channel protein. *Proceedings of the National Academy of Sciences of the United States of America* 90: 4500-4504, 1993.

17. **Cappuccio FP, Kalaitzidis R, Duneclift S, and Eastwood JB**. Unravelling the links between calcium excretion, salt intake, hypertension, kidney stones and bone metabolism. *J Nephrol* 13: 169-177, 2000.

18. **Carey RM**. The Intrarenal renin-angiotensin system in hypertension. *Advances in Chronic Kidney Disease* 22: 204-210, 2015.

19. **Castrop H, and Schießül IM**. Physiology and pathophysiology of the renal Na-K-2Cl cotransporter (NKCC2). *American journal of physiology:*307(9), p. F991-F1002, 2014.

20. **Calinescu O, Paulino C, Kuhlbrandt W, and Fendler K**. Keeping It Simple, Transport Mechanism and pH Regulation in Na^+/H^+ Exchangers. *Journal of Biological Chemistry* 289: 13168-13176, 2014.

21. **Cha B, Tse M, Yun C, Kovbasnjuk O, Mohan S, Hubbard A, Arpin M, and Donowitz M**. The NHE3 juxtamembrane cytoplasmic domain directly binds ezrin: dual role in NHE3 trafficking and mobility in the brush border. *Molecular Biology of the Cell* 17: 2661-2673, 2006.

22. **Chen T, Kocinsky HS, Cha B, Murtazina R, Yang J, Tse CM, Singh V, Cole R, Aronson PS, de Jonge H, Sarker R, and Donowitz M**. Cyclic GMP Kinase II (cGKII) inhibits NHE3 by altering its trafficking and phosphorylating NHE3 at three required sites: identification of a multifunctional phosphorylation site. *Journal of Biological Chemistry* 290: 1952-1965, 2015.

23. **Chow C-W, Khurana S, Woodside M, Grinstein S, and Orlowski J**. The epithelial Na^+/H^+ exchanger, NHE3, is internalized through a clathrin-mediated pathway. *Journal of Biological Chemistry* 274: 37551-37558, 1999.

24. **Chu TS, Peng Y, Cano A, Yanagisawa M, and Alpern RJ**. Endothelin(B) receptor activates NHE-3 by a Ca^{2+}-dependent pathway in OKP cells. *Journal of Clinical Investigation* 97: 1454-1462, 1996.

25. **Counillon L, Franchi A, and Pouyssegur J**. A point mutation of the Na^+/H^+ exchanger gene (NHE1) and amplification of the mutated allele confer amiloride resistance upon chronic acidosis. *Proceedings of the National Academy of Sciences* 90: 4508-4512, 1993.

26. **Del Fattore A, Cappariello A, and Teti A**. Genetics, pathogenesis and complications of osteopetrosis. *Bone* 42: 19-29.

27. **Di Sole F, Babich V, and Moe OW**. The Calcineurin Homologous Protein-1 Increases Na^+/H^+-Exchanger 3 Trafficking via Ezrin Phosphorylation. *Journal of the American Society of Nephrology* 20: 1776-1786, 2009.

28. **Di Sole F, Cerull R, Casavola V, Moe OW, Burckhardt G, and Helmle-Kolb C**. Molecular aspects of acute inhibition of Na^+/H^+ exchanger NHE3 by A2-adenosine receptor agonists. *The Journal of Physiology* 541: 529-543, 2002.

29. **Dimke H, Hoenderop JG, and Bindels RJ**. Hereditary tubular transport disorders: implications for renal handling of Ca^{2+} and Mg^{2+}. *Clin Science (London)*, 118-1 p. 1-18, 2010.

30. **Donowitz M, and Li X**. Regulatory Binding Partners and Complexes of NHE3. *Physiol rev*, 87 (3) p. 825-872, 2007.

31. **Donowitz M, Ming Tse C, and Fuster D**. SLC9/NHE gene family, a plasma membrane and organellar family of Na^+/H^+ exchangers. *Molecular Aspects of Medicine* 34: 236-251, 2013.

32. **Donowitz M, Mohan S, Zhu CX, Chen T-E, Lin R, Cha B, Zachos NC, Murtazina R, Sarker R, and Li X**. NHE3 regulatory complexes. *Journal of Experimental Biology* 212: 1638-1646, 2009.

33. **Ellison DH**. Through a glass darkly: salt transport by the distal tubule. *Kidney Int* 79: 5-8, 2011.

34. **Fierke CA, Calderone TL, and Krebs JF**. Functional consequences of engineering the hydrophobic pocket of carbonic anhydrase II. *Biochemistry* 30: 11054-11063, 1991.

35. **Fliegel L**. The Na^+/H^+ exchanger isoform 1. *The International Journal of Biochemistry & Cell Biology* 37: 33-37, 2005.

36. **Fujita H, Sugimoto K, Inatomi S, Maeda T, Osanai M, Uchiyama Y, Yamamoto Y, Wada T, Kojima T, Yokozaki H, Yamashita T, Kato S, Sawada N, and Chiba H**. Tight junction proteins claudin-2 and -12 are critical for vitamin d-dependent Ca^{2+} absorption between enterocytes. *Molecular Biology of the Cell* 19: 1912-1921, 2008.

37. **Fujiwara Y, Tanoue A, Tsujimoto G, and Koshimizu T-a**. The roles of V1a vasopressin receptors in blood pressure homeostasis: a review of studies on V1a receptor knockout mice. *Clin Exp Nephrol* 16: 30-34, 2012.

38. **Fuster D, and Alexander RT**. Traditional and emerging roles for the SLC9 Na^+/H^+ exchangers. *Pflugers Arch - Eur J Physiol* 466: 61-76, 2014.

39. **Fuster DG, Bobulescu IA, Zhang J, Wade J, and Moe OW**. Characterization of the regulation of renal Na^+/H^+ exchanger NHE3 by insulin. *American journal of physiology*, 292 (2) p. F577-F585, 2007.

40. **Geyer RR, Musa-Aziz R, Qin X, and Boron WF**. Relative CO_2/NH_3 selectivities of mammalian aquaporins 0-9. *American journal of physiology* 304 (3), p. C985-C994, 2013.

41. **Gong Y, Renigunta V, Himmerkus N, Zhang J, Renigunta A, Bleich M, and Hou J**. Claudin-14 regulates renal Ca(++) transport in response to CaSR signalling via a novel microRNA pathway. *The EMBO Journal* 31: 1999-2012, 2012.

42. **Good DW, and Watts BA**. Functional roles of apical membrane Na^+/H^+ exchange in rat medullary thick ascending limb. *American journal of physiology*, 270 p. F691-F699, 1996.

43. **Goodenough DA**. Plugging the leaks. *Proceedings of the National Academy of Sciences* 96: 319-321, 1999.

44. **Greger R, Bleich M, and Schlatter E**. Ion channels in the thick ascending limb of henle loop. *Renal Physiol Biochem* 13: 37-50, 1990.

45. **Gross E, Pushkin A, Abuladze N, Fedotoff O, and Kurtz I**. Regulation of the sodium bicarbonate cotransporter knbc1 function: role of Asp986, Asp988 and kNBC1-carbonic anhydrase II binding. *The Journal of Physiology* 544: 679-685, 2002.

46. **He P, Klein J, and Yun CC**. Activation of Na^+/H^+ Exchanger NHE3 by Angiotensin II Is Mediated by Inositol 1,4,5-Triphosphate (IP3) Receptor-binding Protein Released with IP3 (IRBIT) and Ca^{2+}/Calmodulin-dependent Protein Kinase II. *Journal of Biological Chemistry* 285: 27869-27878, 2010.

47. **Hoenderop JGJ, Nilius B, and Bindels RJM**. Calcium absorption across epithelia. *Physiol Rev*, 85(1) p. 373-422, 2005.

48. **Hoenderop JGJ, van Leeuwen JPTM, van der Eerden BCJ, Kersten FFJ, van derKemp AWCM, Merillat A-M, Waarsing JH, Rossier BC, Vallon V, Hummler E, and Bindels RJM**. Renal $Ca^{(2+)}$ wasting, hyperabsorption, and reduced bone thickness in mice lacking TRPV5. *Journal of Clinical Investigation* 112: 1906-1914, 2003.

49. **Hou J, Rajagopal M, and Yu ASL**. Claudins and the Kidney Volume 75: Annual Review of Physiology. *Annual review of physiology* 75: 479-501, 2013.

50. **Hou J, Renigunta A, Konrad M, Gomes AS, Schneeberger EE, Paul DL, Waldegger S, and Goodenough DA**. Claudin-16 and claudin-19 interact and form a cation-selective tight junction complex. *The Journal of Clinical Investigation* 118: 619-628, 2008.

51. **Ismail EAR, Abul Saad S, and Sabry MA**. Nephrocalcinosis and urolithiasis in carbonic anhydrase II deficiency syndrome. *Eur J Pediatr* 156: 957-962, 1997.

52. **Itoh M, Furuse M, Morita K, Kubota K, Saitou M, and Tsukita S**. Direct Binding of Three Tight Junction-Associated Maguks, Zo-1, Zo-2, and Zo-3, with the Cooh Termini of Claudins. *The Journal of Cell Biology* 147: 1351-1363, 1999.

53. **King LS, Choi M, Fernandez PC, Cartron J-P, and Agre P**. Defective urinary concentrating ability due to a complete deficiency of aquaporin-1. *New England Journal of Medicine* 345: 175-179, 2001.

54. **Kinsella JL, and Aronson PS**. Interaction of NH^{4+} and Li^{+} with the renal microvillus membrane Na^{+}/H^{+} exchanger. *Am J Physiol* 241: C220-226, 1981.

55. **Klier M, Schuler C, Halestrap AP, Sly WS, Deitmer JW, and Becker HM**. Transport Activity of the High-affinity Monocarboxylate Transporter MCT2 Is Enhanced by Extracellular Carbonic Anhydrase IV but Not by Intracellular Carbonic Anhydrase II. *Journal of Biological Chemistry* 286: 27781-27791, 2011.

56. **Krishnan D, Liu L, Wiebe SA, Casey JR, Cordat E, and Alexander RT**. Carbonic anhydrase II binds to and increases the activity of the epithelial sodium proton exchanger, NHE3. *American Journal of Physiol,* 309 (4), F383-92, 2015.

57. **Kurashima K, Yu FH, Cabado AG, Szabo EZ, Grinstein S, and Orlowski J**. Identification of sites required for down-regulation of Na^{+}/H^{+} exchanger NHE3 activity by cAMP-dependent protein kinase: phosphorylation-

dependent and -independent mechanisms. *Journal of Biological Chemistry* 272: 28672-28679, 1997.

58. **Lambers TT, Bindels RJM, and Hoenderop JGJ**. Coordinated control of renal Ca^{2+} handling. *Kidney Int* 69: 650-654, 2006.

59. **Lee-Kwon W, Kim JH, Choi JW, Kawano K, Cha B, Dartt DA, Zoukhri D, and Donowitz M**. Ca^{2+}-dependent inhibition of NHE3 requires PKCŒ± which binds to E3KARP to decrease surface NHE3 containing plasma membrane complexes. *American journal of physiol,* 285(6), p. C1527-C1536,2003.

60. **Li X, Alvarez B, Casey JR, Reithmeier RAF, and Fliegel L**. Carbonic Anhydrase II Binds to and Enhances Activity of the Na^+/H^+ Exchanger. *Journal of Biological Chemistry* 277: 36085-36091, 2002.

61. **Li X, Liu Y, Alvarez BV, Casey JR, and Fliegel L**. A Novel Carbonic Anhydrase II Binding Site Regulates NHE1 Activity, *Biochemistry* 45: 2414-2424, 2006.

62. **Loiselle FB, Morgan PE, Alvarez BV, and Casey JR**. Regulation of the human NBC3 Na^+/HCO_3^-, cotransporter by carbonic anhydrase II and PKA. 2004, p. C1423-C1433.

63. **Ma T, Yang B, Gillespie A, Carlson EJ, Epstein CJ, and Verkman AS**. Severely impaired urinary concentrating ability in transgenic mice lacking aquaporin-1 water channels. *Journal of Biological Chemistry* 273: 4296-4299, 1998.

64. **Margolis DS, Szivek JA, Lai LW, and Lien YH**. Phenotypic characteristics of bone in carbonic anhydrase II-deficient mice. *Calcif Tissue Int* 82: 66-76, 2008.

65. **McDonough AA**. Mechanisms of proximal tubule sodium transport regulation that link extracellular fluid volume and blood pressure. *American journal of physiol regul integr comp,* 298(4), p. R851-R861,2010.

66. **McMurtrie HL, Cleary HJ, Alvarez BV, Loiselle FB, Sterling D, Morgan PE, Johnson DE, and Casey JR**. Mini Review. *Journal of Enzyme Inhibition and Medicinal Chemistry* 19: 231-236, 2004.

67. **Miles EW, Rhee S, and Davies DR**. The Molecular Basis of Substrate Channeling. *Journal of Biological Chemistry* 274: 12193-12196, 1999.

68. **Muto S, Hata M, Taniguchi J, Tsuruoka S, Moriwaki K, Saitou M, Furuse K, Sasaki H, Fujimura A, Imai M, Kusano E, Tsukita S, and Furuse M**. Claudin-2, deficient mice are defective in the leaky and cation-selective paracellular permeability properties of renal proximal tubules. *Proceedings of the National Academy of Sciences of the United States of America* 107: 8011-8016, 2010.

69. **Nagami GT**. Role of angiotensin II in the enhancement of ammonia production and secretion by the proximal tubule in metabolic acidosis. *Am J physiol, 294(4)*, p. F874-F880, 2008.

70. **Nakamura N, Tanaka S, Teko Y, Mitsui K, and Kanazawa H**. Four Na^+/H^+ exchanger isoforms are distributed to Golgi and post-Golgi compartments

and are involved in organelle pH regulation. *Journal of Biological Chemistry* 280: 1561-1572, 2005.

71. **Nesterov V, Dahlmann A, Krueger B, Bertog M, Loffing J, and Korbmacher C**. Aldosterone-dependent and -independent regulation of the epithelial sodium channel (ENaC) in mouse distal nephron. *Am J Physiol*, 303(9) p. F1289-F1299, 2012.

72. **Ng RC, Rouse D, and Suki WN**. Calcium transport in the rabbit superficial proximal convoluted tubule. *Journal of Clinical Investigation* 74: 834-842, 1984.

73. **Orlowski J, and Grinstein S**. Diversity of the mammalian sodium/proton exchanger SLC9 gene family. *Pflugers Arch* 447: 549-565, 2004.

74. **Pan W, Borovac J, Spicer Z, Hoenderop JG, Bindels RJ, Shull GE, Doschak MR, Cordat E, and Alexander RT**. The epithelial sodium/proton exchanger, NHE3, is necessary for renal and intestinal calcium (re)absorption. *Am J Physiol*, 302(8) p. F943-F956, 2012.

75. **Pang T, Su X, Wakabayashi S, and Shigekawa M**. Calcineurin Homologous Protein as an Essential Cofactor for Na^+/H^+ Exchangers. *Journal of Biological Chemistry* 276: 17367-17372, 2001.

76. **Pao AC, Bhargava A, Sole FD, Quigley R, Shao X, Wang J, Thomas S, Zhang J, Shi M, Funder JW, Moe OW, and Pearce D**. Expression and role of serum and glucocorticoid-regulated kinase 2 in the regulation of Na^+/H^+ exchanger 3 in the mammalian kidney. *Am J Physiol,* 299(6), p. F1496-F1506,2010.

77. **Piontek Jr, Winkler L, Wolburg H, Muller SL, Zuleger N, Piehl C, Wiesner B, Krause G, and Blasig IE**. Formation of tight junction: determinants of homophilic interaction between classic claudins. *The FASEB Journal* 22: 146-158, 2008.

78. **Prasad GVR, Coury LA, Finn F, and Zeidel ML**. Reconstituted Aquaporin 1 Water Channels Transport CO_2 across Membranes. *Journal of Biological Chemistry* 273: 33123-33126, 1998.

79. **Preston G, Smith B, Zeidel M, Moulds J, and Agre P**. Mutations in aquaporin-1 in phenotypically normal humans without functional CHIP water channels. *Science* 265: 1585-1587, 1994.

80. **Preston GM, and Agre P**. Isolation of the cDNA for erythrocyte integral membrane protein of 28 kilodaltons: member of an ancient channel family. *Proceedings of the National Academy of Sciences of the United States of America* 88: 11110-11114, 1991.

81. **Preston GM, Carroll TP, Guggino WB, and Agre P**. Appearance of Water Channels in Xenopus Oocytes Expressing Red Cell CHIP28 Protein. *Science* 256: 385-387, 1992.

82. **Purkerson JM, and Schwartz GJ**. The role of carbonic anhydrases in renal physiology. *Kidney Int* 71: 103-115, 2006.

83. **Reithmeier RAF**. A Membrane Metabolon Linking Carbonic Anhydrase with Chloride/Bicarbonate Anion Exchangers. *Blood Cells, Molecules, and Diseases* 27: 85-89, 2001.

84. **Renkema KY, Alexander RT, Bindels RJ, and Hoenderop JG**. Calcium and phosphate homeostasis: Concerted interplay of new regulators. *Annals of Medicine* 40: 82-91, 2008.

85. **Sabolic I, Valenti G, Verbavatz JM, Van Hoek AN, Verkman AS, Ausiello DA, and Brown D**. Localization of the CHIP28 water channel in rat kidney. *Am J Physiol* 263: C1225-1233, 1992.

86. **Sarker R, Gr√∏nborg M, Cha B, Mohan S, Chen Y, Pandey A, Litchfield D, Donowitz M, and Li X**. Casein Kinase 2 Binds to the C Terminus of Na^+/H^+ exchanger 3 (NHE3) and Stimulates NHE3 Basal Activity by Phosphorylating a Separate Site in NHE3. *Molecular Biology of the Cell* 19: 3859-3870, 2008.

87. **Schnermann J, Chou C-L, Ma T, Traynor T, Knepper MA, and Verkman AS**. Defective proximal tubular fluid reabsorption in transgenic aquaporin-1 null mice. *Proceedings of the National Academy of Sciences* 95: 9660-9664, 1998.

88. **Schultheis PJ, Clarke LL, Meneton P, Miller ML, Soleimani M, Gawenis LR, Riddle TM, Duffy JJ, Doetschman T, Wang T, Giebisch G, Aronson PS, Lorenz JN, and Shull GE**. Renal and intestinal absorptive defects in mice lacking the NHE3 Na^+/H^+ exchanger. *Nat Genet* 19: 282-285, 1998.

89. **Simon EE, Merli C, Herndon J, Cragoe EJ, and Hamm LL**. Effects of barium and 5-(N-ethyl-N-isopropyl)-amiloride on proximal tubule ammonia transport. *Am J Physiol*, 262(1 Pt 2) p. F36-F39, 1992.

90. **Sly WS, Hewett-Emmett D, Whyte MP, Yu YS, and Tashian RE**. Carbonic anhydrase II deficiency identified as the primary defect in the autosomal recessive syndrome of osteopetrosis with renal tubular acidosis and cerebral calcification. *Proceedings of the National Academy of Sciences of the United States of America* 80: 2752-2756, 1983.

91. **Sowah D, and Casey JR**. An intramolecular transport metabolon: fusion of carbonic anhydrase II to the COOH terminus of the Cl^-/HCO_3, exchanger, AE1. *Am J Physiol*, 301: p. C336-C346, 2011.

92. **Sterling D, Alvarez BV, and Casey JR**. The Extracellular Component of a Transport Metabolon: extracellular loop 4 of the human ae1 Cl^-/ HCO_3^- exchanger binds carbonic anhydrase IV. *Journal of Biological Chemistry* 277: 25239-25246, 2002.

93. **Sterling D, Reithmeier RAF, and Casey JR**. A transport metabolon: Functional interaction of carbonic anhydrase II and chloride/bicarbonate exchangers. *Journal of Biological Chemistry* 2001.

94. **Sun X, Soleimani M, and Petrovic S**. Decreased Expression of Slc26a4 (Pendrin) and Slc26a7 in the Kidneys of Carbonic Anhydrase II-Deficient Mice. *Cellular Physiology and Biochemistry* 21: 095-108, 2008.

95. **Tani K, and Fujiyoshi Y**. Water channel structures analysed by electron crystallography. *Biochimica et Biophysica Acta (BBA) - General Subjects* 1840: 1605-1613, 2014.

96. **Theilig F, and Wu Q**. ANP-induced signaling cascade and its implications in renal pathophysiology. *Am J Physiol*, 308 (10) p. F1047-F1055, 2015.

97. **van Heeswijk MPE, and van Os CH**. Osmotic water permeabilities of brush border and basolateral membrane vesicles from rat renal cortex and small intestine. *J Membrain Biol* 92: 183-193, 1986.

98. **Vilas G, Krishnan D, Loganathan SK, Malhotra D, Liu L, Beggs MR, Gena P, Calamita G, Jung M, Zimmermann R, Tamma G, Casey JR, and Alexander RT**. Increased water flux induced by an aquaporin-1/carbonic anhydrase II interaction. *Molecular Biology of the Cell* 26: 1106-1118, 2015.

99. **Vince JW, Carlsson U, and Reithmeier RAF**. Localization of the Cl-/HCO3- Anion Exchanger Binding Site to the Amino-Terminal Region of Carbonic Anhydrase II. *Biochemistry* 39: 13344-13349, 2000.

100. **Vince JW, and Reithmeier RAF**. Carbonic Anhydrase II Binds to the Carboxyl Terminus of Human Band 3, the Erythrocyte Cl^-/HCO_3^- ,Exchanger. *Journal of Biological Chemistry* 273: 28430-28437, 1998.

101. **Vince JW, and Reithmeier RAF**. Identification of the Carbonic Anhydrase II Binding Site in the Cl^-/HCO_3^- Anion Exchanger AE1,. *Biochemistry* 39: 5527-5533, 2000.

102. **Waheed A, Zhu XL, Sly WS, Wetzel P, and Gros G**. Rat skeletal muscle membrane associated carbonic anhydrase is 39-kDa, glycosylated, GPI-anchored CA IV. *Archives of Biochemistry and Biophysics* 294: 550-556, 1992.

103. **Weiner ID, and Verlander JW**. Role of NH_3 and NH_4^+ transporters in renal acid-base transport. *Am J Physiol*, 300(1) p. F11-F23, 2011.

104. **Weinman EJ, Wang Y, Wang F, Greer C, Steplock D, and Shenolikar S**. A C-terminal PDZ motif in NHE3 binds NHERF-1 and enhances cAMP inhibition of sodium hydrogen exchange,. *Biochemistry* 42: 12662-12668, 2003.

105. **Weise A, Becker HM, and Deitmer JW**. Enzymatic suppression of the membrane conductance associated with the glutamine transporter SNAT3 expressed in xenopus oocytes by carbonic anhydrase II. *The Journal of General Physiology* 130: 203-215, 2007.

106. **Wiederkehr MR, Zhao H, and Moe OW**. Acute regulation of Na^+/H^+ exchanger NHE3 activity by protein kinase C: role of NHE3 phosphorylation. *Am J Physiol*, 276 (5 Pt 1) p. C1205-C1217,1999.

107. **Zaun HC, Shrier A, and Orlowski J**. Calcineurin B homologous protein 3 promotes the biosynthetic maturation, cell surface stability, and optimal transport of the Na^+/H^+ Exchanger NHE1 isoform. *The Journal of Biological Chemistry* 283: 12456-12467, 2008.

108. **Zhang R, Skach W, Hasegawa H, van Hoek AN, and Verkman AS**. Cloning, functional analysis and cell localization of a kidney proximal tubule water transporter homologous to CHIP28. *The Journal of Cell Biology* 120: 359-369, 1993.

109. **Zhang W, Zitron E, Homme M, Kihm L, Morath C, Scherer D, Hegge S, Thomas D, Schmitt CP, Zeier M, Katus H, Karle C, and Schwenger V**. Aquaporin-1 channel function is positively regulated by protein kinase C. *Journal of Biological Chemistry* 282: 20933-20940, 2007.

110. **Zhu XC, Sarker R, Horton JR, Chakraborty M, Chen T-E, Tse CM, Cha B, and Donowitz M**. Nonsynonymous single nucleotide polymorphisms of NHE3 differentially decrease NHE3 transporter activity. *Am J Physiol*, 308 (9) p. C758-C766, 2015.

111. **Zizak M, Chen T, Bartonicek D, Sarker R, Zachos NC, Cha B, Kovbasnjuk O, Korac J, Mohan S, Cole R, Chen Y, Tse CM, and Donowitz M**. Calmodulin Kinase II constitutively binds, phosphorylates, and inhibits brush border Na^+/H^+ exchanger 3 (NHE3) by a NHERF2 protein-dependent process. *Journal of Biological Chemistry* 287: 13442-13456, 2012.

CHAPTER 2

Carbonic anhydrase II binds to and increases the activity of the epithelial sodium-proton exchanger, NHE3

(Much of this paper has been published as: ***Krishnan D, Liu L, Wiebe SA, Casey JR, Cordat E, Alexander RT,*** Carbonic anhydrase II binds to and increases the activity of the epithelial sodium proton exchanger, NHE3. Am J Physiol Renal Physiol. 2015 Aug 15; 309(4):F383-92. doi: 10.1152/ajprenal.00464.2014. Epub 2015 Jun 3.)

Devishree Krishnan completed all the experiments.

Liu L generated the CAII Myc cDNA.

Shane Wiebe helped to complete experimental revisions.

2.1 Introduction

Intravascular volume is maintained via highly regulated control of sodium homeostasis, best observed along the course of the nephron, where the majority (at least 65%) of Na^+ is reabsorbed from the proximal tubule. Transepithelial reabsorption of sodium from this nephron segment is determined by a series of transport events and enzyme-mediated catalysis. Apical Na^+ influx occurs through the sodium/proton exchanger isoform 3 (NHE3) in exchange for a cytosolic H^+. Cytosolic Na^+ is excreted back into the blood via either the Na^+-K^+-ATPase or the sodium-dependent bicarbonate transporter (NBCe1). The rate-limiting step is apical Na^+ influx via NHE3, whose activity depends on the presence of cytosolic protons. H^+ are generated by the cytosolic carbonic anhydrase isoform II (CAII), an enzyme mediating the catalysis of CO_2 and H_2O into HCO_3^- and a H^+. H_2O and CO_2 enter the cell from the tubular lumen, at least in part through the water channel aquaporin-1 (11, 23, 27). This process also drives HCO_3^- reabsorption, as glycosylphosphatidylinositol (GPI)-linked extracellular carbonic anhydrase IV mediates catalysis of effluxed H^+ to convert HCO_3^- into H_2O and CO_2 (40). NHE3 is one of nine isoforms of the Na^+ /H^+ exchanger family (14). In mammals, NHE1-5 proteins are present in the plasma membrane, and NHE6-9 localize predominantly in endomembrane compartments (13, 14). NHE3 is located in the apical membrane of intestinal and renal epithelia (19). In the kidney, NHE3 is predominantly expressed in the proximal tubule and to a lesser extent in the thick ascending limb of the loop of henle (9). NHE3 participates directly in Na^+ reabsorption and indirectly in the reabsorption of bicarbonate, Ca^{2+}, and the

secretion of ammonium (10, 20, 25). CAII both physically and functionally interacts with a number of transporters, including anion exchanger 1 (AE1), NBCe1, and MCT (6, 7, 24, 38, 39). The best-characterized interaction is between AE1 and CAII. LDADD motif in the cytosolic C-terminus of AE1 binds to the histidine-rich N-terminus of CAII (37, 39). This interaction augments AE1 transport, potentially via enzymatic provision of substrate to the transporter (38). Such an interaction has been dubbed a transport metabolon (33). NHE1 directly interacts with the cytosolic carbonic anhydrase CAII, through the NHE1 ^{790}RIQRCLSDPGPHP^{802} motif in the carboxyl, cytosolic terminus (16, 17). This interaction increases NHE1 activity (16). However, the existence of a direct AE1/CAII physical interaction has been questioned (1, 22). Examination of the cytosolic carboxy terminus of NHE3 revealed a potential CAII binding site (^{710}IKEKDLEL**SD**TEE^{722}), consistent with the motif established for NHE1 (16, 17). Given this, and the known dependence of CAII activity for what is currently appreciated as NHE3-mediated transepithelial Na^+ transport (12, 26), we hypothesized that CAII and NHE3 physically and functionally interact. Consistent with this, a proximity ligation assay (PLA) revealed the close association of the two proteins; we could coimmunoprecipitate CAII with NHE3, and a microtiter plate assay confirmed that the glutathione-**S**-transferase (GST) tagged NHE3 C-terminal domain, containing the putative CAII binding site, binds CAII. Moreover, in the presence of CO_2 and bicarbonate, NHE3 activity is inhibited by acetazolamide, but is not when NHE3 activity is measured in the nominal absence of CO_2 and HCO_3^-.

2.2 Materials and methods

2.2.1. Materials

Restriction enzymes *EcoR1* and *NotI* were from NewEngland Biolabs (Whitby, ON). BL21 Escherichia coli and pcDNA3.1+ were from Invitrogen (Carlsbad, CA). pGEX 6P-1 and glutathione-Sepharose 4B were from GE Healthcare (Mississauga, ON). Recombinant human CAII, nigericin, acetazolamide, and EIPA were from Sigma-Aldrich Canada (Oakville, ON). Antibodies/stains used include rabbit anti-CAII polyclonal antibody (Santa Cruz Biotechnology, Santa Cruz, CA), mouse anti-hemagglutinin (HA; 16B12, Covance, Emeryville, CA), and phalloidin (Invitrogen). DMEM-F12 medium, geneticin, penicillin/streptomycin/glutamine (PSG), and neon transfection reagents were from GIBCO Life Technologies (Burlington, ON). Fetal bovine serum was from VWR International (Mississauga,ON). Opossum kidney cells were from the American Type Culture Collection (ATCC; Manassas, VA). Fugene was from Promega (Madison, WI). Isopropyl ß-D-1-thiogalactopyranoside (IPTG) was from Fermentas Canada, (Burlington, ON).

2.2.2. Cell culture

Opossum kidney (OK) cells were obtained from ATCC. OK cells stably overexpressing NHE3 with three exofacial HA tags, $NHE3_{38HA3}$ (amino acid sequence: YPYDVPDYAS) (2), or pcDNA 3.1+ were generated by transfecting the constructs with FuGENE 6 transfection reagent, then selecting with geneticin. Monoclonal stable cell lines were subsequently isolated by limiting dilution as previously (20). The cells were maintained in DMEM-F12 medium supplemented

with 10% fetal bovine serum, 5% penicillin, streptomycin, glutamine (PSG), and 750 μM geneticin (G418) at 37°C in a 5% CO_2 incubator. OK cells stably expressing $NHE3_{38HA3}$ were transiently transfected with cDNA encoding CAII, CAII-myc, an inactive mutant of CAII (CAII-V143Y) (33), a binding mutant of CAII [CAII-HEX, which is a catalytically active mutant, containing six point mutations (H3P, H4D, K9D, H10K, H15Q, and H17S)] (37), or pcDNA 3.1+, via electroporation with the Neon transfection system (4). For experimental purposes, transfected cells were grown on 11 x 7.5-mm-2D-UAB (Thermo Scientific, Asheville, NC) coverslips.

2.2.3. Immunoblotting

Stably or transiently transfected cells were grown on 10-cm-diameter tissue culture dishes. Cell lysates were prepared with sample buffer containing 4.6% SDS, 0.02% bromophenol blue, 20% glycerol, 2% 2-mercaptoethanol, 130 mM Tris·HCl, pH 6.8, with protease inhibitor cocktail (Calbiochem, Gibbstown, NJ), and benzonase nuclease (Novagen, EMD Chemicals, San Diego, CA). Total cell lysate was incubated at 37 °C for 20 min and then was fractionated on a 12% polyacrylamide gel and then transferred to a polyvinylidenedifluoride membrane. The membrane was first blocked with 5% milk in TBST (150 mM NaCl, 0.1% Tween, 20 mM Tris, pH 7.4) for 2 h at room temperature. Then it was immunoprobed with mouse monoclonal anti-HA antibody (16B12, Covance, Emeryville, CA), rabbit anti-CAII (Santa Cruz Biotechnology), or mouse monoclonal anti-Myc antibody (Cell Signaling Technology, Danvers, MA), all in 1: 1,000 dilution, incubated overnight at 4 °C. Membranes were washed with

TBST then incubated with either secondary horseradish peroxidase (HRP)-conjugated goat anti-mouse or goat anti-rabbit IgG antibody (1:5,000 dilution in TBST, Santa Cruz Biotechnology) for 2 h at room temperature. Finally, the membranes were washed with TBST and after incubation with western Lighting plus ECL reagents (PerkinElmer, Boston, MA), immunoreactive bands were visualized with a Carestream Advanced Fluorescent Imaging F PRO image station (Carestream Health, Rochester, NY).

2.2.4. Measurement of Na^+/H^+ exchange activity in the presence of CO_2

To assess a functional interaction between NHE3 and CAII, we overexpressed NHE3 containing three exofacial HA tags in OK cells to enhance NHE3 expression (20). NHE activity was measured in cells that were grown on coverslips (11 x 7.5 mm, Thermo Scientific) as previously (16). Coverslips were incubated with 5 mM BCECF-AM (Molecular Probes, Eugene, OR) at 37 °C for 10 min. The loaded cells were rinsed with iso Na^+ buffer (140 mM NaCl, 1 mM $MgCl_2$, 1 mM $CaCl_2$, 3 mM KCl, 10 mM glucose, and 5 mM HEPES, pH 7.4) to remove excess probe and then placed inside a fluorescence cuvette where the coverslip was held immobile with a holder device. Intracellular pH (pHi) was determined with a PTI Fluorometer [LPS-220B, Photon Technology International (PTI), London, ON]. The NHE activity of OK cells overexpressing NHE3 or pcDNA3.1+ was measured as the rate of pH recovery after acidifying cells by switching them from iso Na^+-buffered medium to a HCO_3^--buffered medium (130 mM NaCl, 1 mM $MgCl_2$, 1 mM $CaCl_2$, 3 mM KCl, 10 mM glucose, and 25 mM $NaHCO_3$, pH 7.4), bubbled with 5% CO_2 - 95% air; the perfusion rate was kept

constant per experimental condition but varied between sets of experiments from 1.5–8 ml/min to ensure equivalent degree of acidification within experimental groups. Fluorescence measurements were made with dual excitation (440, 490 nm), and a single emission was measured (510 nm). Calibration was performed with high K^+-containing buffer at pH 6.0, 6.5, 7.0, and 7.5 (140 mM KCl, 1 mM $MgCl_2$, 1 mM $CaCl_2$, 10 mM glucose, and 20 mM HEPES) containing 10 mM nigericin for each individual coverslip (34). NHE3 activity was then calculated as the rate of change in pH over the first 30 s from maximal acidification. The rate of pH change was also assessed in the presence of 100 μM EIPA and acetazolamide (Sigma-Aldrich Canada) when indicated.

2.2.5. Measurement of Na^+/H^+ exchanger activity in the absence of CO_2

NHE3 activity was assessed in the absence of CO_2 as previously (2,3). After loading with BCECF-AM as above, the cells were rinsed with iso Na^+ buffer (140 mM NaCl, 1 mM $MgCl_2$, 1 mM $CaCl_2$, 3 mM KCl, 10 mM glucose, and 5 mM HEPES, pH 7.4) to remove excess probe and then placed inside a fluorescence cuvette where the coverslip was held immobile with a holder device. pHi was determined with a PTI-Fluorometer (LPS-220B, PTI). The cells were perfused with iso Na^+ buffer, containing 10 mM NH_4Cl for 10 min before a switch to acidify the cells by perfusing with iso K^+ buffer (140 mM KCl, 1 mM $MgCl_2$, 1 mM $CaCl_2$, 10 mM glucose, and 20 mM HEPES, pH 7.4) for 2 min. pH recovery in cells transfected with NHE3 or pcDNA3.1+ was then induced by perfusing cells with iso Na^+ buffer. Calibration was performed with high K^+-containing buffer with 10 mM nigericin for each individual coverslip as above (34). NHE3 activity was

calculated as the change in pH over the first 30 s after iso Na^+ readdition.

2.2.6. Generation of glutathione-S-transferase constructs and CAII-myc

DNA encoding amino acids 630–730 or 730–830 of rat NHE3 was amplified by PCR. The former region contains a homologous region to the NHE1, CAII binding site (^{710}IKEKDLELSDTEE^{722}) (17). Rat full-length NHE3 was used as the template (2). Primers for the 630–730 region were forward: 5' -CG GAA TTC CTC TAC AGTCGG CAC GAG CT-3' and reverse: 5' -G GGC GGC CGC TCAATG CCT CCA CTG ATC TCT TC-3'. Primers for the 730–830 region were forward: 5' -CG GAA TTC GAA TTT CTG GCC AGCGTC AC-3' and reverse: 5' -G GGC GGC CGC TCA CAT GTG TGTGGA CTC AGG G-3'. Forward primers contained an *EcoRI* restriction site and reverse primers a *NotI* site. After amplification, the PCR fragment was digested with the appropriate enzymes and then ligated into the pGEX 6P1 vector. The generated constructs are subsequently referred to as NHE3-Tail-1 (630 –730) and NHE3-Tail-2 (730–830). CAII-myc was subcloned from a CAII-GFP construct by PCR with forward primer 5'-CCG GAA TTC CGG GCC ACC ATG TCC CATCAC TGG GGG TAC G-3' and reverse primer 5'-AAGGAAAAAAGC GGC CGC TTA TAG GTC CTC CTC GGA GAT CAG CTTTTG TTC TTT GAA GGA AGC TTT GAT TTG CCT G-3'. *EcoRI* and *NotI* restriction sites were engineered into the primers, permitting digestion and ligation into the pcDNA 3.1+ mammalian expression vector. The construct was found to be functional by measuring the rate that lysate from cells overexpressing it acidified a solution bubbled with CO_2 (5). All DNA sequences were confirmed by sequencing at the TAGC Applied Genomics core, University of

Alberta.

2.2.7. Purification of glutathione-S-transferase fusion proteins

GST.NHE3-Tail-1, GST.NHE3-Tail 2, or pGEX 6P1 (empty vector) were purified by methods used previously (16, 32). They were transformed into E. coli BL21 by electroporation (Eppendorf Electroporator 2510,Eppendorf North America, Westbury, NY) and then plated onto LB agar plates with 100 g/ml ampicillin (Sigma-Aldrich Canada) and incubated at 37 °C overnight. A single colony was used to inoculate LB broth, containing 100 µg/ml of ampicillin, which was then incubated overnight at 37 °C in a shaker (Infors HT Ectron, Infors Canada, Anjou, Quebec). A 5 ml culture was subsequently inoculated into 250 ml of LB broth and grown at 37 °C in a shaker until it reached A600 0.6–1.0. Isopropylthiogalactoside (1 mM final concentration) (Fermentas /Thermo Scientific, Ottawa, ON) was added, and the culture was subsequently incubated for 3 h further at 37 °C while shaking. Cultures were then centrifuged at 7,500 g for 10 min in a Beckman-Avanti J-25 centrifuge (Beckmann Coulter, Mississauga, ON) at 4 °C. The bacterial pellet was resuspended in 5 ml of 4 °C PBS with benzamidine, PMSF, and protease inhibitor cocktail (Roche Diagnostics, Laval, Canada) with 75 µl of Triton X-100. Suspended cells were disrupted by sonicating (Braun-sonic 2000 sonicator) with four 45 s pulses at 20 kHz. Cells were then centrifuged at 12,000 g for 10 min at 4 °C. The supernatant was transferred to glutathione Sepharose 4B resin (washed with PBS) and incubated at 20 °C for 2 h. The samples were subsequently centrifuged at 1,500 g for 5 min and then washed with PBS. The fusion proteins were eluted with glutathione buffer (10mM reduced

glutathione in 50 mM Tris·HCl, pH 8.0). The concentration of protein was determined by measuring A_{280} with a Nanodrop spectrophotometer, an extinction coefficient of 1 mg/ml (NanoDrop2000c UV-Vis Spectrophotometers, Thermo Scientific) and BSA standards.

2.2.8. Microtiter plate binding assay

A microtiter plate-binding assay was used to assess a physical interaction between NHE3 and CAII, as per other transporter-CAII interactions (16, 38). Human recombinant CAII (25 nM) was coated on 96-well microtiter plates (96-wellEIA/RIA plate, Costar 3590, Corning, Corning, NY) for 30 min at room temperature in ELISA buffer (150 mM NaCl, and 100 mM Na_2HPO_4, pH 6.0) with 1.25 mg/ml of N-cyclohexyl-N-carbodiimidemetho-p-toluene sulfonate (Sigma-Aldrich Canada). Plates were washed with PBS before blocking with 2% bovine serum albumin in PBS for 2 h at 20 °C. Plates were then washed with PBS and subsequently overlaid with either NHE3-Tail-1, NHE3-Tail-2, or GST alone (50–400 nM) in antibody buffer (100 mM NaCl, 5 mM EDTA, 0.25% gelatin, 0.05% Triton X-100, and 50 mM Tris, pH 7.5), containing 1 mM DTT at 20 °C for 16 h. Note that for experiments examining the effect of pH, the amount of NaCl or pH of solution was altered to the stated content. Plates were next washed with PBS, and the samples were incubated with a rabbit polyclonal anti-GST antibody (1:5,000, Santa Cruz Biotechnolgy) for 2 h at 20 °C. After washing with PBS, plates were incubated with a donkey anti-rabbit IgG polyclonal antibody (1:5,000, Santa Cruz Biotechnolgy), washed again with PBS, and finally incubated with streptavidin conjugated to HRP (Pierce Biotechnology, Rockford, IL) for 1 h at 20 °C. Plates

were developed with TMB substrate reagent (San Jose, CA) and then stopped by adding 200 µl/well of 5 M H_2SO_4. The relative amount of GST-fusion protein binding was finally measured at A_{450} nm in a Synergy Biotek microplate reader.

2.2.9. Proximity ligation assay (PLA)

An association between NHE3 and CAII was assessed by PLA using a previously established methodology (30, 36). OK cells were transfected with cDNA encoding either NHE3 (2), human AE1 (37, 39), or human concentrative nucleoside transporter (hCNT3) (41) and myc-tagged CAII. Two days after transfection, the cells were washed with PBS, lysed in IPB buffer (1% NP-40, 5 mM EDTA, 0.15M NaCl, 0.5% deoxycholate, and 10 mM Tris·HCl, pH 7.5) containing protease inhibitors, washed twice in PBS, and then fixed (3.5% paraformaldehyde, 1 mM $CaCl_2$, 1 mM $MgCl_2$ in PBS, pH 7.4 for 20 min). They were then washed twice with PBS and finally quenched with 50 mM NH_4Cl for 10 min. Fixed cells were permeabilized with 0.1% Triton X-100 in PBS for 1 min at 20 °C and then washed twice for 5 min with Wash Buffer A (Olink Bioscience, Uppsala, Sweden). Samples were then processed for PLA using the Duolink Detection kit (Olink Bioscience), according to the manufacturer's instructions. Briefly, the cells were blocked with manufacturer-provided blocking solution for 30 min at 37 °C, incubated for 1 h at 37 °C in a humidified chamber with a 1:1,000 dilution of rabbit anti-CAII antibody and either mouse anti-HA, IVF12 mouse monoclonal anti-AE1 (a gift from Dr. Michael Jennings, Univ. of Arkansas, Little Rock, AR), or mouse monoclonal anti-hCNT3 (a gift from Dr. James Young, Univ. of Alberta, Edmonton, AB) (41) at 1:500, 1:1,000, and 1:500 dilutions in antibody

diluent, respectively. Samples were then washed twice for 5 min in wash buffer A (manufacturer provided), and then incubated for 1 h at 37 °C with a combination of the corresponding PLA probes (anti-rabbit Plus and anti-mouse Minus, both supplied by the manufacturer) conjugated to specific oligonucleotides. The PLA oligonucleotides were hybridized and circularized by ligation (30 min at 37 °C), and the DNA circle formed was amplified by rolling circle amplification into single-stranded DNA anchored to one of the antibodies. The amplification product was detected by addition of complementary oligonucleotides labeled with Texas Red fluorophore. Coverslips were mounted in the provided mounting medium and observed through a 60X/1.42 PlanApo oil-immersion objective of a spinning-disk confocal microscope (WaveFx, Quorum Technologies, Guelph, ON) on an Olympus IX-81 inverted stand (Olympus, Markham, ON). Z-stack confocal image capture was performed with a C9100-13 EM-CCD Digital Camera (Hamamatsu, Hamamatsu City, Japan), using Volocity software (PerkinElmer, Mississauga ON).

2.2.10. Coimmunoprecipitation

Coimmunoprecipitation (Co-IP) was performed essentially as previously (4). OK cells were cotransfected with $NHE3_{38HA3}$ and CAII-myc by neon transfection as per the PLA (see above). The cells were grown in 10 cm tissue culture dishes for 2 days in DMEM-F12 media in the presence of 5% CO_2 at 37 °C. Once they were 100% confluent, the cells were washed with PBS then collected with 200 µl of elution buffer (1% NP-40, 5 mM EDTA, 0.15 M NaCl, and 10 mM Tris·HCl, pH 8.1) containing protease inhibitor cocktail (1:100, Calbiochem) and PMSF (1:1,000). The homogenized cell lysate was placed on ice for 30 min, then

centrifuged at 12,000 rpm for 10 min at 4 °C. The supernatant was subsequently collected, and the concentration of protein was determined by measuring A_{280} with a Nanodrop spectrophotometer (NanoDrop 2000c UV-Vis Spectrophotometers, Thermo Scientific), using an extinction coefficient of 1 mg/ml and BSA standards. Two separate 50 µl aliquots of Dyna beads protein G (Thermo Fischer) were precleared and then rinsed with 100 µl of elution buffer. To one sample of beads, 2 µg of goat anti-HA antibody was added; to the other sample, 2 µg of rabbit serum was added. Both were then incubated on ice for 20–30 min. Protein cell lysate (300 µg) was added with elution buffer to make the total volume 250 µl, and the samples were incubated overnight at 4 °C. The next day the beads were washed three times with elution buffer containing protease inhibitor cocktail and PMSF. Finally, to elute the bound protein from the beads, 40 µl of sample buffer was added to either the Co-IP, or control sample and to a total protein lysate sample (50 µg), and incubated at 37 °C for 20 min. The samples were then subjected to SDS-PAGE and immunoblotting with anti-myc as above.

2.2.11. Statistical analysis

Data are presented as means SE. Paired or unpaired Student's t-tests or ANOVA was carried out to determine statistical significance as appropriate. Tests were performed using Excel software (Microsoft, Santa Monica, CA), and P values < 0.05 were considered statistically significant.

2.3. Results

2.3.1. Acetazolamide inhibits NHE3 activity in the presence of CO_2 and HCO_3^-.

To assess whether a functional interaction between NHE3 and CAII exists, we stably expressed NHE3 with three exofacial HA epitopes in OK cells (OK-$NHE3_{38HA3}$) (2). This increased NHE3 expression and activity in this cell line and also provided an epitope tag greatly facilitating NHE3 detection and manipulation (3, 20). Cell lysate immunoblotted for the HA epitope revealed a single band of the appropriate molecular weight in cells expressing $NHE3_{38HA3}$, but not cells expressing the vector alone (Fig. 2-1A). Immunoblotting of the same cell lysate revealed endogenous expression of CAII (Fig. 2-1B, bottom band). Immunostaining of OK cells with HA antibody and 4,6-diamidino-2-phenylindole to stain nuclei found NHE3 predominantly present in the apical membrane of OK cells (Fig. 2-1C), consistent with its localization in vivo. NHE3 activity was then assessed as the rate of recovery of pHi induced by an acid load and measured with the fluorescent radiometric pH sensitive dye BCECF-AM. The cells were acidified by switching them from a bicarbonate-free medium to one containing bicarbonate and bubbled with 5% CO_2. OK $NHE3_{38HA3}$ cells demonstrate significantly greater Na^+-dependent recovery of pHi than vector-transfected controls (Fig. 2-1,D–G). Recovery from an acid load under these conditions was both Na^+ dependent (Fig. 2-1, D and E) and inhibited by 100 μM EIPA (Fig. 2-1, F and G), a dose sufficient to block NHE3 activity (35). Recovery from a CO_2-induced acid load was also prevented when a choline-HCO_3^-containing buffer was used instead of the $NaHCO_3$ (dpHi/dT = 0.0014 ± 0.0005 in the presence of Na^+ vs. -0.0004 ± 0.0002

in the absence). This is consistent with NHE3 activity and not the activity of either a bicarbonate transporter or an H^+-ATPase. To examine the possibility of a functional interaction between NHE3 and CAII, we inhibited endogenous CAII with acetazolamide and then repeated the measurement. This greatly attenuated NHE3 activity in the overexpressing cells (Fig. 2-2), consistent with a requirement for CAII activity to significantly augment NHE3 activity.

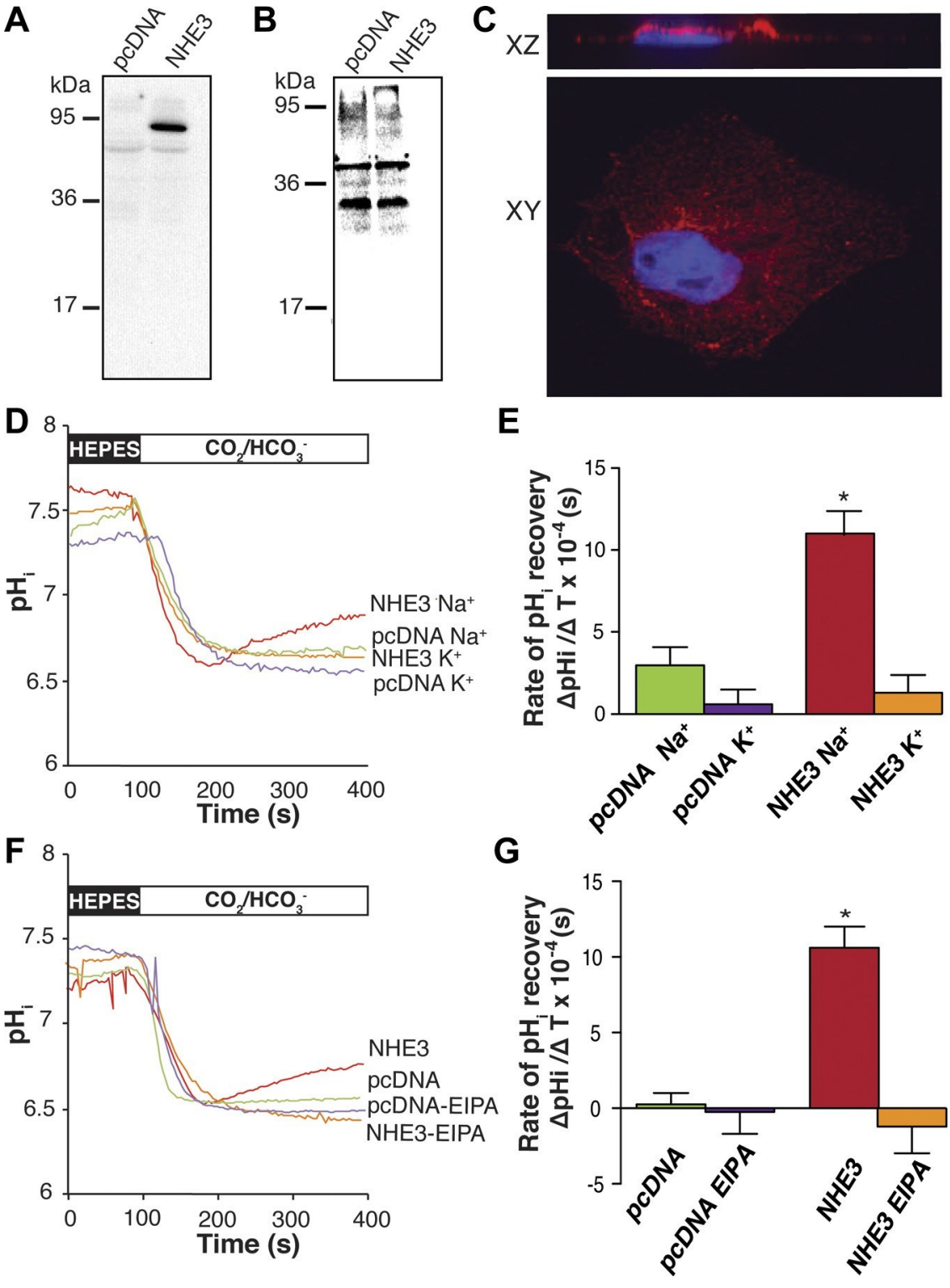
A
pcDNA
NHE3
kDa
95
36
17
B
pcDNA
NHE3
kDa
95
36
17
C
XZ
XY
D
HEPES
CO2/HCO3-
pHi
8
7.5
7
6.5
6
0
100
200
300
400
Time (s)
NHE3 Na+
pcDNA Na+
NHE3 K+
pcDNA K+
E
Rate of pHi recovery
ΔpHi /Δ T x 10-4 (s)
15
10
5
0
*
pcDNA Na+
pcDNA K+
NHE3 Na+
NHE3 K+
F
HEPES
CO2/HCO3-
pHi
8
7.5
7
6.5
6
0
100
200
300
400
Time (s)
NHE3
pcDNA
pcDNA-EIPA
NHE3-EIPA
G
Rate of pHi recovery
ΔpHi /Δ T x 10-4 (s)
15
10
5
0
-5
*
pcDNA
pcDNA EIPA
NHE3
NHE3 EIPA

Figure 2.1. Opossum kidney (OK) cells overexpressing sodium/proton exchanger isoform 3 (NHE3) demonstrate increased sodium-dependent recovery of pH. NHE3 with 3 exofacial hemagglutinin (HA) tags ($NHE3_{38HA3}$) was stably expressed in OK cells. Lysates from cells stably expressing $NHE3_{38HA3}$ or pcDNA were immunoblotted with anti-HA antibody (A) or anti-carbonic anhydrase II (CAII) antibody (B). C: XY and XZ confocal image of a polarized OK cell immunostained with anti-HA (red) and 4,6-diamidino-2-phenylindole (DAPI; blue). D–G: assessment of NHE3 activity. Cells loaded with the pH-sensitive fluorescent probe BCECF-AM were acidified by switching them from HEPES-buffered medium to one containing CO_2/HCO_3^- (either as a Na^+ or K^+ salt; the switch is represented as a change from a black to a white bar). D: representative traces of the change in intracellular pH (pHi) of cells either stably expressing $NHE3_{38HA3}$ or pcDNA (-ve control) overtime in the presence of extracellular sodium (Na^+) or absence of extracellular sodium (K^+). Note: results were similar when choline-HCO_3^- was used. F: representative traces of the change in pHi of cells either stably expressing $NHE3_{38HA3}$ or pcDNA (-ve control) in the presence and absence of 100 μM EIPA. E and G: quantification of initial change (Δ) in pH (over the first 30 s) for each condition displayed in D or F. *$P < 0.05$; n = >6/condition.

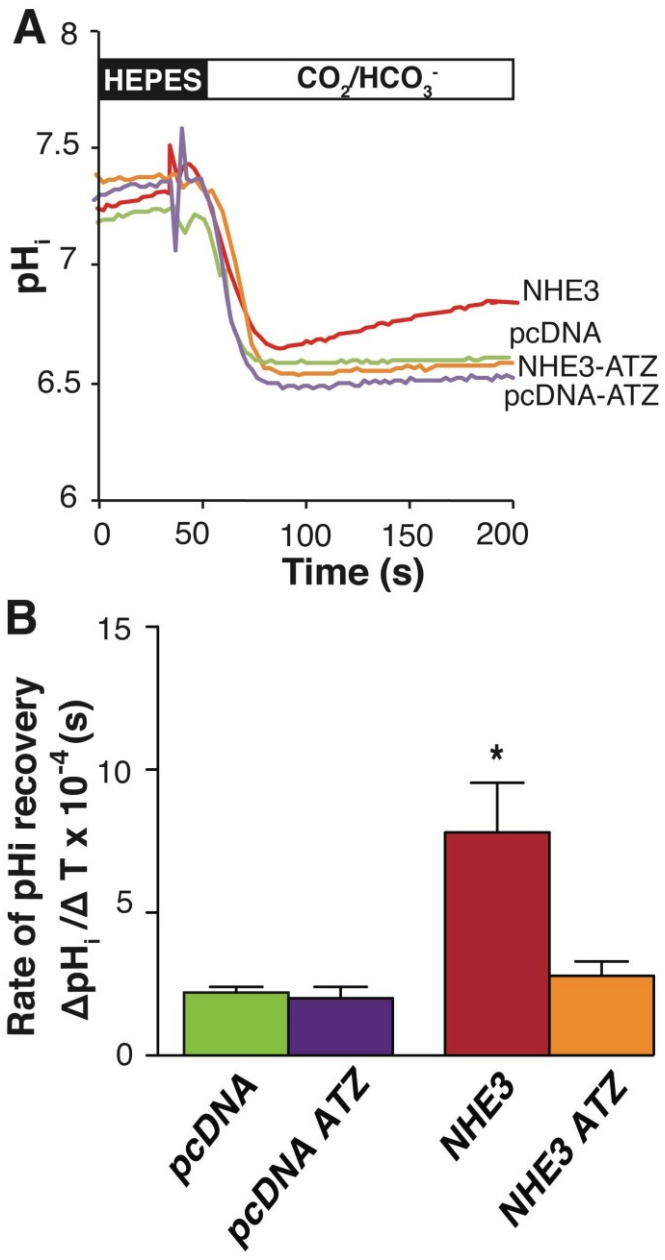

Figure: 2.2. The carbonic anhydrase inhibitor acetazolamide (ATZ) inhibits NHE3. A: representative traces of the initial change in pHi after intracellular acidification induced by switching from a HEPES-buffered solution to one containing HCO_3^- and bubbled with 5% CO_2; the timing of the switch is indicated by the change from a black bar to a white bar over the trace. Traces are from OK cells stably expressing either $NHE3_{38HA3}$ or pcDNA in the presence and absence of 100 µM ATZ. B: quantification of initial NHE3 activity (over the first 30 s) for each condition displayed in A. *P < 0.01; n= > 6/condition.

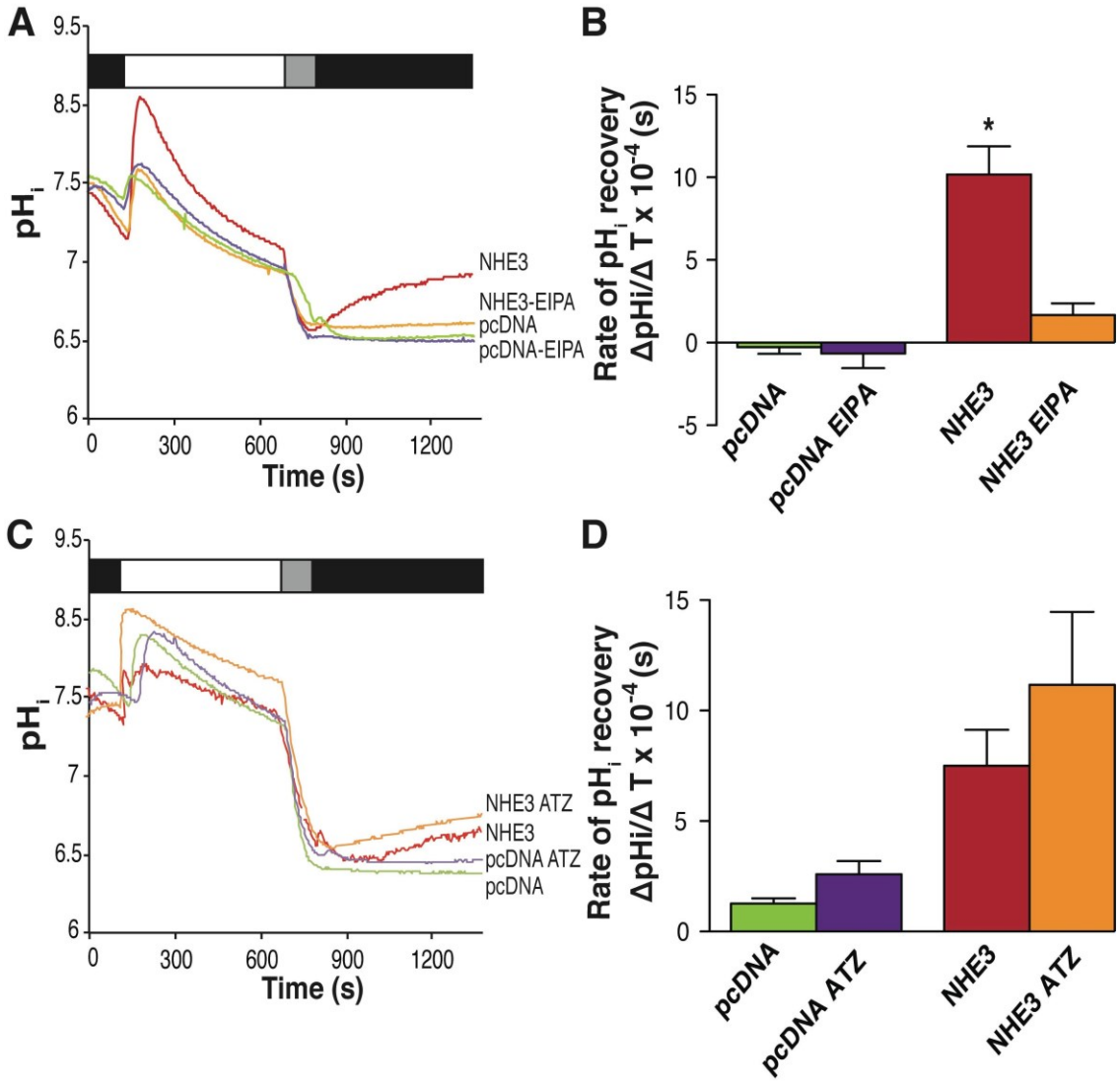

Figure 2.3. ATZ does not inhibit NHE3 activity in the absence of CO_2. NHE3 activity was assessed in the absence of CO_2 and HCO_3^- by prepulsing the cells with NH_4Cl. A: representative traces of the change in pHi of OK cells expressing either $NHE3_{38HA3}$ or pcDNA (negative control) in the presence and absence of 100 µM EIPA. Above the traces is a bar representing the different perfusing solutions: black, Na^+ containing; white, NH_4Cl prepulse; grey, no Na^+ containing buffer. B: quantification of initial NHE3 activity (over the first 30s) for each condition displayed in A. *P < 0.01. C: representative traces of the change in pHi of cells stably expressing either $NHE3_{38HA3}$ or pcDNA (-ve control) in the presence and absence of 100 µM ATZ. The bar above the traces is as described for A. D: quantification of initial NHE3 activity (over the first 100 s) for each condition displayed in C; n = > 6/condition.

2.3.2. Acetazolamide does not inhibit NHE3 activity in the absence of CO_2

To ascertain whether the effect of acetazolamide on NHE3 activity was via inhibition of CAII per se and not by blocking NHE3 directly, we repeated the assay in the absence of bicarbonate and CO_2, in cells acidified by an ammonium chloride prepulse. Under these conditions, cells stably expressing NHE3 also demonstrated significant recovery from an acid load, which was Na^+ dependent and inhibited by 100 μM EIPA (Fig. 2-3, A and B). However, under these conditions, acetazolamide had no effect on the rate of recovery from an acid load in NHE3 expressing cells (Fig. 2-3, C and D). These results are consistent with CAII increasing NHE3 activity and not with acetazolamide directly inhibiting NHE3. CAII association and activity are necessary to enhance NHE3 activity. To confirm that CAII activity is required to augment NHE3 mediated transport, we overexpressed $NHE3_{38HA3}$ with either wild-type CAII or the catalytically inactive CAII mutant (CAII-V143Y) (33) and then repeated the functional assay in the presence of bicarbonate and CO_2. The rate of pHi recovery was significantly higher in cells expressing NHE3 than in those expressing CAII alone (Fig. 2-4, A and B). NHE3 activity was further increased by coexpression with wild-type CAII. However, this increase in activity was not observed when the catalytically inactive CAII-V143Y was coexpressed with NHE3 (Fig. 2-4, A and B). These studies revealed an increase of NHE3 activity induced by CAII but not catalytically inactive CAII (Fig. 2-4, A and B). To assess whether CAII activity was sufficient to enhance NHE3 activity, we overexpressed NHE3 with a CAII mutant that fails to bind other transporters due to elimination of an N-terminal polybasic sequence,

CAII-HEX (7, 37), and repeated the functional studies in the presence of bicarbonate and CO_2. Coexpression with CAII-HEX did not increase NHE3 activity beyond coexpression with the empty vector alone (Fig. 4, A and B). Importantly, when we immunoblotted the remaining cells for NHE3 or CAII we did not observe a significant difference in expression of either protein (Fig. 4,C and D). Taken together, these results demonstrate that CAII activity and physical interaction are required to increase NHE3 activity.

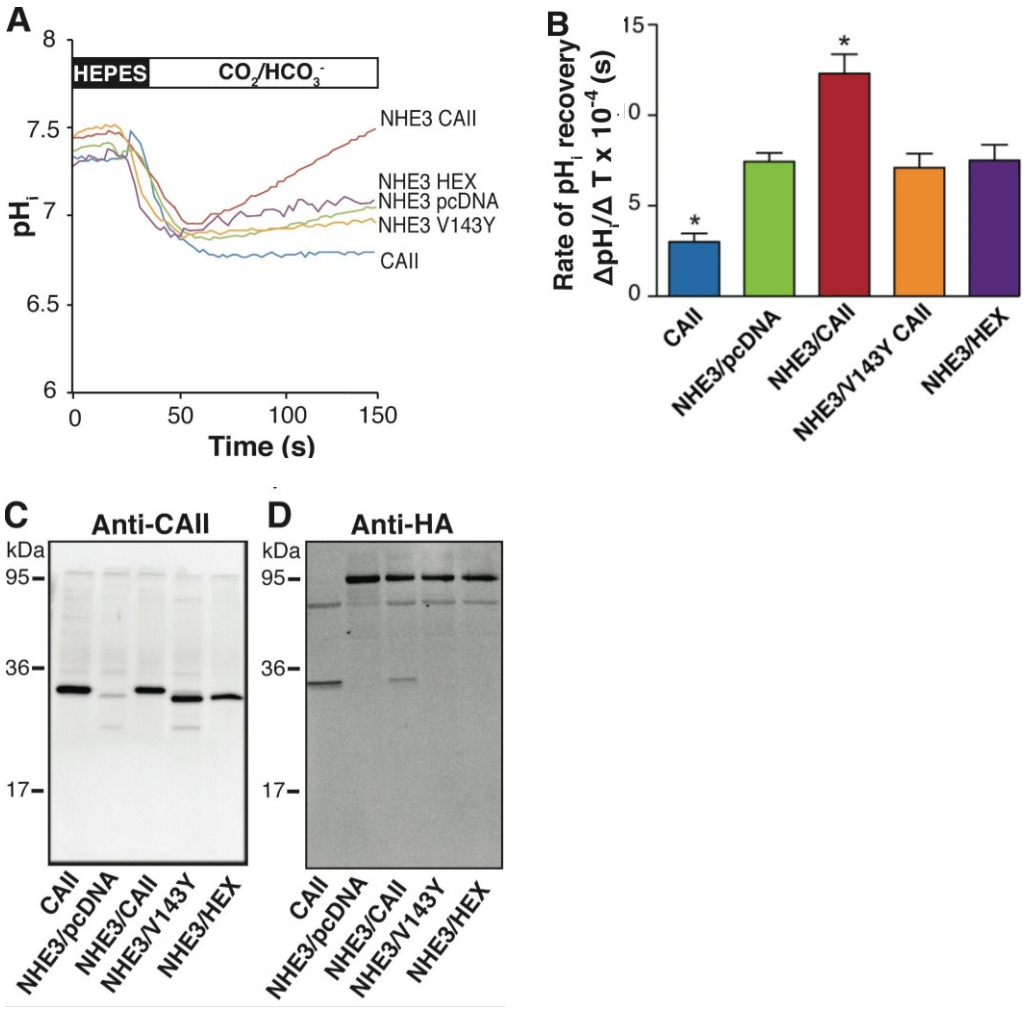

Figure 2.4. CAII activity and binding are required to enhance NHE3 activity. A: representative images of the change in pHi of OK cells transfected with either NHE3 and CAII, NHE3 and CAII-V143Y (functionally inactive mutant), CAII alone, NHE3 and CAII-HEX (functionally active but can't bind transporters), or pcDNA and NHE3 after acidification induced by switching from a HEPES-buffered solution to one containing HCO_3^- and bubbled with 5% CO_2. The change in perfusion buffers is represented by a change from a black to a white bar above the traces. B: quantification of initial NHE3 activity (over the first 30 s) for each condition displayed in A. *P < 0.001 relative to NHE3- and pcDNA-transfected cells. C and D: immunoblots of cell lysate from experiments in A and B to determine CAII (C) or HA (NHE3) expression (D).

2.3.3. NHE3 and CAII associate closely

NHE3 and CAII are both expressed in the brush-border membrane of the proximal tubule (9, 36); however, given the resolution of the light microscope, these two proteins could still be 250 nm away from one another. To assess a closer physical interaction, we cotransfected myc-tagged CAII and either NHE3, hCNT3, or AE1 and then performed a PLA (30). hCNT3 is a plasma membrane nucleoside transport protein, not known to interact with CAII, while a CAII-AE1 coassociation has been reported previously, including by PLA (36, 38). We observed a PLA signal when AE1 and CAII were coexpressed, indicating the ability of the PLA to detect a protein-protein interaction. The absence of a PLA signal in CAII and hCNT3 coexpressing cells illustrates the specificity of the PLA technique (Fig.2-5, A and B). The coexpression of NHE3 and CAII also generated a significant PLA signal consistent with a close association of the two proteins (Fig. 2-5C). Importantly, we were able to detect all transfected proteins on immunoblots, indicating that the lack of a PLA signal in CAII and hCNT3 coexpressing cells did not arise from the absence of protein expression (Fig. 2-5D).

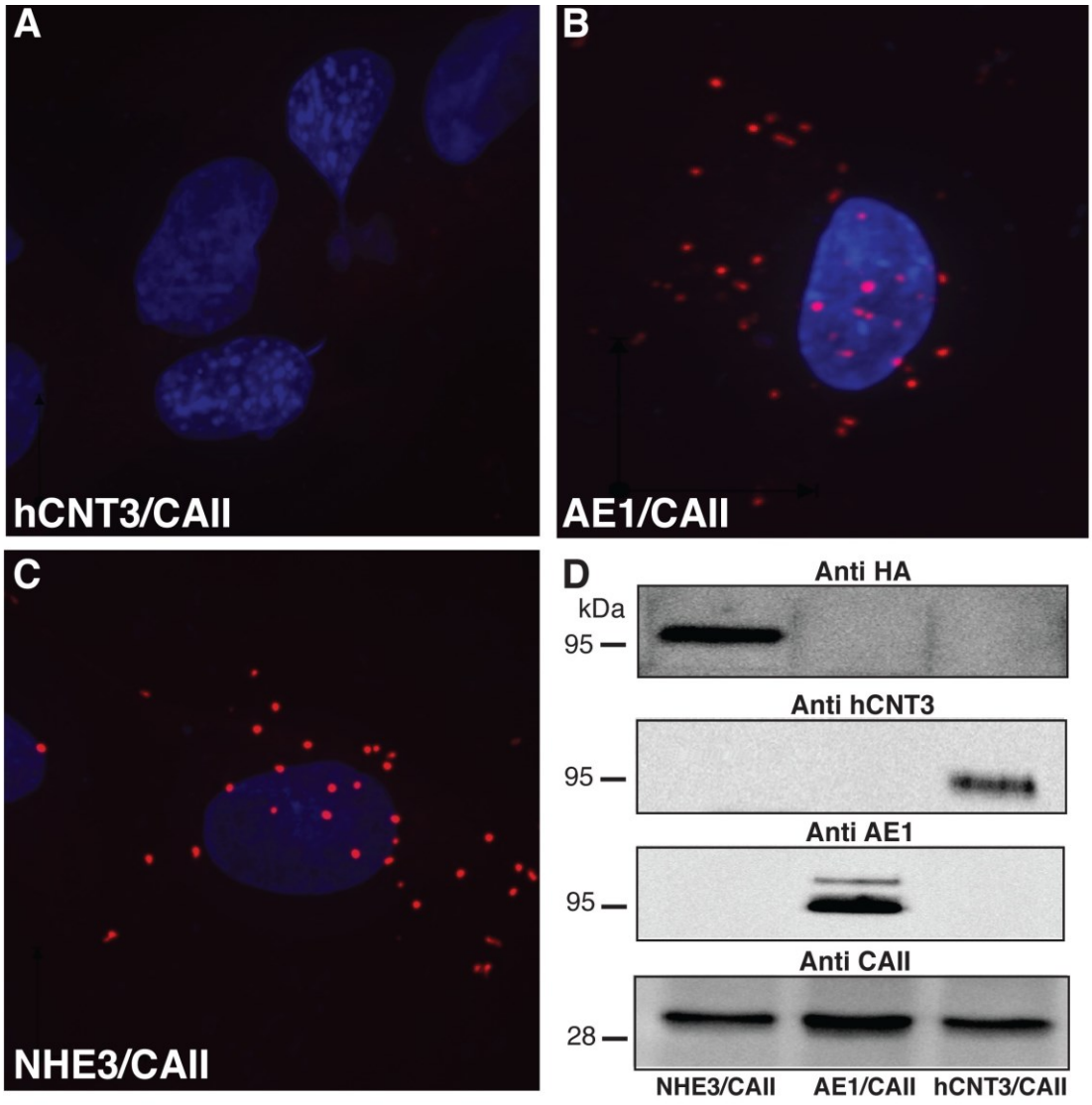

Figure 2.5. CAII associates closely with NHE3. Representative images are shown from a proximity ligation assay performed on OK cells transfected with CAII and either hCNT3 (negative control; A), AE1 (positive control; B), or NHE3 (C). Note: in all representative images (A–C), the nuclei were stained with DAPI (blue). D: immunoblots probed for hCNT3, AE1, HA (for NHE3), and CAII on lysate from cells expressing NHE3 and CAII, AE1 and CAII, or hCNT3 and CAII.

2.3.4. CAII binds the C-terminus of NHE3

To determine whether NHE3 and CAII physically associate, we coexpressed $NHE3_{38HA3}$ and CAII-myc in OK cells. We then immunoprecipitated NHE3 with an anti-HA antibody and immunoblotted with anti-myc. We used total protein cell lysate as a positive control and immunoprecipitated with rabbit serum as a negative control. CAII was immunoprecipitated by NHE3, but not rabbit serum (Fig. 2-6A). To examine whether there is a direct physical interaction between the cytosolic carboxyl terminus of NHE3 and CAII, we expressed amino acids 630–730 (NHE3-Tail-1) or 730–831 (NHE3-Tail-2) of rat NHE3 as GST fusion proteins (Fig. 2-6B). NHE3-Tail-1 contains the putative CAII binding site (^{710}IKEKDLELSDTEE^{722}). We then performed a microtiter plate-binding assay with these two constructs (16). Recombinant human CAII was fixed to the plate and then overlaid with different concentrations of the GST-fusion protein (50–400 nM). The degree of binding was then assessed by applying an anti-GST antibody followed by a HRP secondary and measuring the development of a colorimetric reaction. The assay was also performed with GST alone, and the results were subtracted from both Tail constructs. We observed significantly greater binding of NHE3-Tail-1 to CAII than NHE3-Tail-2 (Fig. 2-6C). These data infer a direct interaction between the cytosolic terminus of NHE3 and CAII. Finally, we tested the effects of varying pH and ionic strength on the interaction between CAII and NHE3, using the microtiter plate assay. Binding of GST alone was measured and subtracted from all values. Maximal binding between NHE3-Tail-1 and CAII occurred at 100 mM NaCl; this was set to 100% (Fig. 2-7A). Increasing ionic

strength past this decreased the interaction, and above 400 mM NaCl completely eliminated the interaction (Fig. 2-7A). We found that the NHE3/CAII interaction was strongly pH dependent. There was increased interaction at an alkaline pH (8.0), and the interaction was prevented at an acidic pH, i.e., 6.0 (Fig. 2-7B). Half-maximal binding was observed at pH 7.2. Therefore, the interaction between NHE3 and CAII is dependent on both ionic strength and pH, consistent with an electrostatic interaction.

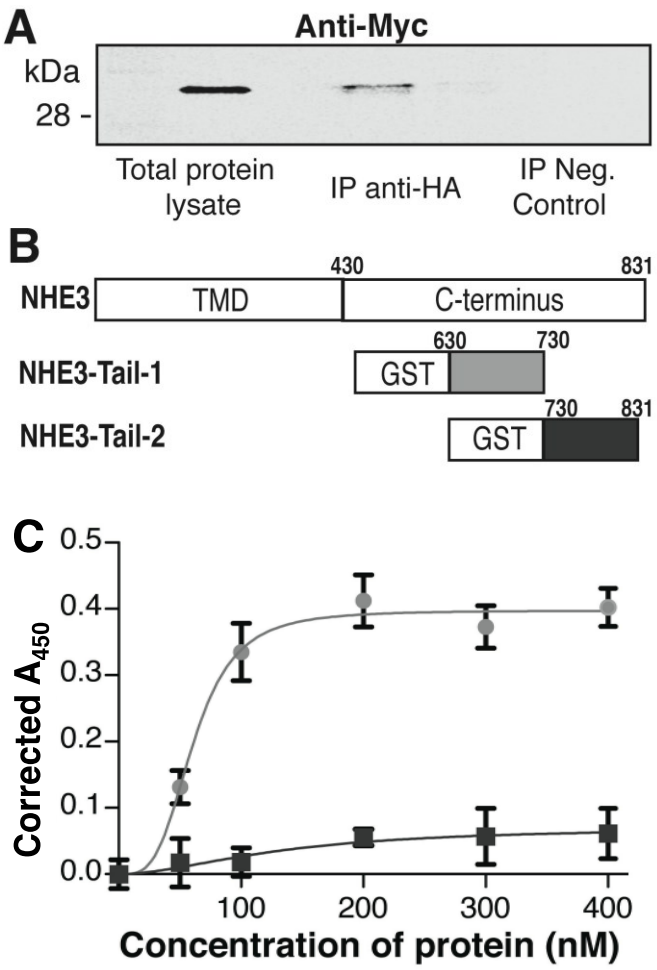

Figure 2.6. CAII binds the C terminus of NHE3. A: NHE3-CAII coimmunoprecipitation (IP). OK cells cotransfected with $NHE3_{38HA3}$ and CAII-myc were lysed and immunoprecipitated with either anti-HA (to pull down NHE3) or in the presence of rabbit IgG (negative control) and then immunoblotted for anti-myc (CAII). A sample of total protein lysate was included. Note: a blank lane was left between samples on the gel. B: schematic representation of the glutathione-S-transferase (GST)-fusion constructs generated from the cytosolic carboxy terminus of NHE3. Note: NHE3-Tail-1 contains a potential CAII binding site homologous to NHE1 (^{710}IKEKDLELSDTEE^{722}). C: CAII was fixed to a 96- well plate, which was subsequently overlaid with the concentration of the GST-fusion protein listed on the X-axis. After washing, the samples were incubated with an anti-GST antibody and then the appropriate secondary antibody. The net relative amount of GST-fusion protein binding was assessed by a colorimetric reaction measured at A_{450}, which is subtracted from the background obtained with only GST protein. The round symbols represent NHE3 tail 1 and square symbols NHE3 tail 2.

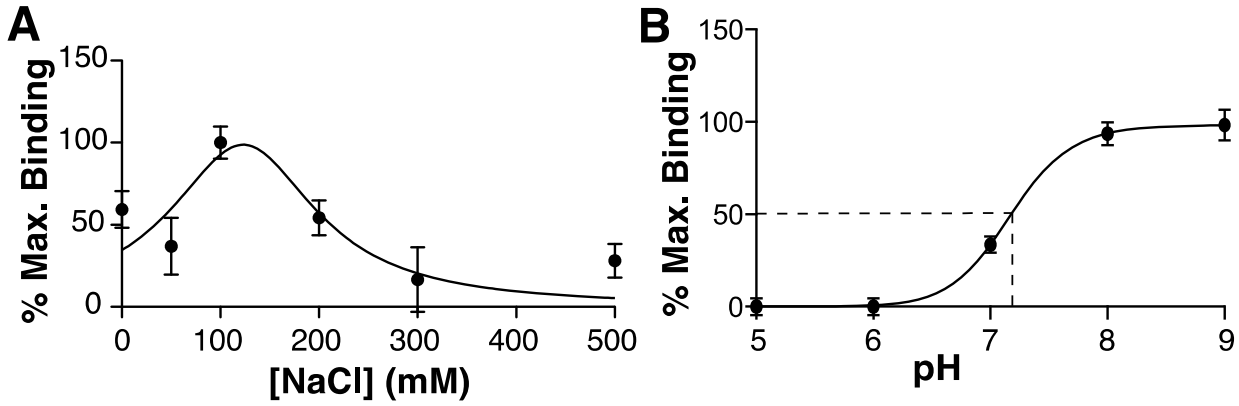

Figure 2.7. CAII binding to the C terminus of NHE3 is NaCl concentration and pH sensitive. A: a microtitre plate binding assay was used to probe the nature of the physical interaction between NHE3 and CAII as per Fig. 2.6. However, the antibody buffer used to apply the fusion proteins contained varying concentrations of NaCl, from 100–500 mM or a range of pH (5–9). Note: results are corrected for the background obtained with only GST protein as above.

2.4. Discussion

NHE3 has an important role in renal function by reabsorbing Na^+, HCO_3^-, and H_2O from the proximal tubule (28). We provide several lines of evidence that NHE3 and CAII physically interact. A PLA confirmed a close association of the two proteins when expressed in a proximal tubular epithelial cell culture model. Co-IP confirmed a physical association between NHE3 and CAII and microtiter plate assays identified a region in the cytosolic terminus of NHE3 required for CAII binding. We also provide evidence that NHE3 and CAII functionally interact. Coexpression of NHE3 with CAII increased NHE3 activity, which depended on CAII catalysis, since augmented NHE3 activity was only prevented by acetazolamide in the presence of CAII substrate. Moreover, coexpression of NHE3 and a catalytically dead CAII did not increase NHE3 activity. Finally, a NHE3-CAII physical interaction is required to increase NHE3 activity, as a CAII construct lacking the putative transporter-binding motif failed to increase NHE3 activity. Together, these data support a physical and functional interaction between CAII and NHE3 in the proximal tubule. We examined the interaction between NHE3 and CAII in a proximal tubule model, as this is a site of prodigious sodium and water reabsorption facilitated in large part by NHE3 activity (28). NHE3-CAII cooperation likely helps to maximize NHE3 function, permitting this process. NHE3 is also expressed throughout the intestine, where it plays a similar role in sodium and water reabsorption (15, 28). CAII is also expressed throughout the small and large bowel (18, 21, 29). We thus speculate that a physical and functional interaction between NHE3 and CAII in the mucosal membrane of the

intestine may also serve to increase sodium and water absorption there.

CAII forms a transport metabolon with AE1, enhancing its activity (33). A metabolon is a complex of enzymes from one metabolic pathway coupled together so as to facilitate substrate movement from one active site to the next (31). Transport metabolons are a functional coupling of an enzyme to a transporter that increases flux through the transporter. The AE1 transport metabolon appears to require a direct physical interaction between the enzyme and the transporter (33), although there are also data suggesting a direct physical interaction is not required (1, 22). NHE1 and CAII also physically and functionally interact (16). Using similar experimental approaches, we found that both the putative transporter binding site in CAII and CAII catalysis are necessary to increase NHE3 activity. The interaction between NHE3 and CAII is different from the interaction between CAII and the monocarboxylate transporters, as CAII activity is required for increased NHE3 activity (7, 8). Our observations therefore support a mechanism whereby association of CAII with NHE3 increases transporter activity. We found that the region between amino acids 630 and 730 in the cytosolic carboxy terminus of NHE3 binds CAII. We found this interaction to be pH sensitive. Consistent with a role for amino-terminal CAII histidine residues in mediating the interaction with NHE3, the interaction was titrated with a pKa of 7.2, and enhanced at alkaline pH. This pKa is nearly identical to the pKa established for the AE1-CAII interaction, which is mediated through amino-terminal histidines in CAII, as mutation of histidine residues in the CAII N-terminal region prevents binding to AE1 (37, 38). Increasing ionic strength inhibited the NHE3-CAII interaction, suggesting that it is

potentially an ionic interaction. Although the interaction was also inhibited at lower ionic strength, perhaps due to another factor such as altered protein conformation, however, this is purely speculative. We observed maximal interaction between CAII and the cytosolic C-terminus of NHE3 at pH 8 and above. Although there was some binding at the lower pH of our functional assays, the effect of an NHE3-CAII interaction would nonetheless be attenuated in our studies, underestimating its effect. Previous studies of sodium/proton exchangers found maximal transport activity when the cytosol was acidic. This makes intuitive sense for housekeeping transporters such as NHE1, as the role of this exchanger is to rid the cytosol of protons generated by metabolism. In this case, reduced activity at a physiological pH would prevent alkalinization of the cell. However, NHE3 does not appear to play a housekeeping role such as this; instead, it is implicit to the reabsorption of sodium from intestinal and renal epithelia and therefore plays a central role in volume regulation (28). Consequently, there may be a need to maintain NHE3 activity at physiological pH or even an alkaline pH. Perhaps the binding of CAII to the cytosolic terminus of NHE3 mediates this? NHE3 is activated by an acidic pH. However, functional studies have been performed predominantly in the absence of HCO_3^- and CO_2. Hence the activating effect of CAII on NHE3 activity would not have been recognized.

In summary, we show Co-IP of NHE3 with CAII, close association in renal epithelial cells, and direct interaction by GST-binding studies. This physical interaction between NHE3 and CAII contributes to increased NHE3 activity. However, a physical interaction is insufficient to increase NHE3 activity, as CAII

catalysis is also required. Thus NHE3 and CAII both physically and functionally interact, an association likely facilitating the vast amount of salt and water reabsorption from the proximal tubule and intestine.

References

1. **Al-Samir S, Papadopoulos S, Scheibe RJ, Meissner JD, Cartron JP, Sly WS, Alper SL, Gros G, Endeward V.** Activity and distribution of intracellular carbonic anhydrase II and their effects on the transport activity of anion exchanger AE1/SLC4A1. *J Physiol* 591: 4963–4982, 2013.

2. **Alexander RT, Furuya W, Szászi K, Orlowski J, Grinstein S.** Rho GTPases dictate the mobility of the Na^+/H^+ exchanger NHE3 in epithelia: role in apical retention and targeting. *Proc Natl Acad Sci* USA 102: 12253–12258, 2005.

3. **Alexander RT, Malevanets A, Durkan AM, Kocinsky HS, AronsonPS, Orlowski J, Grinstein S.** Membrane curvature alters the activation kinetics of the epithelial Na^+/H^+ exchanger, NHE3. *J Biol Chem* 282:7376–7384, 2007.

4. **Almomani EY, King JC, Netsawang J, Yenchitsomanus PT, Malasit P, Limjindaporn T, Alexander RT, Cordat E.** Adaptor protein 1complexes regulate intracellular trafficking of the kidney anion exchanger1 in epithelial cells. *Am J Physiol Cell Physiol* 303: C554–C566, 2012.

5. **Alvarez BV, Vithana EN, Yang Z, Koh AH, Yeung K, Yong V, Shandro HJ, Chen Y, Kolatkar P, Palasingam P, Zhang K, Aung T, Casey JR.** Identification and characterization of a novel mutation in the carbonic anhydrase IV gene that causes retinitis pigmentosa. *Invest OphthalmolVis Sci* 48: 3459–3468, 2007.

6. **Becker HM, Deitmer JW.** Carbonic anhydrase II increases the activity of the human electrogenic Na^+/cotransporter. *J Biol Chem* 282: 13508–13521, 2007.

7. **Becker HM, Deitmer JW.** Nonenzymatic proton handling by carbonic anhydrase II during H^+-lactate cotransport via monocarboxylate transporter1. *J*

Biol Chem 283: 21655–21667, 2008.

8. **Becker HM, Klier M, Schuler C, McKenna R, Deitmer JW.** Intramolecular proton shuttle supports not only catalytic but also noncatalytic function of carbonic anhydrase II. *Proc Natl Acad Sci USA* 108: 3071–3076, 2011.

9. **Biemesderfer D, Rutherford PA, Nagy T, Pizzonia JH, Abu-Alfa AK, Aronson PS.** Monoclonal antibodies for high-resolution localization of NHE3 in adult and neonatal rat kidney. *Am J Physiol Renal Physiol* 273:F289–F299, 1997.

10. **Bobulescu IA, Dubree M, Zhang J, McLeroy P, Moe OW.** Effect of renal lipid accumulation on proximal tubule Na^+/H^+ exchange and ammonium secretion. *Am J Physiol Renal Physiol* 294: F1315–F1322,2008.

11. **Bondy C, Chin E, Smith BL, Preston GM, Agre P.** Developmental gene expression and tissue distribution of the CHIP28 water-channel protein. *Proc Natl Acad Sci USA* 90: 4500–4504, 1993.

12. **Dirks JH, Cirksena WJ, Berliner RW.** Micropuncture study of the effect of various diuretics on sodium reabsorption by the proximal tubules of the dog. *J Clin Invest* 45: 1875–1885, 1966.

13. **Donowitz M, Ming Tse C, Fuster D.** SLC9/NHE gene family, a plasmamembrane and organellar family of Na^+/H^+ exchangers. *Mol Aspects Med* 34: 236–251, 2013.

14. **Fuster DG, Alexander RT.** Traditional and emerging roles for the SLC9 Na^+/H^+ exchangers. *Pflügers Arch* 466: 61–76, 2014.

15. **Gawenis LR, Stien X, Shull GE, Schultheis PJ, Woo AL, Walker NM, Clarke LL.** Intestinal NaCl transport in NHE2 and NHE3 knockout mice. *Am J*

Physiol Gastrointest Liver Physiol 282: G776–G784, 2002.

16. **Li X, Alvarez B, Casey JR, Reithmeier RAF, Fliegel L.** Carbonic anhydrase II binds to and enhances activity of the Na^+/H^+ exchanger. *JBiol Chem* 277: 36085–36091, 2002.

17. **Li X, Liu Y, Alvarez BV, Casey JR, Fliegel L.** A novel carbonic anhydrase II binding site regulates NHE1 activity. *Biochemistry* 45: 2414–2424, 2006.

18. **Okamoto K, Hanazaki K, Akimori T, Okabayashi T, Okada T, Kobayashi M, Ogata T.** Immunohistochemical and electron microscopic characterization of brush cells of the rat cecum. *Med Mol Morphol* 41: 145–150, 2008.

19. **Orlowski J, Kandasamy RA, Shull GE.** Molecular cloning of putative members of the Na/H exchanger gene family. cDNA cloning, deduced amino acid sequence, and mRNA tissue expression of the rat Na/H exchanger NHE-1 and two structurally related proteins. *J Biol Chem* 267:9331–9339, 1992.

20. **Pan W, Borovac J, Spicer Z, Hoenderop JG, Bindels RJ, Shull GE, Doschak MR, Cordat E, Alexander RT.** The epithelial sodium/proton exchanger, NHE3, is necessary for renal and intestinal calcium (re)absorption. *Am J Physiol Renal Physiol* 302: F943–F956, 2012.

21. **Parkkila S.** Distribution of the carbonic anhydrase isoenzyme I, II, and VI in the human alimentary tract. *Gut* 35: 646–650, 1994.

22. **Piermarini PM, Kim EY, Boron WF.** Evidence against a direct interaction between intracellular carbonic anhydrase II and pure C-terminal domains of SLC4 bicarbonate transporters. *J Biol Chem* 282: 1409–1421,2007.

23. **Prasad GV, Coury LA, Finn F, Zeidel ML.** Reconstituted aquaporin 1 water

channels transport CO_2 across membranes. *J Biol Chem* 273:33123–33126, 1998.

24. **Pushkin A, Abuladze N, Gross E, Newman D, Tatishchev S, Lee I, Fedotoff O, Bondar G, Azimov R, Ngyuen M, Kurtz I.** Molecular mechanism of kNBC1, carbonic anhydrase II interaction in proximal tubule cells. *J Physiol* 559: 55–65, 2004.

25. **Rievaj J, Pan W, Cordat E, Alexander RT.** The Na^+/H^+ exchanger isoform 3 is required for active paracellular and transcellular Ca^{2+} transport across murine cecum. *Am J Physiol Gastrointest Liver Physiol* 305: G303–G313, 2013.

26. **Rubio CR, de Mello GB, Mangili OC, Malnic G.** H^+ ion secretion in proximal tubule of low-CO_2/HCO_3^- perfused isolated rat kidney. *PflügersArch* 393: 63–70, 1982.

27. **Schnermann J, Chou CL, Ma T, Traynor T, Knepper MA, Verkman AS.** Defective proximal tubular fluid reabsorption in transgenic aquaporin-1 null mice. *Proc Natl Acad Sci* USA 95: 9660–9664, 1998.

28. **Schultheis PJ, Clarke LL, Meneton P, Miller ML, Soleimani M, Gawenis LR, Riddle TM, Duffy JJ, Doetschman T, Wang T, Giebisch G, Aronson PS, Lorenz JN, Shull GE.** Renal and intestinal absorptive defects in mice lacking the NHE3 Na^+/H^+ exchanger. *Nat Genet* 19:282–285, 1998.

29. **Sjöblom M, Singh AK, Zheng W, Wang J, Tuo Bg Krabbenhöft A, Riederer B, Gros G, Seidler U.** Duodenal acidity sensing, but not epithelial HCO_3^-, supply is critically dependent on carbonic anhydrase II expression. *Proc Natl Acad Sci* USA 106: 13094–13099, 2009.

30. **Soderberg O, Gullberg M, Jarvius M, Ridderstrale K, Leuchowius KJ,**

Jarvius J, Wester K, Hydbring P, Bahram F, Larsson LG, Landegren U. Direct observation of individual endogenous protein complexes in situ by proximity ligation. *Nat Methods* 3: 995–1000, 2006.

31. **Srere PA, Sumegi B, Sherry AD.** Organizational aspects of the citric acid cycle. *Biochem Soc Symp* 54: 173–178, 1987.

32. **Sterling D, Alvarez BV, Casey JR.** The extracellular component of a transport metabolon: extracellular loop 4 of the human AE1 Cl^-/HCO_3^-exchanger binds carbonic anhydrase IV. *J Biol Chem* 277: 25239–25246,2002.

33. **Sterling D, Reithmeier RAF, Casey JR.** A transport metabolon: functional interaction of carbonic anhydrase II and chloride/bicarbonate exchangers. *J Biol Chem* 276: 47886–47894, 2001.

34. **Thomas JA, Buchsbaum RN, Zimniak A, Racker E.** Intracellular pH measurements in Ehrlich ascites tumor cells utilizing spectroscopic probes generated in situ. *Biochemistry* 18: 2210–2218, 1979.

35. **Tse CM, Levine SA, Yun CH, Brant SR, Pouyssegur J, Montrose MH, Donowitz M.** Functional characteristics of a cloned epithelial Na^+/H^+exchanger (NHE3): resistance to amiloride and inhibition by protein kinase C. *Proc Natl Acad Sci* USA 90: 9110–9114, 1993.

36. **Vilas G, Krishnan D, Loganathan SK, Malhotra D, Liu L, Beggs MR, Gena P, Calamita G, Jung M, Zimmermann R, Tamma G, Casey JR, Alexander RT.** Increased water flux induced by an aquaporin-1/carbonic anhydrase II interaction. *Mol Biol Cell* 26: 1106–1118, 2015.

37. **Vince JW, Carlsson U, Reithmeier RAF.** Localization of the Cl^-/HCO_3^-anion

exchanger binding site to the amino-terminal region of carbonic anhydrase II. *Biochemistry* 39: 13344–13349, 2000.

38. **Vince JW, Reithmeier RA.** Carbonic anhydrase II binds to the carboxyl terminus of human band 3, the erythrocyte Cl^-/HCO_3^- exchanger. *J BiolChem* 273: 28430–28437, 1998.

39. **Vince JW, Reithmeier RAF.** Identification of the carbonic anhydrase II binding site in the Cl^-/HCO_3^- anion exchanger AE1. *Biochemistry* 39:5527–5533, 2000.

40. **Waheed A, Zhu XL, Sly WS, Wetzel P, Gros G.** Rat skeletal muscle membrane associated carbonic anhydrase is 39-kDa, glycosylated, GPI-anchored CA IV. *Arch Biochem Biophys* 294: 550 –556, 1992.

41. **Zhang J, Tackaberry T, Ritzel MW, Raborn T, Barron G, Baldwin SA, Young JD, Cass CE.** Cysteine-accessibility analysis of transmembrane domains 11–13 of human concentrative nucleoside transporter 3. *Biochem J* 394: 389–398, 2006.

CHAPTER 3

Increased Water Flux Induced by an Aquaporin-1/Carbonic Anhydrase II interaction

Parts of this chapter have been published in: Vilas G*, Krishnan D*, Loganathan SK*, Malhotra D, Liu L, Beggs MR, Gena P, Calamita G, Jung M, Zimmermann R, Tamma G, Casey JR, Alexander RT.
Mol Biol Cell. 2015 Mar 15;26(6):1106-18. doi: 10.1091/mbc.E14-03-0812.
Epub 2015 Jan 21

- Represents equal contribution to the work

I completed all the experiments in **Figures** 3-2, 3-3, 3-4, 3-13, 3-14,3-15, 3-16, 3-17, **Table** 3-I, 3- II, 3-III.

The experiments in **Figures** 3-5, 3-6, 3-7, 3-8, 3-9, 3-10, 3-11, 3-12 were completed by Loganathan SK .

3.1. Introduction

Intravascular volume is maintained by a complex interplay between organ systems with a central role of renal sodium and water handling. The glomerulus filters a large quantity of water daily, the majority is reabsorbed by the proximal tubule. Indeed the rate of water absorption from the proximal tubule is significantly higher than water can flow across a lipid bilayer (40). This observation led C. van Os to predict the presence of a water "channel" in proximal tubular membranes (40). Consistent with this hypothesis was the Nobel Prize winning work of Peter Agre, who identified aquaporin-1 (AQP1) from red blood cells (31, 32). Subsequently this protein was identified in the proximal tubule and thin descending limb of the loop of Henle, where it mediates water reabsorption (9, 35, 36, 46). Transepithelial sodium movement across the proximal tubule creates a concentration gradient that drives water reabsorption back into the blood (24). Sodium moves across the apical plasma membrane of the proximal tubular cell in exchange for the efflux of a proton, a process mediated by the sodium proton exchanger isoform 3 (NHE3). The catalysis of water and CO_2 into a H^+ and HCO_3^-, via cytosolic carbonic anhydrase II (CAII), participates in the reabsorption of water and sodium by providing a H^+ for the exchange reaction. Water, a substrate of CAII, enters the proximal tubular cell via AQP1. CO_2, the other substrate of CAII, also likely permeates AQP1 tetramers, although this idea is disputed (11, 12, 16, 27, 28). Clearly AQP1 is necessary for the large amount of water reabsorbed from the proximal tubule, however the afore mentioned facts provide rationale for

CAII involvement in this process as well. Consistent with this, carbonic anhydrase inhibitors are diuretics.

CAII interacts with membrane transport proteins including the chloride/bicarbonate exchanger AE1 (42, 43), the sodium/hydrogen exchanger NHE1 (20, 21), the sodium bicarbonate cotransporter 1, NBC1 (3, 4, 23, 33), and the monocarboxylate transporters MCT1 (5) and MCT4 (3). Close association with CAII enhances the rate of transport by a number of mechanisms, including the removal of product and/or the provision of substrate. Given that AQP1 moves water and potentially CO_2 across a membrane, both substrates of CAII, we postulated that CAII and AQP1 might physically and functionally interact.

The cytosolic carboxy terminus of human AQP1 contains a LDADD motif, the exact sequence binding CAII in AE1 (43). AQP1 and CAII colocalize in the apical membrane of the proximal tubule, consistent with their association. Co-expression of AQP1 and CAII increased plasma membrane water permeability in mammalian cells, an effect that required the interacting regions of both CAII and AQP1. Corroborating a specific interaction between AQP1 and CAII, co-expression of CAII with aquaporin-2 (AQP2), the isoform mediating ADH-induced water reabsorption from the renal distal tubule, did not increase membrane water permeability. A proximity ligation assay confirmed that CAII and AQP1 are in close juxtaposition. A mutagenesis program, employing N-ethyl-nitrourea, generated CAII-deficient mice (19). Red blood cell ghosts had increased water permeability when supplemented with CAII but not with albumin. Further, renal cortical membranes isolated from CAII-deficient mice demonstrate decreased

water flux compared with wild-type membranes. Metabolic cage studies performed on these animals found them to be polyuric, polydipsic and to produce dilute urine, despite increased renal AQP1 expression. Renal cortical membranes isolated from CAII-deficient mice demonstrate decreased water flux compared to wild-type membranes. Altogether, these data support a CAII-AQP1 physical interaction that increases water flux through AQP1.

3.2. Materials and methods

DMEM, fetal bovine serum, calf serum, and penicillin-streptomycin-glutamine (PSG) were from Invitrogen (Carlsbad, CA). Cell culture dishes were from Corning (Corning, NY). Complete Protease Inhibitor was from Roche Applied Science (Indianapolis, IN). The BCA Protein Assay Kit and Immobilized Streptavidin Resin were from Pierce (Rockford, IL). Monoclonal antibodies against HA (clone 16B12) were from Covance (Princeton, NJ). Antibodies against AQP1, CAII, and the Na^+/K^+-ATPase were from Santa Cruz Biotechnology (Santa Cruz, CA). The IVF12 monoclonal anti-AE1 antibody was a kind gift from Michael Jennings (University of Arkansas, Little Rock, AR), and the anti-hCNT3 antibody was a kind gift of James Young (University of Alberta, Edmonton, Canada; (45)). Secondary coupled Alexa Fluor 488 and DyLight 549 antibodies were from Jackson ImmunoResearch Laboratories (West Grove, PA). The fluorescein-conjugated *L. tetragonolobus* lectin was from Vector Laboratories (Burlingame, CA). Horseradish peroxidase (HRP)–conjugated donkey anti-mouse immunoglobulin G was from GE Healthcare Bio-Sciences (Piscataway, NJ). The Duolink proximity ligation assay kit was from Olink Bioscience (Uppsala, Sweden).

3.2.1. Animal studies

Wild-type FVB/N mice were purchased from Jackson Laboratories (Bar Harbor, ME). Generation and genotyping of wild-type and the CAII-deficient mice were performed as described previously (7). Mice were housed in virus-free conditions and maintained on a 12-h light/dark schedule. Standard pelleted chow

(PicoLab Rodent Diet 5053; 20% [wt/wt] protein, 4.5% [wt/wt] fat, 0.81% [wt/wt] calcium, 1.07% [wt/wt] potassium, 0.30% [wt/wt] sodium; and 2.2 IU/g vitamin D_3) and drinking water were available ad libitum. Both male and female animals between 8 and 14 wk of age were used. The animals were anesthetized with pentobarbital, and blood was withdrawn by perforating the orbital vessels. Kidneys were then removed and snap frozen in liquid nitrogen, and 3-μm sections were processed and stained as described previously (30). All experiments were performed in compliance with the animal ethics board at the University of Alberta, Health Sciences Section, protocol number 576.

3.2.2. Preparation of mammalian expression constructs.

An untagged version of human AQP1 was generated by PCR and cloned into the pcDNA 3.1(-) mammalian expression vector, using the primers 5′-CGGGATCCGACCATGGCCAGCGAGTTCAAGAAGA-3′ and 5′-CCC-TCGAGCTATTTGGGCTTCATCTCCAC-3′ containing the cloning restriction sites *Bam*HI and *Xho*I, respectively. Wild type, V143Y, and HEX CAII were amplified by PCR using the appropriate *X. laevis* pGEMHE expression vectors as template and cloned in pcDNA3.1 (-) mammalian expression vector. Amplification of wild-type and V143Y cDNA fragments was performed using the primers 5′-CGGAATTCGCCACCATGTCCCATCACTGGGGGTA-3′ and 5′-GGGG-TACCTTATTTGAAGGAAGCTTTGATTTGC-3′, containing the cloning restriction sites *Eco*RI and *Kpn*I, respectively. HEX-CAII was amplified using the forward 5′-CGGCTAGCGCCACCATGTCCCCTCAGTGGGGGTA-3′ and reverse 5′-GCTCTAGATTATTTGAAGGAAGCTTTGATTTGC-3′ primers

containing an *Nhe*I and an *Xba*I site, respectively. TS4 CAII, which demonstrates increased catalytic activity, was a kind gift of Robert McKenna (University of Florida, Gainesville, FL; (14)). This mutant was subcloned into pcDNA 3.1(-) by PCR using the forward primer 5′-CTAGCTAGCATGTCCCATCACTGG-3′, which contains an *Nhe*I site, and the reverse primer 5′-CTAGCTCGAGTTATTTGAAGGAAGCTTT-3′, which contains an *Xho*I site.

3.2.3. Preparation of ΔCABI and ΔCABII AQP1 mutants.

Two AQP1 mutants in which either the CAII binding motif I (CABI; amino acids E251, E252, Y253, and D254) or CAII binding motif II (CABII, D256, D258, and D259) mutagenized to alanine were generated using the PCR-based QuikChange Lightning Site-Directed Mutagenesis Kit (Stratagene, La Jolla, CA). The reactions were carried out on mammalian AQP1 expression vectors as template and following the manufacturer's protocol. Mutations were introduced in the AQP1 sequence using two different sets of self-complementary mutagenic primers: 5′-accagcggccaggtggcggcggctgccctggatgccgacgac-3′ (sense ΔCABI) and 5′-gtcgtcggcatccagggcagccgccgccacctggccgctggt-3′ (antisense ΔCABI) or 5′-ggagtatgacctggctgccgccgccatcaactccaggg-3′ (sense ΔCABII) and 5′-ccctggagttgatggcggcggcagccaggtcatactcc-3′ (antisense ΔCABII), respectively. After the amplification step, the original unaltered cDNA templates were digested with *Dpn*I restriction enzyme. The identity and fidelity of all the clones used were confirmed by sequencing.

3.2.4. Protein expression

Proteins were expressed by transient transfection of HEK293 cells using the calcium phosphate transfection method (34). Cells were grown and transfected in DMEM, supplemented with 5% (vol/vol) fetal bovine serum, 5% (vol/vol) calf serum, and 1× PSG and kept in an incubator at 37 °C and 5% CO_2 saturation. All experiments involving transfected cells were carried out 40–48 h post transfection.

3.2.5. Membrane water permeability measurements

HEK293 cells were grown on poly-L-lysine–coated 25-mm glass coverslips and cotransfected with eGFP and AQP1, wild-type or V143Y CAII, or pcDNA 3.1 (empty vector) in a 1:8 molar ratio (41). Coverslips were mounted in a 35-mm-diameter Attofluor Cell Chamber (Molecular Probes, Eugene, OR). During experiments, the chamber was perfused at 3.5 ml/min with isotonic bicarbonate-buffered MBSS solution (in mM: 68.3 NaCl, 5.4 KCl, 0.4 $MgCl_2$, 0.4 $MgSO_4$, 25 $NaHCO_3$, 2 $CaCl_2$, 5.5 glucose, 100 D-mannitol, 10 HEPES, pH 7.4, 300 mOsm/kg) and then with hypotonic (200 mOsm/kg) bicarbonate-buffered MBSS solution, pH 7.4 (same composition as previous, but lacking D-mannitol). Both buffers were continuously bubbled with 5% CO_2 (balance, air) and adjusted to pH 7.4 with NaOH. The chamber was placed on the stage of a Wave FX spinning disc confocal microscope with a Yokogawa CSU10 scanning head. The microscope has a motorized *XY* stage with piezo focus drive (MS-4000 XYZ Automated Stage; ASI, Eugene, OR). Acquisition was performed with a Hamamatsu C9100-13 digital camera (EMCCD) and a 20x objective (air immersion, numerical aperture 0.75) during excitation with the FiTC/GFP laser (491 nm). eGFP fluorescence data

were acquired at 1 point/s. Lasers were from Spectral Applied Research (Richmond Hill, Canada). Quantitative image analysis was performed with Volocity 4.2 software. The dilution in fluorescence within a specific region of interested was recorded and normalized to the original fluorescence in the region of interest within the defined optical section (F/F_0). The rate of dilution in fluorescence, a measure of water permeability, was then normalized, first to total cellular AQP1 (or AQP2; setting AQP1/AQP2 expression alone to 100%). Finally, the dilution in fluorescence was then divided by the fraction of AQP1/AQP2 at the membrane (as measured by cell surface biotinylation; Figure 3-8). To validate this assay, we performed it in the presence of increasing amounts of AQP1. This demonstrated a linear relationship between AQP1 expression and normalized dilution of expression (Figure 3-8).

3.2.6. Immunoblotting

Equal amounts of total protein were separated by SDS–PAGE and electrotransferred onto Immobilon-P polyvinylidene fluoride membranes (Millipore, Billerica, MA) for 1 h at a constant current of 400 mA. After transfer, membranes were rinsed in TBS (in mM: 150 NaCl, 50 Tris-HCl, pH 7.5) and incubated with TBS-TM (TBS containing 0.1% [vol/vol] Tween-20 and 5% [wt/vol] skim milk) for 1 h at room temperature with gentle rocking to block nonspecific binding. Membranes were then incubated for 16 h at 4 °C with gentle rocking in the presence of either mouse anti-HA, rabbit or goat anti-AQP1, goat anti-AQP2, or rabbit anti-CAII at 1:1000 in TBS-TM. After successive washes with TBS and TBS-T (TBS containing 0.1% [vol/vol] Tween-20), the membranes

were incubated with a 1:5000 dilution of the appropriate HRP-conjugated secondary antibody in TBS-TM for 1 h at 20 °C and then washed further with TBS and TBS-T. Proteins were detected using Western Lightning Chemiluminescence Reagent Plus (PerkinElmer, Waltham, MA) and visualized using a Kodak Image Station 440CF (Kodak, Rochester, NY). Quantitative densitometric analyses were performed using Kodak Molecular Imaging Software, version 4.0.3.

3.2.7. Peptide spot assay

Peptides 15 amino acids in length corresponding to progressively more C-terminal fragments of the cytosolic C-terminus of AQP1, were synthesized onto cellulose membranes (17). The membranes were blocked for 4 h at room temperature in TBS-TM and then incubated with 40 μg of recombinant CAII (Sigma-Aldrich) or the equivalent molar amount of BSA in TBS-TM overnight at 4 °C, respectively. The membranes were then washed with TBS-T before incubation with rabbit anti-CAII at 1:10,000 in TBS-TM, washed, and finally incubated in secondary antibody before visualizing as described.

3.2.8. Proximity ligation assay

HEK293 cells plated in 100-mm dishes containing glass poly-L-lysine–coated coverslips were transfected with cDNAs encoding WT, ΔCABI, ΔCABII, and ΔCAB AQP1, AE1, or hCNT3. Two days post transfection, coverslips were recovered, and the remaining plated cells were washed with PBS, lysed in IPB buffer (1% NP-40, 5 mM EDTA, 0.15 M NaCl, 0.5% deoxycholate, 10 mM Tris-HCl, pH 7.5) containing protease inhibitors and stored frozen until further use. Coverslips were washed twice in PBS, fixed with 3.5% paraformaldehyde, 1 mM

$CaCl_2$, and 1 mM $MgCl_2$ in PBS, pH 7.4, for 20 min, washed twice with PBS, and then quenched with 50 mM NH_4Cl for 10 min. Fixed cells were permeabilized with 0.1% Triton X-100 in PBS for 1 min at room temperature and washed twice for 5 min with Wash Buffer A (Olink Bioscience). Samples were then processed for PLA using the Duolink Detection kit (Olink Bioscience), according to the manufacturer's instructions. Briefly, coverslips were blocked with blocking solution for 30 min at 37 °C and incubated for 1 h at 37 °C in a humidified chamber with a 1:1000 dilution of rabbit anti-CAII antibody and goat anti-AQP1, IVF12 mouse monoclonal anti-AE1, or mouse monoclonal anti-hCNT3 at 1:500, 1:1000, and 1:500 dilutions in antibody diluent, respectively. Samples were then washed twice for 5 min in wash buffer A and then incubated for 1 h at 37 °C with a combination of the corresponding PLA probes (anti-rabbit Plus and anti-mouse Minus or anti-goat Minus) conjugated to unique oligonucleotides. The PLA oligonucleotides were hybridized and circularized by ligation (30 min at 37 °C), and the formed DNA circle was then amplified by rolling circle amplification into single-stranded DNA anchored to one of the antibodies. The amplification product was detected by addition of complementary oligonucleotides labeled with Texas red fluorophore. Coverslips were mounted in the provided mounting media and observed through a 60x/1.42 PlanApo oil immersion objective. *Z*-stack confocal image capture was performed with a C9100-13 EMCCD digital camera using Volocity software.

3.2.9. Preparation of red blood cell ghosts and renal cortical membrane vesicles, and stopped-flow light scattering measurement of water permeability

Whole blood was extracted from wild-type FVB/N mice by cardiac puncture. Red blood cells were isolated by centrifugation for 5 min at 5000 rpm. Red blood cells were washed with 0.9% NaCl three times at 4 °C. The red blood cells were then lysed by the addition of 5 mM $NaPO_4$, pH 7.4, with protease inhibitor cocktail and 1 mM phenylmethylsulfonyl fluoride. After 10 min, the membranes were pelleted by centrifugation at 27,000 rpm for 20 min at 4 °C. The hemolysate was then removed by aspiration and the lysis step repeated until membranes became white (usually thrice more). Ghosts were resealed in the presence of 250 μM recombinant CAII (Sigma-Aldrich) or BSA by incubation in PBS containing 1 mM $CaCl_2$ for 30 min at 37 °C. Finally, the resealed ghosts were washed three times with PBS before stopped-flow light scattering was performed.

Renal cortexes from wild-type and CAII-deficient mice were homogenized with a glass/Teflon homogenizer (500 rpm) in ice-cold buffer containing 220 mM mannitol, 70 mM sucrose, 5 mM ethylene glycol tetraacetic acid [EGTA], and 1 mM EDTA, 20 mM Tris-HCl, pH 7.4. Nucleus- and mitochondrion-enriched fractions were removed by centrifugation at 500 × *g* and 6000 × *g* for 10 min, respectively. A plasma membrane–enriched fraction was then obtained by centrifugation at 17,000 × *g* for 1 h at 4°C. The pellet was gently resuspended in homogenization buffer, creating plasma membrane vesicles. The size of vesicles was determined with an N5 Submicron Particle Size Analyzer (Beckman Coulter,

Palo Alto, CA) and was not different between genotypes (59.92 ± 3.8 vs. 59.7 ± 2.8 nm).

Osmotic water permeability of renal plasma membrane vesicles and red blood cell ghosts was determined by stopped-flow light scattering, as described previously (8). Briefly, the time course of vesicle volume change was followed at 20 °C by changes in intensity of scattered light at the wavelength of 450 nm, using a BioLogic MPS-20 (BioLogic, Claix, France) stopped-flow reaction analyzer with a 1.6-ms dead time and 99% mixing efficiency in <1 ms. Aliquots of vesicles were diluted into a hypotonic (220 mOsm) isolation medium (124 mM mannitol, 70 mM sucrose, 1 mM EDTA, 5 mM EGTA, 20 mM Tris-HCl, pH 7.4). One of the syringes of the stopped-flow apparatus was filled with the vesicle suspension, and the other was filled with the same buffer to which mannitol was added to reach a final osmolarity of 500 mOsm to establish a hypertonic gradient (140 mOsm) upon mixing. The final protein concentration after mixing was 100 μg/ml. Immediately after applying a hypertonic gradient, water outflow occurs and the vesicles shrink, causing an increase in scattered light intensity. The data were fitted to a single-exponential function, and the related rate constant (K_i, in seconds^{-1}) of water efflux was determined. The coefficient of osmotic water permeability (P_f), an index reflecting the osmotic water permeability of the analyzed membranes, was calculated using the equation [$P_f = K_i V_o/A_v V_w \Delta C$] where K_i is the fitted exponential rate constant, V_0 is the initial mean vesicle volume determined as described, A_v is the mean vesicle surface, V_w is the molar volume of water, and

ΔC is the osmotic gradient. The medium osmolarity was verified by a vapor-pressure osmometer (Wescor, Logan, UT).

3.2.10. Statistical analysis

Data are presented as means ± SE. Paired or unpaired Student's *t* tests or analysis of variance were carried out to determine statistical significance as appropriate. Tests were performed using Excel software (Microsoft, Redmond, WA), and values <0.05 were considered statistically significant.

3.3 Results

3.3.1. The cytosolic C-terminus of AQP1 contains two potential CAII binding sites

The physical interaction between CAII and AE1 is mediated by an acidic cluster of amino acids, L^{886}DADD, in the cytosolic C-terminal domain of AE1 (43). A carbonic anhydrase binding motif was subsequently defined as a hydrophobic amino acid followed by a sequence of four amino acids, with at least two acid residues (43). Examination of the amino acid sequence in the cytosolic C-terminus of human AQP1 revealed two potential carbonic anhydrase II binding sites (CABs), VE^{251}EYD and LD^{256}ADD (Figure 3-1A). Surprisingly, the second CAB (CABII) is identical to AE1's CAII binding motif. Moreover, this sequence is conserved across species (Figure 3-1A). Examination of the cytosolic termini of the other aquaporins failed to identify a similar acidic cluster (Figure 3-1B). The presence of sequential CABs in the cytosolic C-terminus of AQP1 raises the possibility of altered water flux through AQP1 upon CAII interaction.

Figure 3.1: The cytosolic C- terminus of AQP1 has two CAII binding motifs. Examination of the human AQP1 amino acid sequence identified two consensus carbonic anhydrase binding (CAB) sites in the cytosolic C-terminus. (A) Sequence alignment of the CABs found in AQP1 genes in the indicated species. CAB1 is depicted in blue and CABII in red throughout. (B) Comparison of the same region of the other aquaporins does not reveal this motif.

3.3.2. AQP1 is coexpressed in proximal tubular brush border membranes with CAII

To assess the possibility of an intrarenal interaction between CAII and AQP1, we examined the localization of CAII in the kidney. Murine renal sections immune stained with an anti-CAII antibody revealed strong cortical staining in tubular epithelial cells lacking a predominant brush border, consistent with cortical collecting duct localization. Fainter cortical staining was apparent in most of the remaining tubules, consistent with the morphology of the proximal tubule (Figure 3-2A). Closer examination of the weaker cortical tubular epithelial cell staining revealed predominant brush border expression of CAII (Figure 3-2B), a location where AQP1 is expressed (29, 46). To assess whether the two proteins were in the same subcellular domain, we immunostained serial sections for AQP1 and CAII (Figure 3-2 C and D). Predominant AQP1 and CAII staining was observed at the brush border membrane. The CAII brush border membrane staining was specific, as no signal was observed when sections from CAII-deficient mice were immune stained (Figure 3-3). Finally, to confirm proximal tubular localization of CAII, we coimmunostained murine renal sections with anti-CAII antibody and *Lotus tetragonolobus* lectin, a proximal tubule marker (13). This demonstrated significant overlap in staining (Figure 3-2 E-E"). These findings are consistent with AQP1 and CAII brush border colocalization.

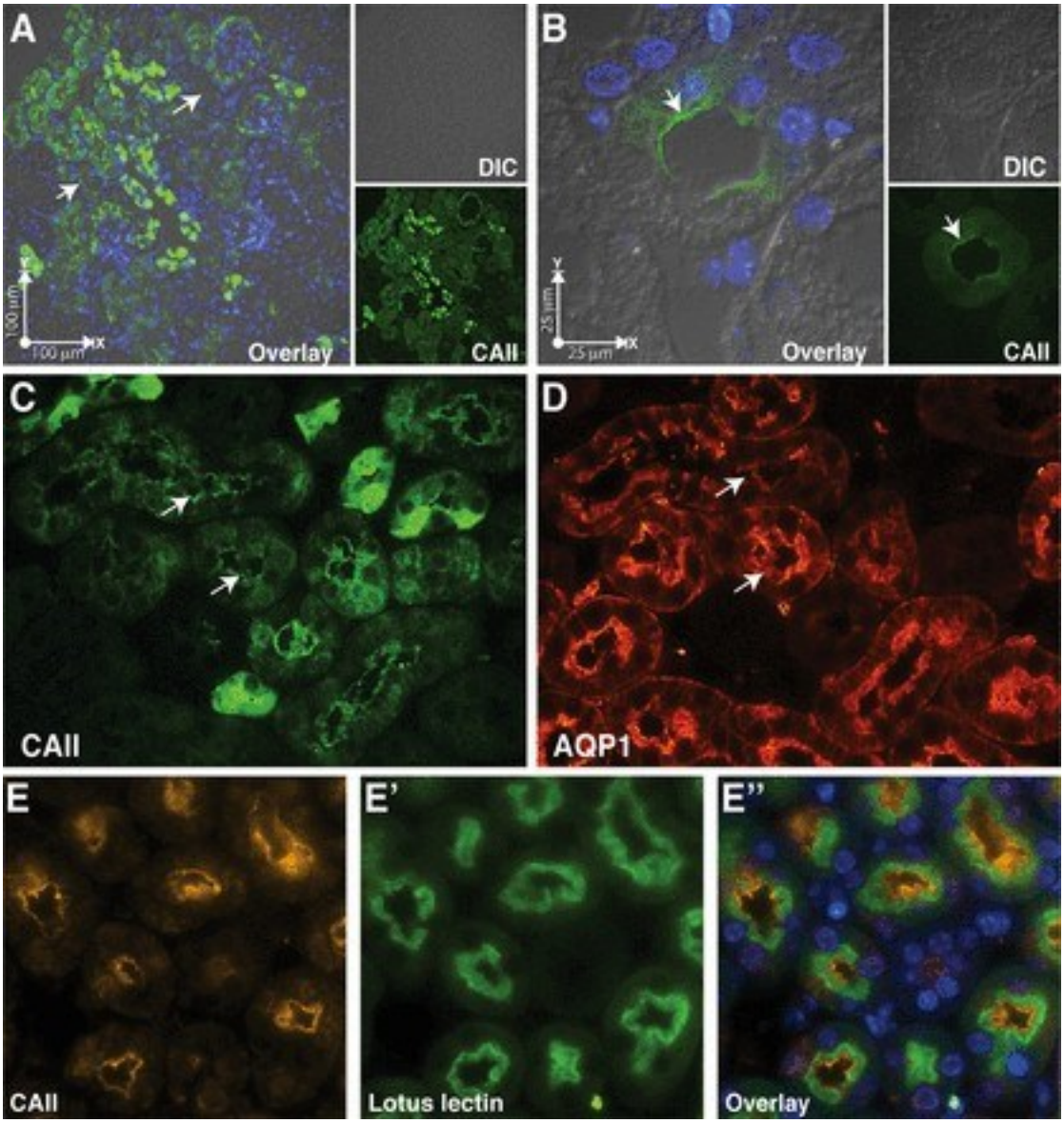

Figure 3.2: CAII and AQP1 colocalize in mouse proximal tubular brush border membrane. (A,B) A kidney section immunostained for CAII (green) and with the nuclear stain 4',6-diamidino-2-phenylindole. A) A low power cortical image, with arrows pointing to proximal tubular staining. B) A high-power image with an arrow pointing to the brush border. Individual channels are displayed at both high and low power. C, D) Serial sections immunostained for C) CAII and D) AQP1. E-E') Image of the renal cortex, immunostained for CAII E and with a proximal tubular marker, L.tetragonolobus lectin (E'). An overlay of the two channels is presented in E".

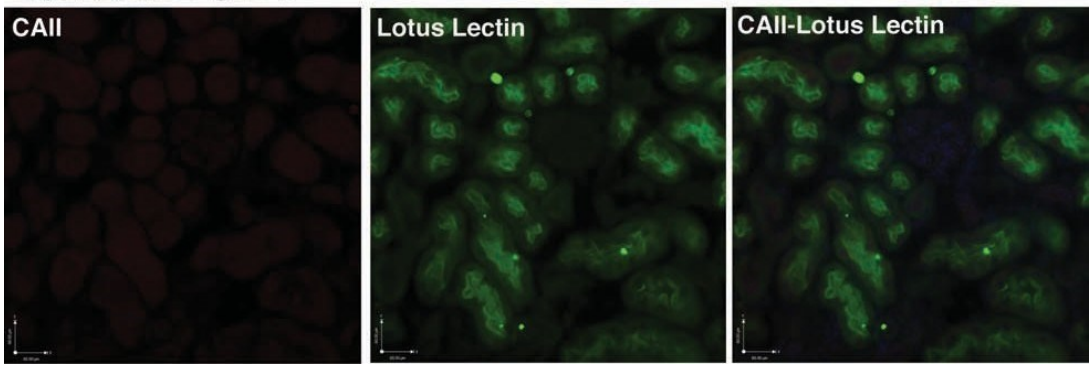

Figure 3.3: Negative control for CAII staining in Car2 deficient mice.
Immunostaining as per Figure 3-2E, but performed on renal sections from Car2 deficient mice. Scale bar is 60 μm in each case.

3.3.3. CAII binds to the acidic motifs in the tail of AQP1

To assess a possible direct physical interaction between CAII and the cytosolic C-terminus of AQP1, we prepared an array of synthetic 15 amino acid peptides corresponding to sequential overlapping sequences of the AQP1 C-terminus. After blotting onto derivatized cellulose membranes, the array was incubated with either purified CAII or albumin, after which the membrane was probed with an anti-CAII antibody. Visualization of the membrane revealed clear association of CAII with peptides containing both the EEYD and LDADD motifs (Figure 3-4). Specificity of the interaction was indicated by the failure of albumin to show immunoreactivity. These data support a direct physical interaction between CAII and the acidic motifs in the AQP1 C-terminus.

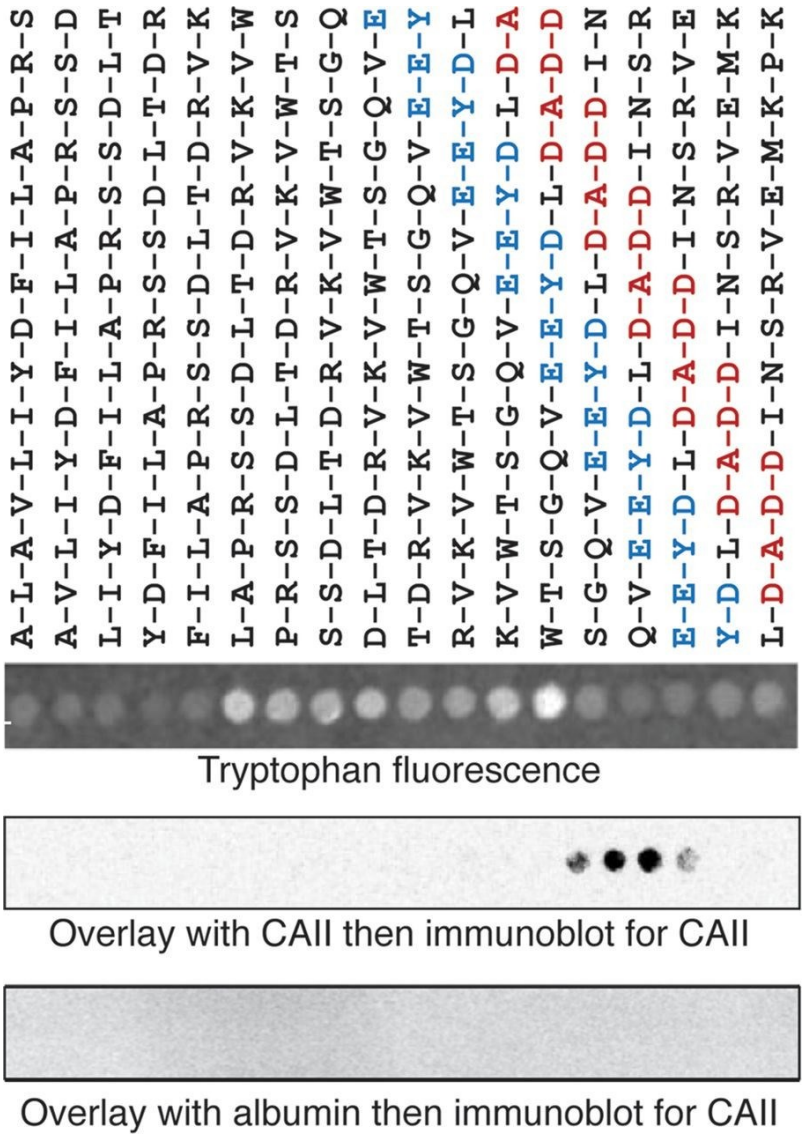

Figure 3.4: A peptide overylay assay reveals that CAII interacts with the acidic clusters in the C-terminus of AQP1. Fifteen- amino acid pepetides corresponding to overlapping progressively more C-terminal sequences in AQP1 were spotted onto cellulose membranes and visualized with ultraviolet fluorescence (tryptophan fluorescence). The exact peptide sequence is detailed above the blot. Recombinant CAII or albumin was incubated with the membrane before a primary anti-CAII antibody, followed by the appropriate secondary antibody, and then visualization. Displayed are representative overlays from 3 separate experiments.

3.3.4. CAII increases water flux through AQP1 in kidney cells

To examine the effects of CAII on AQP1-mediated water permeation in a mammalian renal cell, we performed experiments in HEK293 cells (Figure 3-5). Cells were cotransfected with enhanced green fluorescent protein (eGFP) and combinations of AQP1 with WT-CAII, V143Y-CAII, or HEX-CAII or vector alone. We used the dilution of cytosolic eGFP fluorescence in a region of interest of an optical slice measured by confocal microscopy as an index of cell volume changes after cells were shifted to a hypotonic medium (Figure 3-5A). The cytosolic concentration of eGFP is inversely proportional to cell volume, and the rate of change of eGFP concentration is a surrogate for the rate of volume change. The rate of cell volume change is directly proportional to the amount of AQP1 expressed in this assay over the range of DNA transfected (Figure 3-6).

The rate of cell volume change of HEK293 cells expressing AQP1 alone was significantly greater than for cells expressing CAII, V143Y-CAII, HEX-CAII, or empty vector alone (Figure 3-7). To account for possible differences in the abundance of AQP1 at the plasma membrane due to coexpression of CAII, we normalized the data to the cell surface expression of AQP1 as determined by cell surface biotinylation (Figure 3-8A). The rate of fluorescence change (normalized to the activity of vector transfected cells) of cells cotransfected with AQP1 and CAII was significantly higher than that of cells transfected with AQP1 alone (Figure 3-5B). The normalized rate of fluorescence change of cells expressing AQP1 and either V143Y-CAII or HEX-CAII was significantly greater than that of cells expressing AQP1 alone. Although the increase in water flux induced by

coexpression of the CAII mutants was lower in magnitude than for WT-CAII, there was no statistically significant difference between the rate of fluorescence change of AQP1/CAII and either AQP1/V143Y-CAII– or AQP1/HEX-CAII–transfected cells, likely due to endogenous CAII activity in this model system. Further, coexpression of AQP2 with CAII failed to augment water flux beyond that of AQP2 alone (Figure 3-9). The mammalian cell swelling data suggest that a physical interaction between CAII and AQP1 specifically increases AQP1-mediated water-flux.

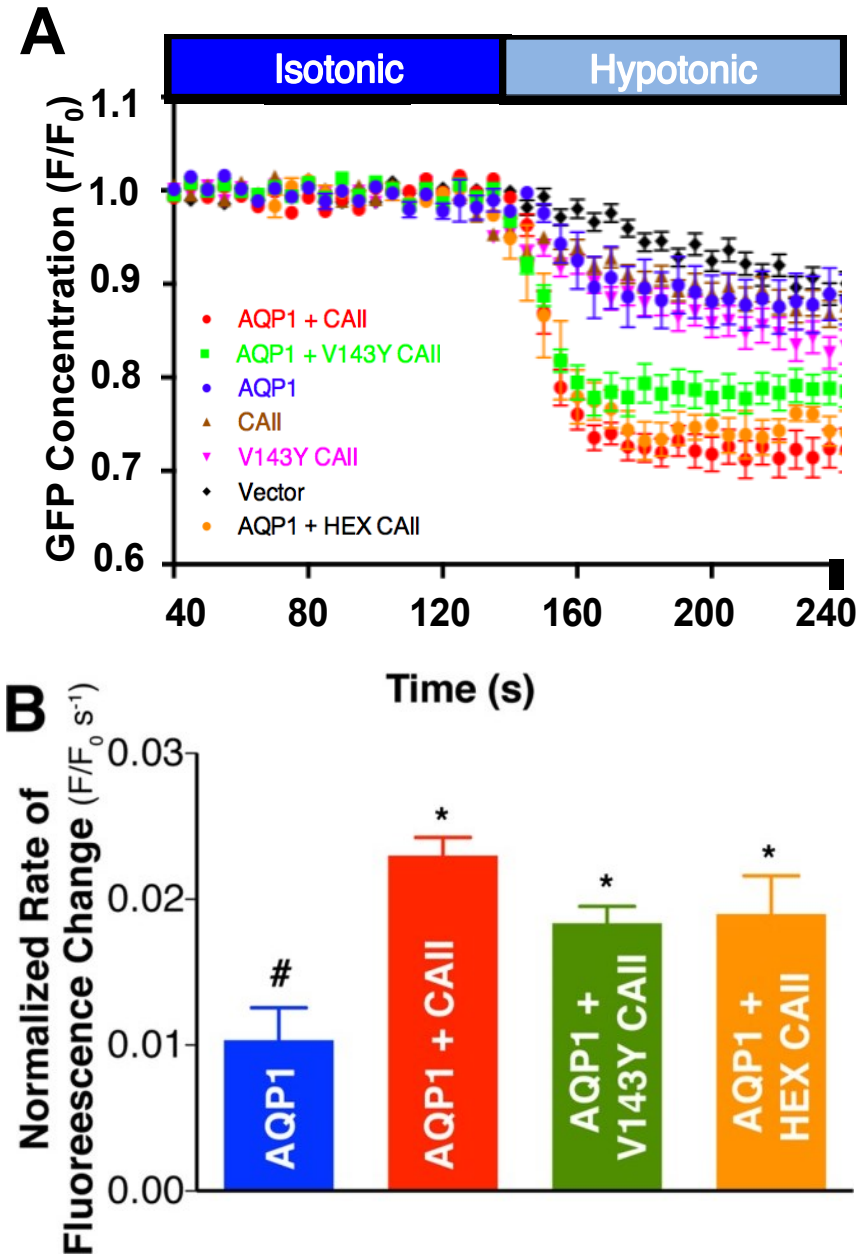

Figure 3.5: CAII expression increases water flux through AQP1 expressed in HEK293 cells. (A) AQP1 water transport activity was measured by confocal fluorescence microscopy on transfected HEK293 cells. Cells were perfused alternately with isotonic (dark blue bar) and hypotonic (light blue bar) medium, and GFP fluorescence was quantified digitally. GFP concentration as assessed by fluorescence in a representative region of interest (ROI) normalized to initial fluorescence in that ROI (F/F_0) is plotted vs. time. (B) Rate of fluorescence change corrected for activity of vector-transfected cells and normalized to AQP1 cell surface expression. Cell surface expression was determined by biotinylation and is presented in Figure 3-8. Asterisk represents a statistically significant difference ($p < 0.05$) compared with AQP1, and number sign (#) represents a statistically

significant difference from AQP1 + CAII.

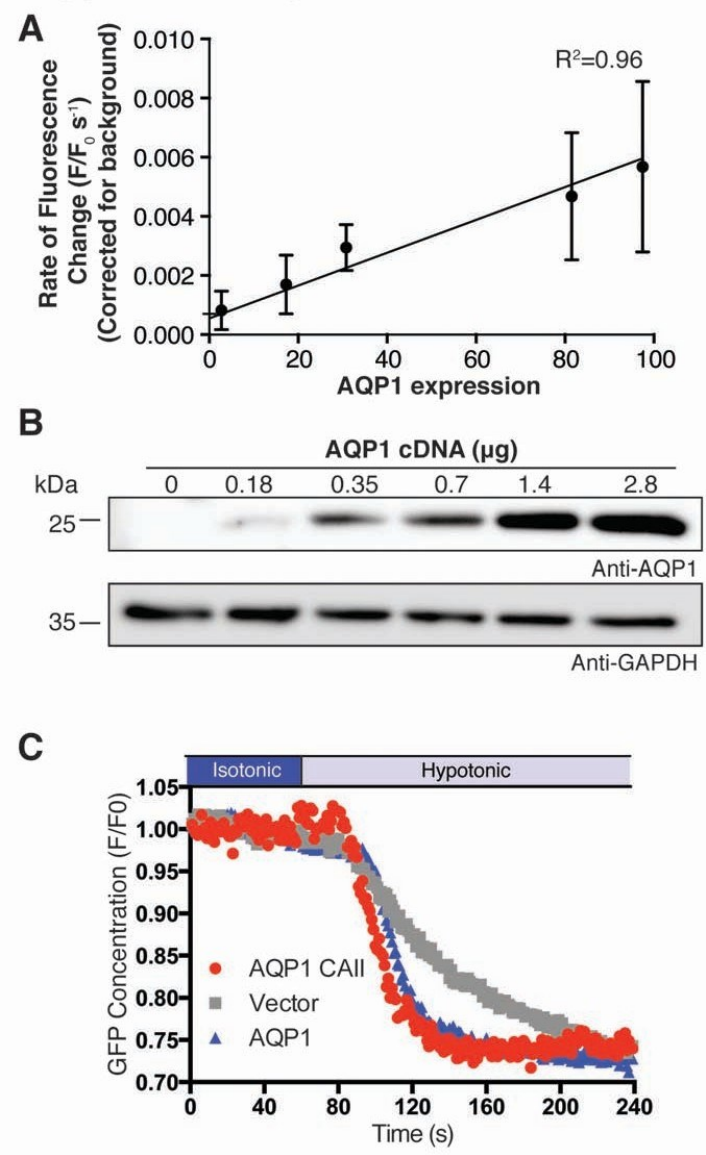

Figure 3.6: The amount of aquaporin-1 expression correlates with water permeability of HEK293 cells, as measured by the dilution of fluorescence. A) Plot of rate of fluorescence change (a measure of water permeability) vs aquaporin-1 expression. B) Immunoblot probed for aquaporin-1 and GAPDH from cell lysate obtained from HEK293 cells transfected with increasing amounts of aquaporin-1 cDNA. C) Representative (i.e. not averaged) traces from the data displayed in Figure 3-5.

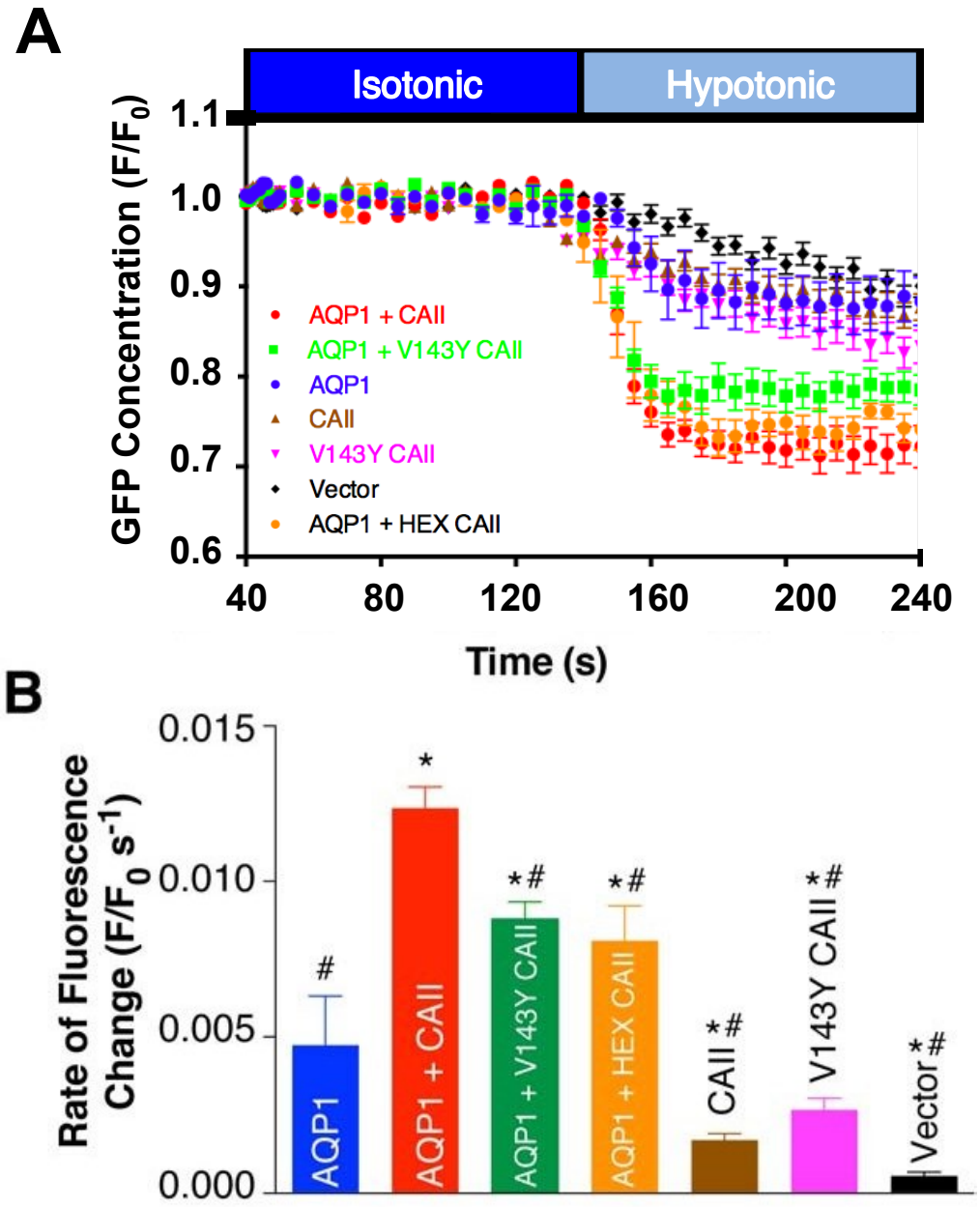

Figure 3.7: CAII expression increases water flux through AQP1 expressed in HEK293 cells. A) AQP1 water transport activity was measured by confocal fluorescence microscopy on transfected HEK293 cells. Cells were perfused alternately with isotonic (dark blue bar) and hypotonic (light blue bar) medium, and GFP fluorescence was quantified digitally. GFP concentration of a confocal slice as assessed by fluorescence in a representative region of interest (ROI) normalized to initial fluorescence in that ROI (F/Fo) is plotted vs. time. B) Initial rate of fluorescence change that has not been normalized to total or cell surface AQP1 expression. * represents $p< 0.05$ compared to AQP1 alone and # represents $p< 0.05$ compared to AQP1 + CAII. N >3 per condition.

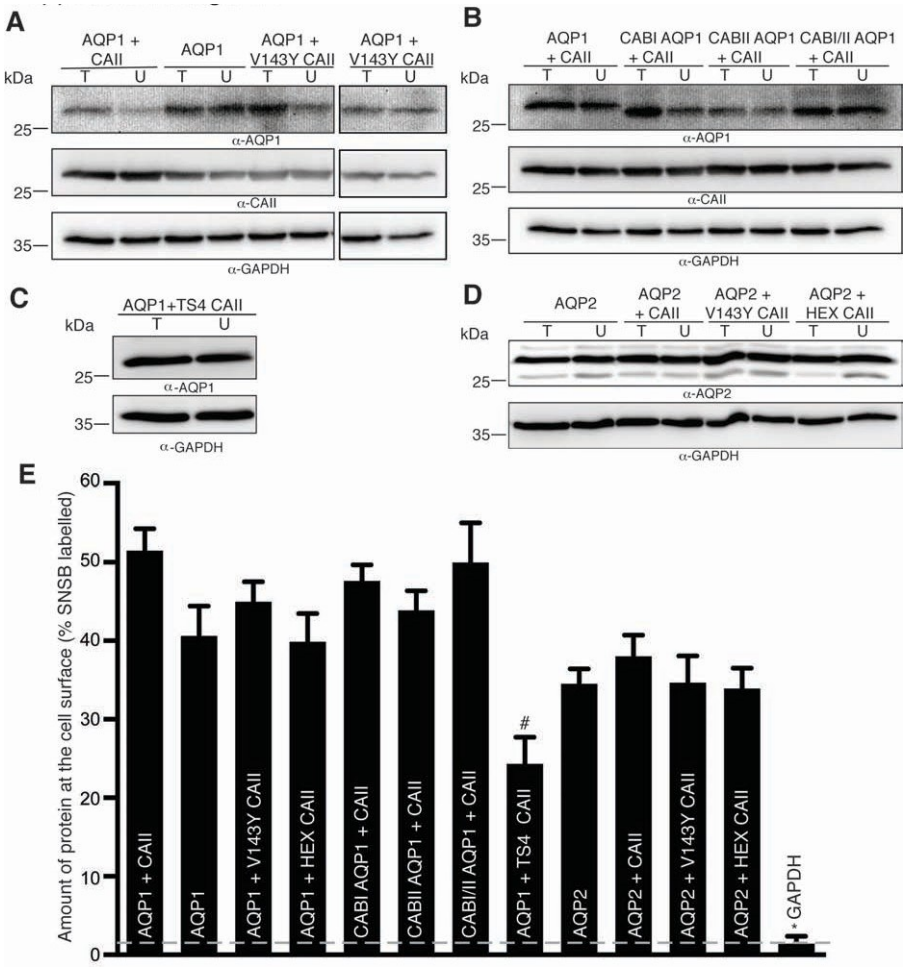

Figure 3.8. Cell surface biotinylation data used to normalize water permeability studies performed in HEK293 cells. A) Total cell lysate (T) and the unbound fraction (U) of biotinylated cells transfected with AQP1 +/- CAII, V143Y-CAII or HEX-CAII mutant immunoblotted for AQP1, top blot, CAII, middle blot or GAPDH, bottom blot. B) Total cell lysate (T) and the unbound fraction of biotinylated cells (U) transfected with CAII +/- AQP1 or the AQP1 CAB mutants immunoblotted forAQP1, top blot, CAII, middle blot or GAPDH, bottom blot. C) Total and unbound fraction of lysate from cells transfected with AQP1 and the TS4-CAII mutant subjected to SDS PAGE and immunoblotted forAQP1, top blot, or GAPDH, bottom blot. D) Total cell lysate (T) and the unbound fraction of biotinylated cells transfected with AQP2 +/- CAII, V143Y-CAII or HEX-CAII mutant immunoblotted for AQP1, top blot, or GAPDH, bottom blot. Depicted are representative immunoblots for panels A-D. E) Quantification of cell surface expression of AQP1, AQP2 or the AQP1 CAB mutants ($n > 3$ for all conditions and #represents $p < 0.05$ relative to AQP1 expression alone).

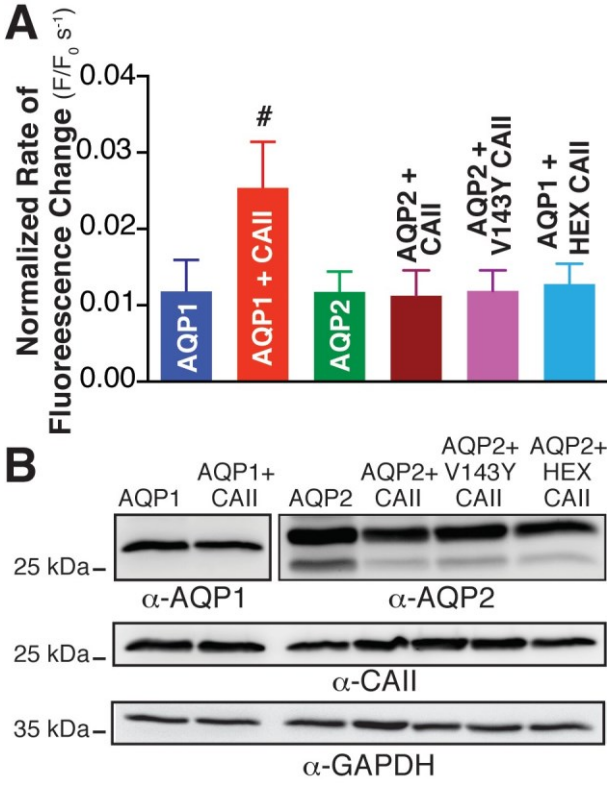

Figure 3.9: CAII expression does not increase water flux through AQP2 expressed in HEK293 cells. Aquaporin-mediated (AQP1 and AQP2) water transport activity was measured by confocal fluorescence microscopy of transfected HEK293 cells as per Figure 3-5. (A) Rate of fluorescence change corrected for activity of vector-transfected cells and normalized to AQP1 or AQP2 cell surface expression. Cell surface expression was determined by biotinylation and is presented in Figure 3-8. Number sign (#) represents a statistically significant difference ($p < 0.05$) compared with AQP1; $n > 3$ per condition. (B) Immunoblots demonstrating total cellular expression of AQP1, AQP2, CAII, and glyceraldehyde-3-phosphate dehydrogenase (GAPDH).

3.3.5. AQP1 and CAII associate in mammalian cells

To further delineate the molecular details of the interaction between AQP1 and CAII, we engineered AQP1 mutants in which the two CAB motifs were individually or doubly mutated to alanine (AQP1-CABI, AQP1-CABII, and AQP1-CABI/II, respectively; Figure 3-10A). These constructs were transfected into HEK293 cells, and the association between these proteins and endogenous CAII was assessed by in situ proximity ligation assays (PLAs, (37)). The in situ PLA permits the binding of a red fluorophore if the two target antigens, detected with antibodies, are within 40 nm of one another (37). AE1, which associates with CAII (42, 43), and the human nucleoside transport protein hCNT3 were used as positive and negative controls, respectively. Confocal microscopy analysis of AE1-transfected cells processed for in situ PLA revealed a significant fluorescent signal, confirming a close physical association of AE1 and CAII (Figure 3-10C). In contrast, when the interaction between hCNT3 and CAII was investigated, no proximity signal was detected (Figure 3-10C) despite significant expression of hCNT3 and CAII (Figure 3-6C and Figure 3-11). AQP1-transfected cells processed for in situ PLA produced a significant fluorescence signal, consistent with close physical association of AQP1 and CAII (Figure 3-10C). We observed a fluorescence signal in cells transfected with AQP1-CABI and CAII but less than for wild-type AQP1–transfected cells. We were unable to detect a significant proximity signal in cells expressing either AQP1-CABII or AQP1-CABI/II (Figure 3-10C). We confirmed expression of the transfected proteins as well as CAII by analyzing the remnant of the cells used for the assay by immunoblot (Figure 3-

10B). These results suggest that AQP1 and CAII interact and that CABII of AQP1 is most responsible for this. The reduced number of amplification foci in AQP1-CABI compared with WT-AQP1 suggests that this region also contributes to the association of CAII with AQP1.

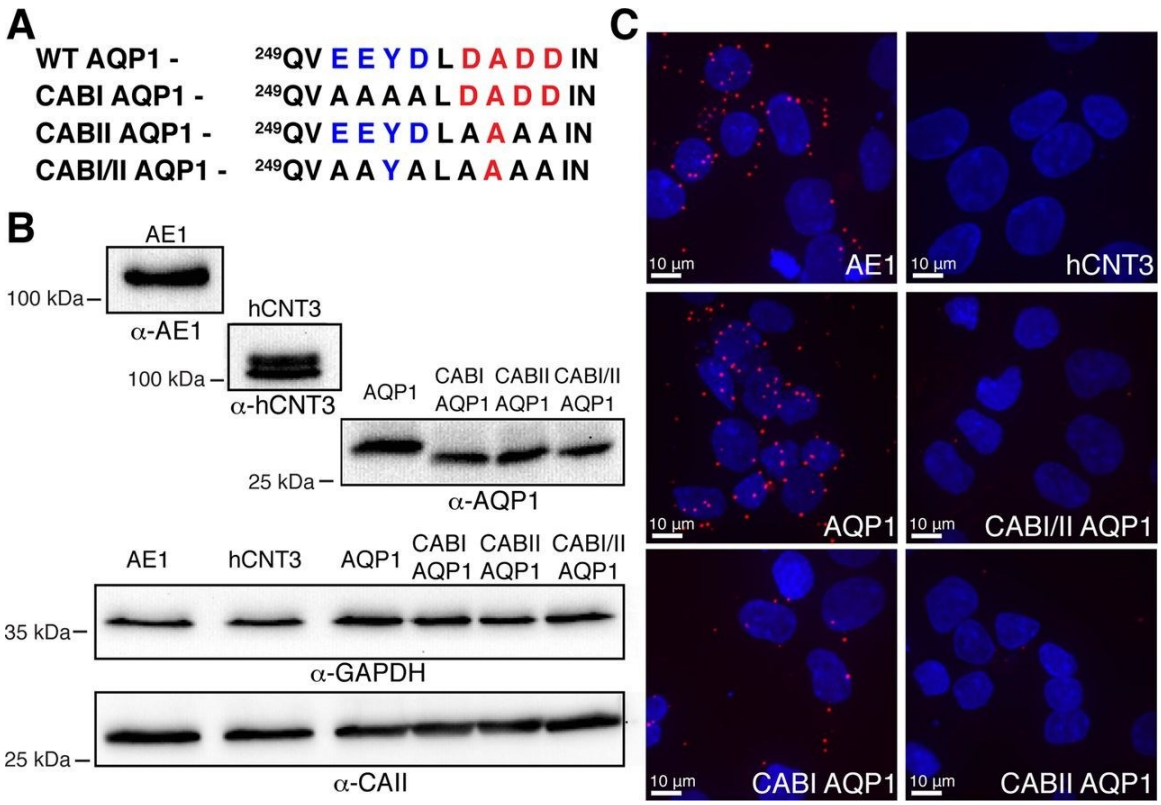

Figure 3.10: AQP1 and CAII are in close proximity. (A) The CAB mutants generated. The CAB1 motif is in blue, and the CABII motif is in red. **(**B) Immunoblots of cell lysates from transfections used in the proximity ligation assays. The primary antibody used is depicted under the blot, and the cDNA transfected is displayed in bold above the blot. GAPDH was probed as a loading control. (C) Cells transfected with the indicated cDNAs were processed in a proximity ligation assay, using an anti-CAII antibody in each case, along with anti-AE1 (AE1), anti-AQP1 (AQP1, CAB1AQP1, CABIIAQP1, CABI/IIAQP1), or anti-hCNT3 (hCNT3).

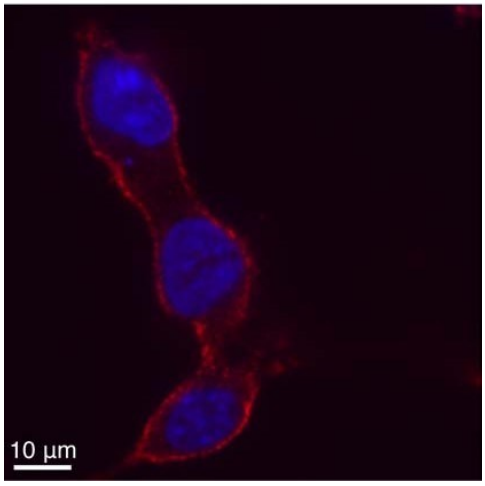

Figure 3.11. hCNT3 is expressed at the cell surface despite the absence of a PLA signal. HEK293 cells were transfected with hCNT3 cDNA, 72 h later they were fixed, permeabalized and immunostained with a primary anti-hCNT3 antibody followed by an AlexaFluor 594 secondary antibody. The nuclei are costained with DAPI.

3.3.6. CABI and CABII are required to increase the water conductance of AQP1

We next compared the ability of AQP1 CAB mutants to induce cell swelling upon hypotonic challenge in HEK293 cells (Figure 3-12). Cells coexpressing CABI-AQP1 and CAII had a significantly increased swelling rate compared with cells transfected with empty vector or AQP1 alone (Figure 3-12B). This rate of cell swelling was not statistically different from that of AQP1- and CAII-expressing cells (Figure 3-12B). In contrast, when CABII-AQP1 or CABI/CABII-AQP1 mutants were coexpressed with CAII, cell-swelling rates were not different from that of cells expressing AQP1 alone (Figure 3-12B). These results did not arise from differences in the expression of the AQP1 constructs, as they were normalized to cell surface AQP1 abundance, which was determined by cell surface biotinylation (Figure 3-8B). These data are consistent with the PLA data, supporting a predominant role for CABII in localizing CAII to AQP1 and in augmenting water flux through it.

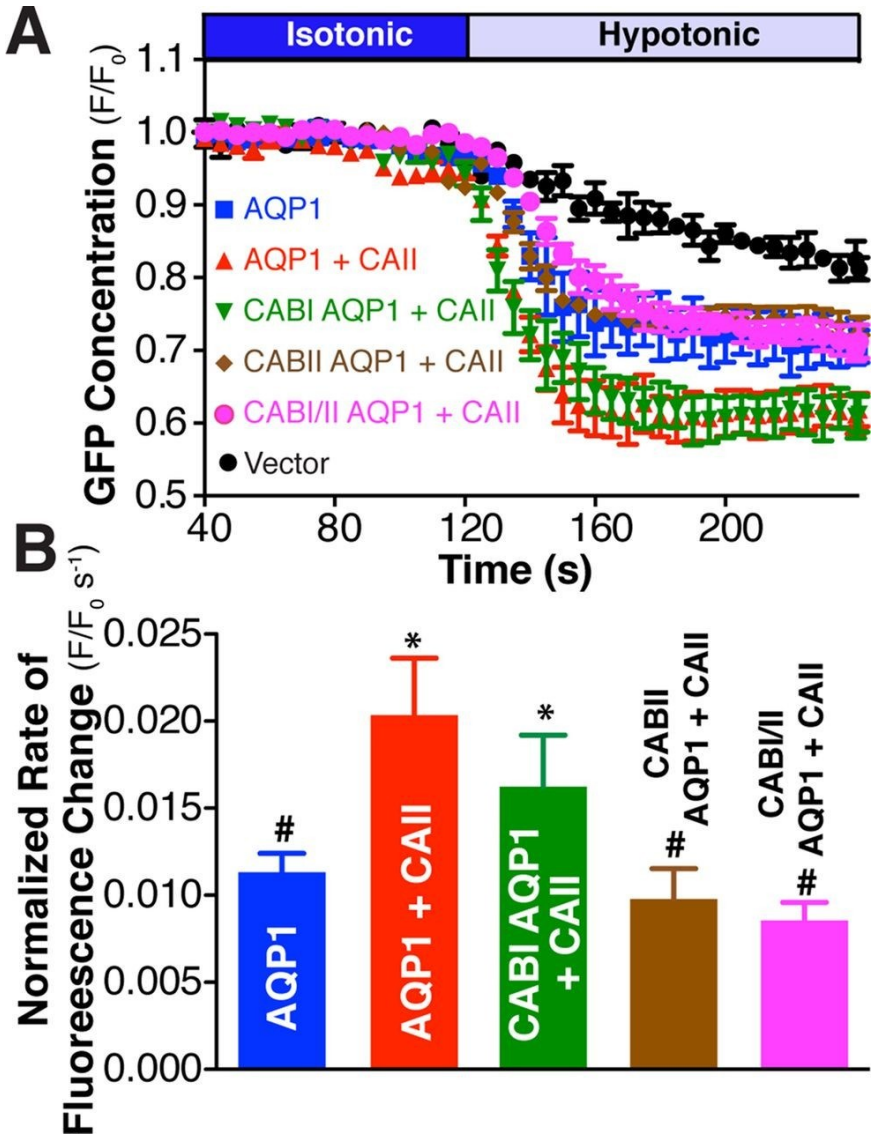

Figure 3.12: CABII is necessary to mediate increased water flux through AQP1 by CAII. AQP1 Water transport activity was measured by confocal fluorescence microscopy of HEK293 cells transfected with AQP1 CAB mutants in the presence and absence of CAII. **(**A) Cells were perfused initially with isotonic (dark blue bar) and then hypotonic (light blue bar) medium, and eGFP fluorescence was recorded. eGFP concentration as assessed by fluorescence in a representative ROI normalized to initial fluorescence in that ROI (F/F_0) is plotted vs time. The constructs transfected are indicated on the left side of the curves. (B) Rate of fluorescence change corrected for activity of vector-transfected cells and normalized to AQP1 amount at the cell surface. Cell surface expression was determined by biotinylation and is presented in Figure 3-8. Asterisk represents a statistically significant difference ($p < 0.05$) compared with AQP1, and number sign (#) represents a statistically significant difference from AQP1 + CAII.

3.3.7. CAII increases water permeability of red blood cell ghosts

We next measured water permeability of mouse red blood cell ghosts resealed in the presence of 250 μM CAII or bovine serum albumin (BSA). This provides a 50-fold molar excess of CAII per AQP1 (given that wild-type mice have a red blood cell volume of 90×10^{-15} l and that red blood cells contain 200×10^3 AQP1 molecules/cell (1)). Immunoblots of ghost lysates resealed in the absence of added CAII demonstrate the nominal absence of CAII from the ghosts (Figure 3-13A). To assess whether CAII was occluded in the red cell ghosts, we treated ghosts with trypsin in the presence or absence of the detergent Triton X-100. Ghost lysis with detergent was required for CAII digestion (Figure 3-13B). These data support the presence of CAII inside ghosts, where it is available to interact with the cytosolic C-terminus of AQP1. Finally, we measured water permeability across ghosts supplemented with BSA or CAII and found a near doubling of osmotic water permeability (P_f) in the ghosts supplemented with CAII relative to BSA supplementation (Figure 3-13, C and D). These results are consistent with a role of CAII in increasing water conduction through AQP1 in red blood cell membranes.

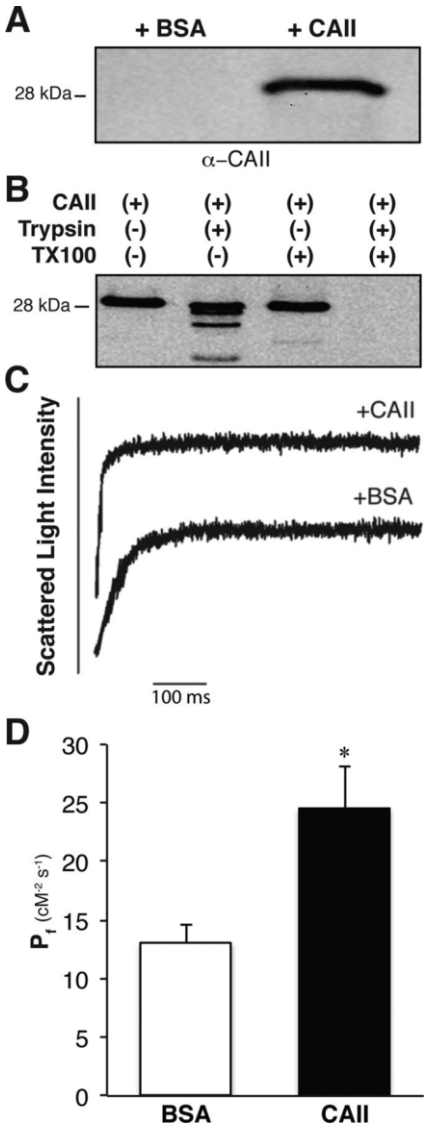

Figure 3.13: CAII increases the water permeability of red blood cell ghosts. (A) Immunoblot of ghost lysate resealed in the presence of BSA or CAII and probed with anti-CAII. (B) Immunoblot of ghost lysate resealed in the presence of CAII and treated with trypsin, Triton X-100, or both. (C) Representative light scattering traces from red blood cell ghosts supplemented with BSA or CAII. (D) Coefficient of osmotic water permeability (P_f) of red blood cell ghosts supplemented with bovine serum albumin or CAII. Asterisk represents a statistically significant difference ($p < 0.05$) compared with BSA-supplemented sample.

3.3.8. CAII-deficient mice are polydipsic, polyuric and have dilute urine

To examine the physiological significance of the interaction between AQP1 and CAII, we investigated water handling in an animal model devoid of CAII. To this end, we examined CAII-deficient mice, which were generated by random mutagenesis (19). These animals lack detectable CAII in all tissue examined, including the kidney (38). Wild-type and CAII-deficient mice were housed in metabolic cages for 24 h, to measure water ingestion and collect urine. After this, we measured blood gases (Table 3-I) and isolated kidneys. The animals did not demonstrate a metabolic acidosis as we added alkali (sodium citrate) to their drinking water in order to reduce mortality. They did, however, have a respiratory acidosis as previously reported (Table 3-I and (22)). We observed a significant increase in water consumption and total urine volume in the CAII-deficient mice, which we do not believe has been reported previously. This is despite the smaller mass of CAII–deficient mice relative to wild-type littermates (Table 3-II). We proceeded to measure electrolyte excretion, urine pH and osmolarity (Table 3-III). Consistent with a known defect in urinary acidification (19, 22), CAII-deficient mice demonstrate increased urinary pH (Table III). Urinary excretion of sodium, chloride, potassium and creatinine were not different between genotypes, however, the CAII-deficient mice have dilute urine relative to the wild-type animals (Table 3-III). CAII deficient mice are therefore polydipsic, polyuric and have dilute urine relative to their wild-type littermates. These findings are consistent with impaired tubular water reabsorption.

Table 3.1: Blood-gas analysis of wild-type and CAII-deficient mice

	pH	P_{CO2} (mm Hg)	$[HCO_3^-]$ (mM)	Hct (%)	Hb (g/l)
WT (n=8)	7.33 ± 0.01	41 ± 1	22 ± 1	42 ± 1	14.3 ± 0.2
CAII-Def (n=7)	7.18 ± 0.02**	59 ± 3**	22 ± 1	40 ± 3	13.6 ± 1.0

Values are mean ± SE. *$P \leq 0.05$ when compared with control, **$P \leq 0.01$ when compared with wild-type. Hct = hematocrit, Hb = hemoglobin.

Table 3.2: Metabolic cage data from Wild-type and CAII-deficient mice

	Animal mass (g)	Volume H_2O Consumed, (ml/24 h)	Chow Eaten, (g/24 h)	Urine Volume, (ml/24 h)
WT (n=9)	26.2 ± 1.8	6.3 ± 0.4	5.8 ± 0.4	0.5 ± 0.2
CAII-Def (n=6)	19.7 ± 1.4*	7.7 ± 0.4*	5.7 ± 0.6	1.7 ± 0.5*

Values are mean ± SE. *$P \leq 0.05$ when compared with control.

Table 3.3: Urine analysis of wild-type and CAII-deficient mice

	pH	Na^+ excretion, (µmol/24 h)	K^+ excretion, (µmol/24 h)	Cl^- excretion, (µmol/24 h)	Creatinine excretion (µmol/24 h)	Osmolality (mOsm)
WT (n=7)	7.3 ± 0.1	229 ± 54	270 ± 66	253 ± 62	0.07 ± 0.02	3360 ± 330
CAII-Def (n=5)	8.5 ± 0.1**	274 ± 112	300 ± 121	277 ± 115	0.10 ± 0.02	1920 ± 220*

Values are mean ± SE. *$P \leq 0.05$ when compared with control, **$P \leq 0.01$ when compared with wild-type.

3.3.9. AQP1 expression is increased in CAII-deficient mice

The putative nephron segment responsible for increased water excretion in CAII-deficient mice was examined by measuring the renal expression of AQP1 and AQP2. CAII expression was not detectable in the CAII-deficient mice by immunoblot (Figure 3-14A), or by quantitative real time PCR (Figure 3-15). Expression of AQP2 was not different between CAII-deficient and wild-type mice (Figure 3-16), however, renal AQP1 protein (Figure 3-14B) and mRNA expression were increased in the CAII-deficient mice (Figure 3-15).

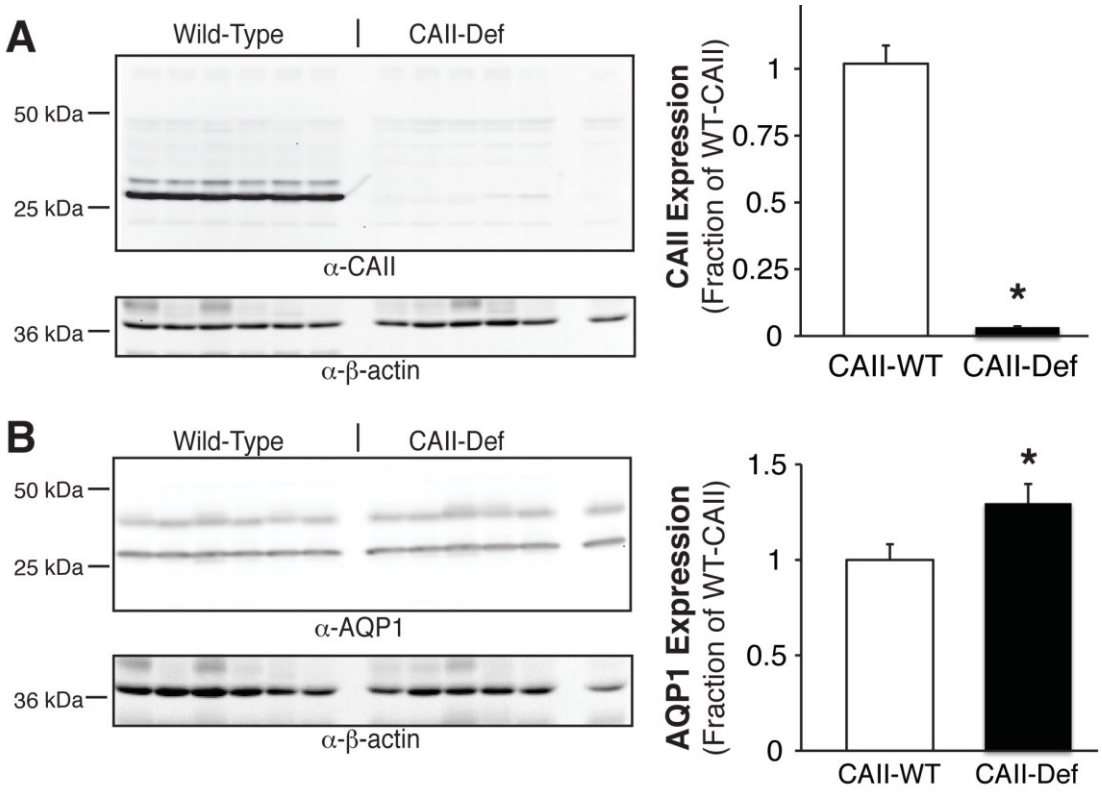

Figure 3.14: Renal AQP1 expression is increased in CAII-deficient mice. Whole kidney lysates were prepared from eight wild-type (WT) and eight CAII-deficient mice (CAII-Def). Immunoblots of these lysates were probed for A) CAII and B) AQP1. Afterwards the individual immunoblots were stripped and reprobed for b-actin. Protein expression normalized to β-actin is depicted to the right of the immunoblots. * Represents a statistically significant difference ($p < 0.05$) compared to wild-type kidney lysate.

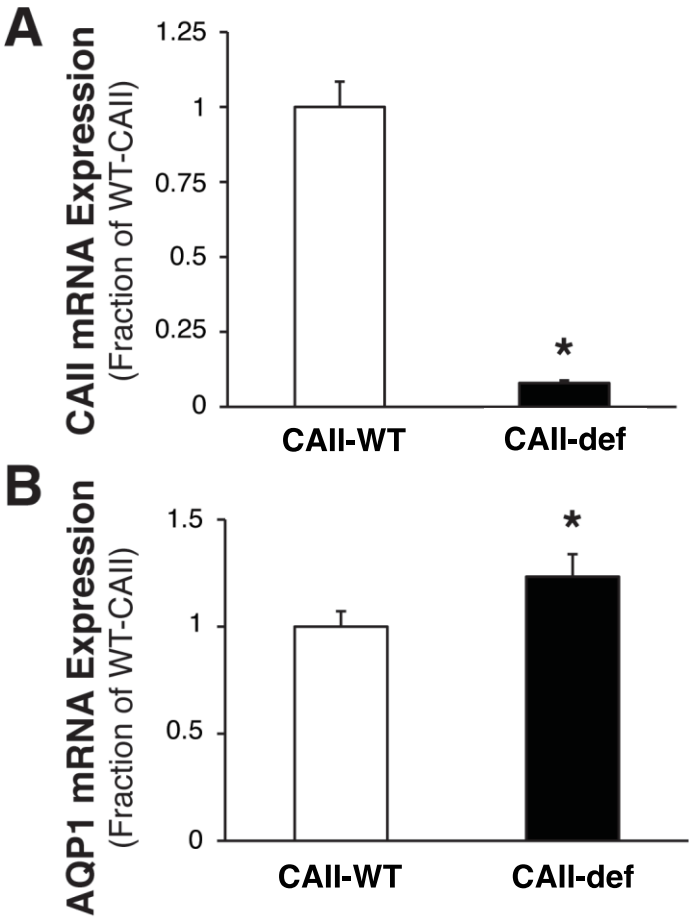

Figure 3.15: AQP1 mRNA expression increases in CAII-deficient mice. Isolation of mRNA from whole kidney were prepared from eight wild-type (WT) and eight CAII-deficient mice (CAII-Def). qPCR analysis for A) CAII and B) AQP1. mRNA expression normalized to β-actin. * Represents a statistically significant difference ($p < 0.05$) compared to wild-type mRNA.

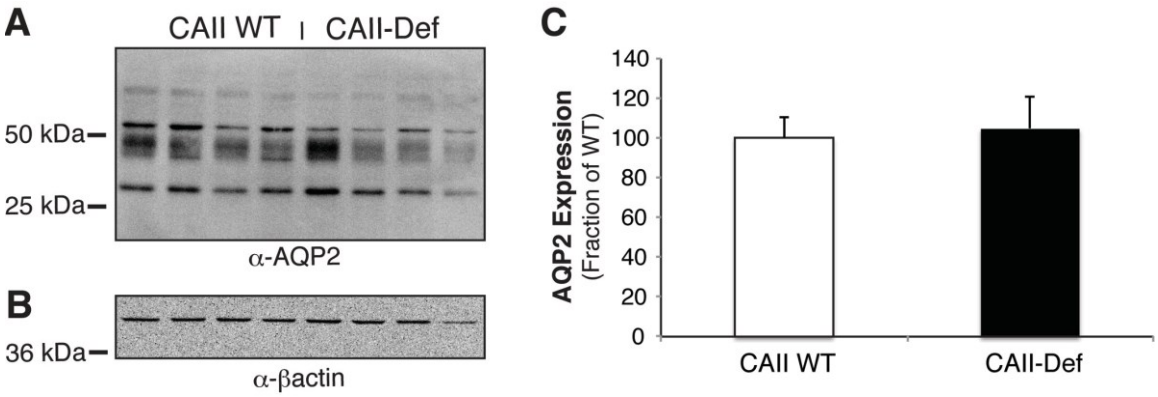

Figure 3.16: No change in AQP2 mRNA expression in CAII-deficient mice. Whole kidney lysates were prepared from eight wild-type (WT) and eight CAII-deficient mice (CAII-Def). Immunoblots of these lysates were probed for A) AQP2 . B) Afterwards the individual immunoblots were stripped and reprobed for β-actin. Protein expression normalized to β-actin is depicted to the right of the immunoblots. No significant change was observed in AQP2 expression in CAII deficient mice.

3.3.10. Water flux across renal cortical membranes isolated from kidneys of CAII-deficient mice is increased despite decreased AQP1 expression

To evaluate the physiological relevance of the interaction between AQP1 and CAII, we compared the P_f of renal cortical membrane–enriched vesicles from wild-type and CAII-deficient mice. Vesicles from wild-type and CAII-deficient mice were not different in size. Vesicles generated from renal cortical membranes of wild-type animals swelled at approximately twice the rate of those generated from CAII-deficient mice (Figure 3-17, A and B). This did not arise from a difference in the amount of AQP1 in the membrane fraction, as there was increased AQP1 expression in cortical membranes isolated from CAII-deficient mice (Figure 3-17, C and D). These results are consistent with CAII increasing the flow of water through AQP1 in the proximal tubule.

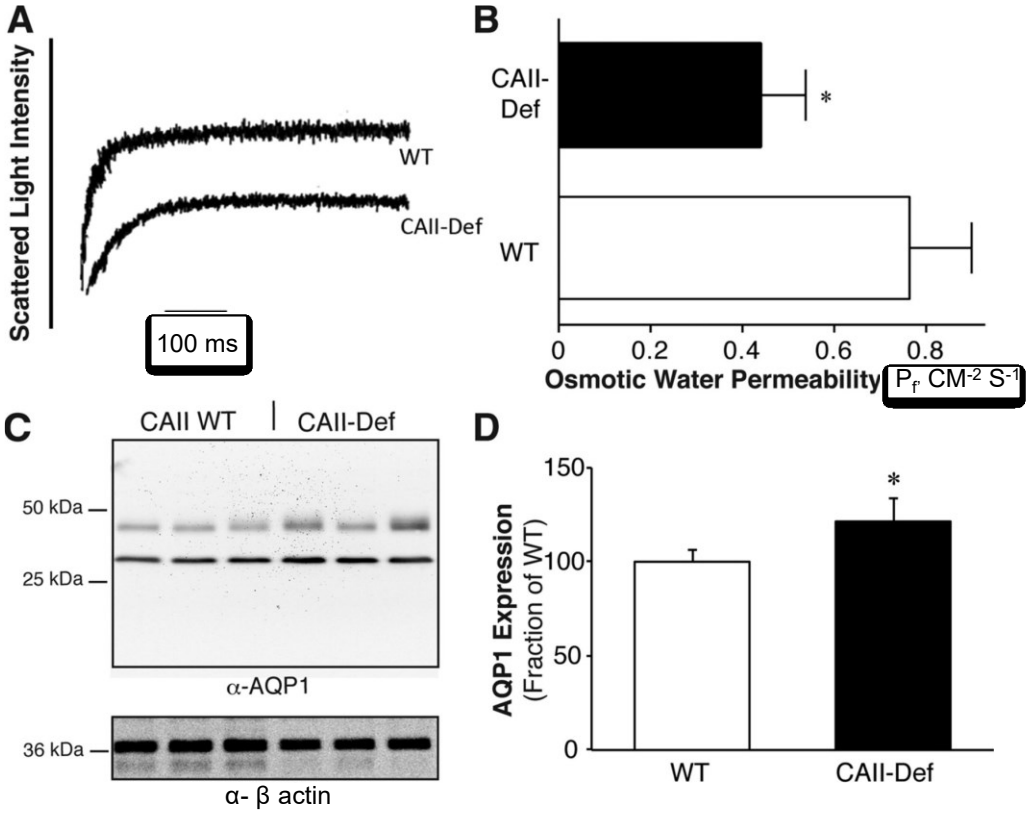

Figure 3.17: CAII-deficient cortical kidney membrane vesicles have reduced water permeability. (A) Representative traces of the light scattering induced by renal cortical membranes from WT and CAII-deficient mice. (B) Osmotic water permeability of kidney cortical membrane vesicles prepared from WT and CAII-deficient mice. (C) Representative immunoblots of cortical kidney membranes isolated from six WT and six CAII-deficient (CAII-def) mice probed for AQP1 and β-actin. (D) Quantification of AQP1 membrane expression normalized to β-actin. Asterisk represents a statistically significant difference ($p < 0.05$) compared with WT.

3.4. Discussion

Data presented here support a physical and functional interaction between CAII and AQP1. The cytosolic C-terminus of AQP1 has two potential CAII binding sites, one of which is identical to AE1's CAII binding region, LDADD. Coexpression studies with AQP1 and CAII in a mammalian cell line demonstrate that CAII enhances water permeation through AQP1. CAII did not increase water permeation through AQP2 in this model system. For CAII to increase water conductance through AQP1, both the AE1 binding region of CAII and the second CAB in AQP1 are essential. PLAs revealed that CAII and AQP1 associate closely in kidney cells and that this association requires an intact CABII in AQP1. Water permeability studies on red blood cell ghosts found increased water flux when the ghosts were resealed in the presence of CAII. Consistent with a role for this interaction *in vivo*, CAII-deficient mice have polyuria, polydipsia and dilute urine relative to their wild-type littermates. AQP1 expression was increased in CAII-deficient mice, potentially as compensation for decreased water conductance through the channel. Water flux across renal cortical membrane vesicles from CAII-deficient mice was greatly reduced relative to vesicles derived from wild-type animals, implying reduced water flux across the proximal tubule of CAII-deficient mice despite higher AQP1 expression. Taken together, these studies identify CAII as an enhancer of water conductance through AQP1.

How might CAII increase water flux through AQP1? A physical association is required, as mutation of the potential binding site in CAII or the potential binding sites in AQP1 significantly attenuated the increased water flux through

AQP1 mediated by wild-type CAII. Moreover, elimination of CABII from the cytosolic C-terminus of CAII not only eliminated the increased water conductance through AQP1 mediated by coexpression with CAII, it also prevented the close association of these two proteins as assessed by a proximity ligation assay. Of importance, these studies do not demonstrate a direct interaction between AQP1 and CAII, as another molecule may contribute to this complex. However, the peptide overlay assay data does support a direct interaction.

The interaction between CAII and other membrane transport proteins increases the transport rate via a mechanism that requires CAII activity. It appears that this is also the case with the interaction between CAII and AQP1, at least in oocytes, since the expression of AQP1 with catalytically inactive V143Y-CAII attenuated the increased flux of water through AQP1 mediated by wild-type CAII. Under these conditions, the proximity of CAII to AQP1 would not have been altered. How CAII activity increases water flux through AQP1 is uncertain. CAII has been proposed to form linear arrays out from the cytosolic face of MCT1 that serve to shuttle protons away from the surface of the transporter (5). In so doing, CAII reduces the local concentration of a substrate of the transporter. This in turn would increase the concentration gradient and consequently the driving force for proton flux through MCT1. Perhaps a similar phenomenon occurs with AQP1 and CAII, but instead of a proton shuttle, water is rapidly funneled away from AQP1 so as to create a larger concentration gradient for it.

We focused on the interaction of CAII and AQP1 in the proximal tubule of the kidney. We did so because this is the site of the greatest amount of water flux

in the body and consequently where increased water flux through AQP1 would be most beneficial. AQP1 and CAII are also expressed in red blood cells. Of interest, the Cl^-/HCO_3^- exchanger AE1 is also abundant in red blood cells, where its transport activity is increased by CAII interaction (20). Our experiments on red blood cell ghosts imply an interaction between CAII and AQP1 in red blood cells. This would be beneficial to the efficient removal of protons from peripheral muscles as well as CO_2. Moreover, this interaction would also facilitate the movement of water and CO_2 into alveoli during respiration, potentially increasing the efficiency of respiration. There is an approximate fivefold excess of CAII in red blood cells relative to AQP1, supporting the possibility of this interaction *in vivo* (1, 39). Blood gas analysis of CAII deficient mice is consistent with this (Table 3-I). The CAII deficient mice demonstrate a respiratory acidosis as documented previously (22). This could, however, simply be due to the absence of CAII, and not secondary to decreased water flux through AQP1.

Acetazolamide is a diuretic that is predominantly prescribed for the prevention of altitude sickness (2, 25). Acetazolamide causes both a diuresis and a mild metabolic acidosis with compensatory tachypnea. In the renal proximal tubule, sodium reabsorption requires the exchange of a luminal Na^+ for a cytosolic H^+ via NHE3. The cytosolic H^+ is provided by the catalysis of H_2O and CO_2 into H^+ and HCO_3^- by CAII. Inhibition of CAII would decrease the substrate available for NHE3, the proximal tubular sodium–proton exchanger, thereby decreasing sodium absorption from the proximal tubule and consequently inducing a natriuresis. The utility of this inhibition to induce a diuresis is limited by

tubuloglomerular feedback. Acetazolamide also blocks water flux through AQP1 directly (15, 26). This could also induce a diuresis. Our findings support a further role for CAII activity in mediating water flux through AQP1. The attenuated water flux across the proximal tubule arising from CAII inhibition might also contribute to the diuresis caused by acetazolamide.

Our observation that CAII increases water flux through AQP1 is not the first suggestion that flux through the channel might be regulated. Increased cGMP increases both water flux and ion permeation through AQP1 (6, 44). Direct phosphorylation of the cytosolic AQP1 C-terminus by protein kinase C also increases water flux through AQP1 (47). Of interest, hypotonic stimuli rapidly translocate endomembrane AQP1 to the plasma membrane, an effect mediated by increased intracellular Ca^{2+} (10). Our findings therefore contribute to the growing body of literature suggesting that water flow through AQP1 might not be static but instead is potentially dynamically regulated.

AQP1 mediates water flux across the capillary endothelium, playing a significant role in ultrafiltration during peritoneal dialysis. Ultrafiltration failure is a common reason for discontinuing peritoneal dialysis and switching to hemodialysis (18). The design of a small molecule that binds to the DADD motif could increase water flux through AQP1 in peritoneal mesothelium, increasing ultrafiltration during peritoneal dialysis. A recent report describes how another small molecule, AqF026, increases water flux by 20% through AQP1 by binding to a separate site of AQP1, the D loop (44). Given the data presented here, a molecule

occupying the DADD motif would be predicted to have a similar if not larger effect on water flux through AQP1.

In nephron, proximal tubule is the place where majority of water reabsorption takes place and coincidently both AQP1 and CAII present in the same segment. CAII interacts with AQP1 in proximal tubule and increases the water reabsorption. This plays a potential role in urine concentration.

In conclusion, we demonstrate that CAII augments water conductance through AQP1 in a mammalian cell culture model. Moreover, the two proteins closely associate with one another in cell culture and colocalize at the brush border membrane of the renal proximal tubule. Maximal water flux through AQP1 requires both CAII activity and the proposed interaction motifs of both AQP1 and CAII. Supplementation with CAII increases water permeability of red blood cell ghosts. The absence of CAII in vivo results in decreased water flux across brush border membrane vesicles from CAII-deficient mice, potentially explaining the polyuria and polydipsia observed in these animals. A CAII-AQP1 interaction likely permits the maximal reabsorption of water from the proximal tubule and may potentially be manipulated to cause a diuresis or increase ultrafiltration in peritoneal dialysis patients.

References

1. **Anstee DJ**. The functional importance of blood group-active molecules in human red blood cells. *Vox Sang* 100: 140-149, 2011.

2. **Bartsch P, and Swenson ER**. Clinical practice: Acute high-altitude illnesses. *N Engl J Med* 368: 2294-2302, 2013.

3. **Becker H, Klier M, and Deitmer J**. Nonenzymatic Augmentation of Lactate Transport via Monocarboxylate Transporter Isoform 4 by Carbonic Anhydrase II. *J Membrane Biol* 234: 125-135, 2010.

4. **Becker HM, and Deitmer JW**. Carbonic anhydrase II increases the activity of the human electrogenic Na^+/HCO_3^- cotransporter. *J Biol Chem* 282: 13508-13521, 2007.

5. **Becker HM, and Deitmer JW**. Nonenzymatic Proton Handling by Carbonic Anhydrase II during H^+-Lactate Cotransport via Monocarboxylate Transporter 1. *Journal of Biological Chemistry* 283: 21655-21667, 2008.

6. **Boassa D, and Yool AJ**. A fascinating tail: cGMP activation of aquaporin-1 ion channels. *Trends Pharmacol Sci* 23: 558-562, 2002.

7. **Brown BF, Quon A, Dyck JR, and Casey JR**. Carbonic anhydrase II promotes cardiomyocyte hypertrophy. *Can J Physiol Pharmacol* 90: 1599-1610, 2012.

8. **Calamita G, Ferri D, Gena P, Carreras FI, Liquori GE, Portincasa P, Marinelli RA, and Svelto M**. Altered expression and distribution of aquaporin-9 in the liver of rat with obstructive extrahepatic cholestasis. *Am J Physiol Gastrointest Liver Physiol* 295: G682-690, 2008.

9. **Chou CL, Knepper MA, Hoek AN, Brown D, Yang B, Ma T, and Verkman AS**. Reduced water permeability and altered ultrastructure in thin descending limb of Henle in aquaporin-1 null mice. *J Clin Invest* 103: 491-496, 1999.

10. **Conner MT, Conner AC, Bland CE, Taylor LH, Brown JE, Parri HR, and Bill RM**. Rapid aquaporin translocation regulates cellular water flow: mechanism of hypotonicity-induced subcellular localization of aquaporin 1 water channel. *J Biol Chem* 287: 11516-11525, 2012.

11. **Endeward V, Musa-Aziz R, Cooper GJ, Chen L-M, Pelletier MF, Virkki LV, Supuran CT, King LS, Boron WF, and Gros G**. Evidence that aquaporin 1 is a major pathway for CO_2 transport across the human erythrocyte membrane. *The FASEB Journal* 20: 1974-1981, 2006.

12. **Fang X, Yang B, Matthay MA, and Verkman AS**. Evidence against aquaporin-1-dependent CO_2 permeability in lung and kidney. *J Physiol* 542: 63-69, 2002.

13. **Faraggiana T, Malchiodi F, Prado A, and Churg J**. Lectin-peroxidase conjugate reactivity in normal human kidney. *J Histochem Cytochem* 30: 451-458, 1982.

14. **Fisher Z, Boone CD, Biswas SM, Venkatakrishnan B, Aggarwal M, Tu C, Agbandje-McKenna M, Silverman D, and McKenna R**. Kinetic and structural characterization of thermostabilized mutants of human carbonic anhydrase II. *Protein Eng Des Sel* 25: 347-355, 2012.

15. **Gao J, Wang X, Chang Y, Zhang J, Song Q, Yu H, and Li X**. Acetazolamide inhibits osmotic water permeability by interaction with aquaporin-1. *Anal Biochem* 350: 165-170, 2006.

16. **Geyer RR, Musa-Aziz R, Qin X, and Boron WF**. *Relative CO_2/NH_3 selectivities of mammalian aquaporins 0-9*. 2013, p. C985-C994.

17. **Hilpert K, Winkler DF, and Hancock RE**. Peptide arrays on cellulose support: SPOT synthesis, a time and cost efficient method for synthesis of large numbers of peptides in a parallel and addressable fashion. *Nat Protoc* 2: 1333-1349, 2007.

18. **Kawaguchi Y, Hasegawa T, Nakayama M, Kubo H, and Shigematu T**. Issues affecting the longevity of the continuous peritoneal dialysis therapy. *Kidney Int Suppl* 62: S105-107, 1997.

19. **Lewis SE, Erickson RP, Barnett LB, Venta PJ, and Tashian RE**. N-ethyl-N-nitrosourea-induced null mutation at the mouse Car-2 locus: an animal model for human carbonic anhydrase II deficiency syndrome. *Proc Natl Acad Sci U S A* 85: 1962-1966, 1988.

20. **Li X, Alvarez B, Casey JR, Reithmeier RAF, and Fliegel L**. Carbonic Anhydrase II Binds to and Enhances Activity of the Na^+/H^+ Exchanger. *Journal of Biological Chemistry* 277: 36085-36091, 2002.

21. **Li X, Liu Y, Alvarez BV, Casey JR, and Fliegel L**. A Novel Carbonic Anhydrase II Binding Site Regulates NHE1 Activity,. *Biochemistry* 45: 2414-2424, 2006.

22. **Lien Y-HH, and Lai L-W**. *Respiratory acidosis in carbonic anhydrase II-deficient mice*. 1998, p. L301-L304.

23. **Loiselle FB, Morgan PE, Alvarez BV, and Casey JR**. *Regulation of the human NBC3 Na^+/HCO_3^- cotransporter by carbonic anhydrase II and PKA*. 2004, p. C1423-C1433.

24. **Lorenz JN, Schultheis PJ, Traynor T, Shull GE, and Schnermann Jr**. Micropuncture analysis of single-nephron function in NHE3-deficient mice. *Am J Physiol*, 277 (3 Pt 2) p. F447-F453,1999.

25. **Low EV, Avery AJ, Gupta V, Schedlbauer A, and Grocott MP**. Identifying the lowest effective dose of acetazolamide for the prophylaxis of acute mountain sickness: systematic review and meta-analysis. *Bmj* 345: e6779, 2012.

26. **Ma B, Xiang Y, Mu SM, Li T, Yu HM, and Li XJ**. Effects of acetazolamide and anordiol on osmotic water permeability in AQP1-cRNA injected Xenopus oocyte. *Acta Pharmacol Sin* 25: 90-97, 2004.

27. **Musa-Aziz R, Chen LM, Pelletier MF, and Boron WF**. Relative CO_2/NH_3 selectivities of AQP1, AQP4, AQP5, AmtB, and RhAG. *Proc Natl Acad Sci U S A* 106: 5406-5411, 2009.

28. **Nakhoul NL, Davis BA, Romero MF, and Boron WF**. Effect of expressing the water channel aquaporin-1 on the CO_2 permeability of Xenopus oocytes. *Am J Physiol* 274: C543-548, 1998.

29. **Nielsen S, Smith BL, Christensen EI, Knepper MA, and Agre P**. CHIP28 water channels are localized in constitutively water-permeable segments of the nephron. *The Journal of Cell Biology* 120: 371-383, 1993.

30. **Pan W, Borovac J, Spicer Z, Hoenderop JG, Bindels RJ, Shull GE, Doschak MR, Cordat E, and Alexander RT**. The epithelial sodium/proton exchanger, NHE3, is necessary for renal and intestinal calcium (re)absorption. *Am J Physiol*, 302: p. F943-F956,2012.

31. **Preston GM, and Agre P**. Isolation of the cDNA for erythrocyte integral membrane protein of 28 kilodaltons: member of an ancient channel family. *Proc Natl Acad Sci U S A* 88: 11110-11114, 1991.

32. **Preston GM, Carroll TP, Guggino WB, and Agre P**. Appearance of Water Channels in Xenopus Oocytes Expressing Red Cell CHIP28 Protein. *Science* 256: 385-387, 1992.

33. **Pushkin A, Abuladze N, Gross E, Newman D, Tatishchev S, Lee I, Fedotoff O, Bondar G, Azimov R, Ngyuen M, and Kurtz I**. Molecular mechanism of kNBC1–carbonic anhydrase II interaction in proximal tubule cells. *J Physiol* 559: 55-65, 2004.

34. **Ruetz S LA, Kopito RR**. Function and biosynthesis of erythroid and nonerythroid anion exchangers. *Soc Gen Physiol Ser* 48: 193-200, 1993.

35. **Sabolic I, Valenti G, Verbavatz JM, Van Hoek AN, Verkman AS, Ausiello DA, and Brown D**. Localization of the CHIP28 water channel in rat kidney. *Am J Physiol* 263: C1225-1233, 1992.

36. **Schnermann J, Chou C-L, Ma T, Traynor T, Knepper MA, and Verkman AS**. Defective proximal tubular fluid reabsorption in transgenic aquaporin-1 null mice. *Proceedings of the National Academy of Sciences* 95: 9660-9664, 1998.

37. **Soderberg O, Gullberg M, Jarvius M, Ridderstrale K, Leuchowius K-J, Jarvius J, Wester K, Hydbring P, Bahram F, Larsson L-G, and Landegren U**. Direct observation of individual endogenous protein complexes in situ by proximity ligation. *Nat Meth* 3: 995-1000, 2006.

38. **Spicer SS, Lewis SE, Tashian RE, and Schulte BA**. Mice carrying a CAR-2 null allele lack carbonic anhydrase II immunohistochemically and show vascular calcification. *The American Journal of Pathology* 134: 947-954, 1989.

39. **Tashian RE CN**. Biochemical genetics of carbonic anhydrase. *Adv Hum Genet* 7: 1-56, 1976.

40. **van Heeswijk MPE, and van Os CH**. Osmotic water permeabilities of brush border and basolateral membrane vesicles from rat renal cortex and small intestine. *J Membrain Biol* 92: 183-193, 1986.

41. **Vilas GL, Loganathan SK, Liu J, Riau AK, Young JD, Mehta JS, Vithana EN, and Casey JR**. Transmembrane water-flux through SLC4A11: a route defective in genetic corneal diseases. *Human Molecular Genetics* 22: 4579-4590, 2013.

42. **Vince JW, and Reithmeier RAF**. Carbonic Anhydrase II Binds to the Carboxyl Terminus of Human Band 3, the Erythrocyte Cl^-/HCO_3^- Exchanger. *Journal of Biological Chemistry* 273: 28430-28437, 1998.

43. **Vince JW, and Reithmeier RAF**. Identification of the Carbonic Anhydrase II Binding Site in the Cl^-/HCO_3^- Anion Exchanger AE1,. *Biochemistry* 39: 5527-5533, 2000.

44. **Yool AJ, Morelle J, Cnops Y, Verbavatz J-M, Campbell EM, Beckett EAH, Booker GW, Flynn G, and Devuyst O**. AqF026 Is a Pharmacologic Agonist of the Water Channel Aquaporin-1. *Journal of the American Society of Nephrology* 24: 1045-1052, 2013.

45. **Zhang J, Tackaberry T, Ritzel MW, Raborn T, Barron G, Baldwin SA, Young JD, and Cass CE**. Cysteine-accessibility analysis of transmembrane domains 11-13 of human concentrative nucleoside transporter 3. *Biochem J* 394: 389-398, 2006.

46. **Zhang R, Skach W, Hasegawa H, van Hoek AN, and Verkman AS**. Cloning, functional analysis and cell localization of a kidney proximal tubule water transporter homologous to CHIP28. *The Journal of Cell Biology* 120: 359-369, 1993.

47. **Zhang W, Zitron E, Homme M, Kihm L, Morath C, Scherer D, Hegge S, Thomas D, Schmitt CP, Zeier M, Katus H, Karle C, and Schwenger V**. Aquaporin-1 channel function is positively regulated by protein kinase C. *Journal of Biological Chemistry* 282: 20933-20940, 2007.

CHAPTER 4

Effect of dietary sodium on urinary calcium secretion

The experiments where mice were fed with different sodium containing diets was performed by Dr. Henrik Dimke, however, analysis of this experiment, including immunoblotting and quantitative real-time PCR was performed by Devishree Krishnan

The human experiment was carried out by Dr. Bramm, however, urinary analysis of calcium, creatinine and sodium was completed by Devishree Krishnan.

4.1. Introduction

Calcium (Ca^{2+}) homeostasis is important for many physiological functions. It is maintained by the gut, bone and kidney (9, 17). Ingested calcium is absorbed from the intestine into the blood. Absorbed Ca^{2+} can be either deposited into bone or filtered by the glomerulus and reabsorbed along the nephron or excreted in the urine (17). The excretion of urine with more/less Ca^{2+} is referred to as hyper or hypocalciuria respectively. In the nephron, 65% of Ca^{2+} is reabsorbed from the proximal tubule, 20% by the thick ascending limb, 10% by the distal convoluted tubule and connecting tubules and there is no reabsorption from the collecting ducts (9, 19). Recently Worcester and colleagues demonstrated that in individuals with hypercalciuria, the proximal tubule failed to reabsorb calcium from the glomerular filtrate, causing their disease (22).

Calcium is reabsorbed from the proximal tubule, via a passive paracellular process that is dependent on sodium reabsorption. The active transcellular flux of sodium across the proximal tubule could mediate passive paracellular calcium reabsorption by two potential mechanisms. 1. The removal of water from the lumen may concentrate the calcium concentration, which is then reabsorbed down a chemical gradient or 2. Water flux from lumen to blood drives calcium into the interstitium via a process called solvent drag. This latter process is essentially convection-mediated transport of calcium by the osmotically driven water. Regardless of the exact mechanism, both processes infer proximal tubule sodium transport facilitates calcium reabsorption from this segment (3, 17). The majority of sodium reabsorption from the proximal tubule occurs through the apical

membrane via the sodium proton exchanger isoform 3, NHE3 (2, 12, 15). Pan et al have implicated NHE3 in Ca^{2+} homeostasis (17). NHE3 knockout mice have hypercalciuria and osteopenia.

Ingested Ca^{2+} is absorbed into the blood through the intestine via two distinct pathways: transcellular and paracellular (2). Transcellular absorption from the intestine is mediated at least in part by TRPV6, calbindin-D_{9K} and PMCa1b. Claudin-2 and -12 are involved in paracellular absorption, putatively making a Ca^{2+} permeable pore (2). In the proximal tubule, Ca^{2+} reabsorption occurs paracellularly through the tight junction (TJ). The TJ proteins involved in this reabsorption are claudins. Claudin-2 has been specifically implicated, however the identity of other claudins involved in this transport process are not known (14). What has been appreciated is that the paracellular transport of Ca^{2+} across the proximal tubule is dependent on Na^{+} transport via NHE3 (Figure 4.1B).

In the thick ascending limb (TAL) of the loop of Henle, claudin-16 and -19 form a paracellular cation permeable pore permitting the reabsorption of Ca^{2+} (Figure 4.1C) (10, 11, 20). Increased claudin-14 expression in the TAL occurs in response to CaSR signaling. Claudin-14 acts as a cation blocker to increase urinary Ca^{2+} excretion thereby maintaining blood Ca^{2+} levels (5). In the distal convoluted tubule (DCT), Ca^{2+} transport occurs by active transcellular transport. TRPV5, Calbindin D_{28K} and NCX are the proteins involved in this process (Figure 4.1D). PTH and the active form of vitamin D increase the expression of these proteins, inducing Ca^{2+} reabsorption from the DCT (6, 9).

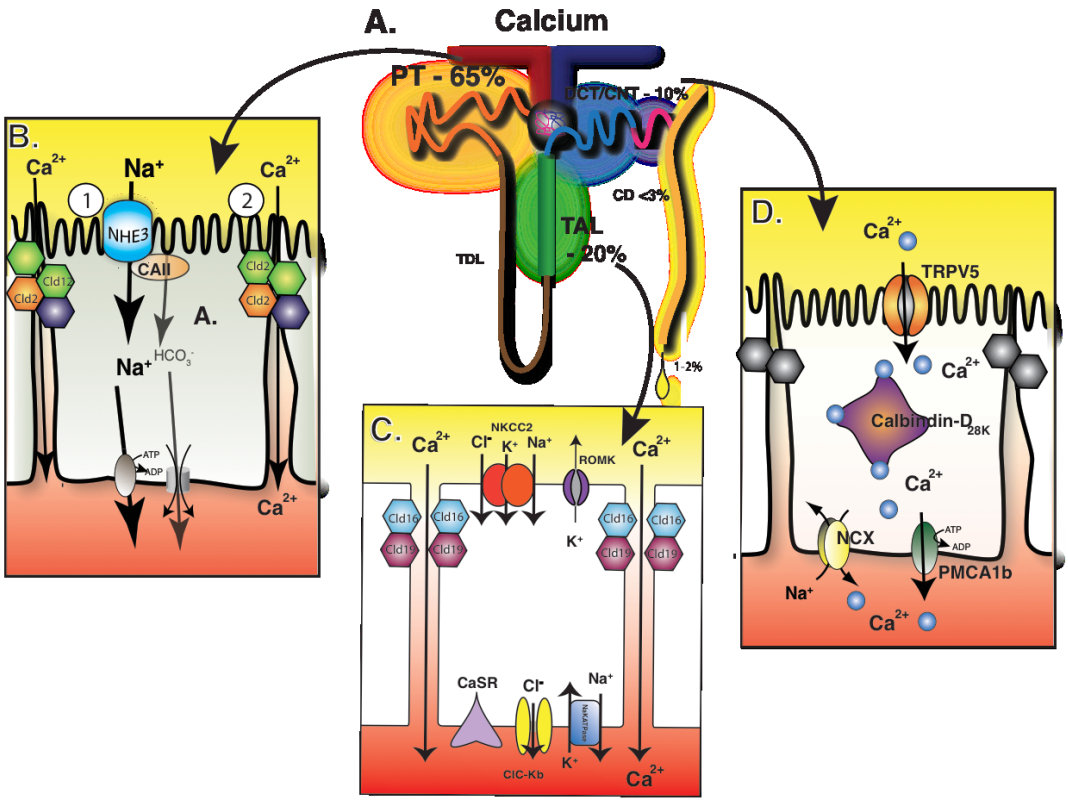

Figure 4.1: Schematic representation of calcium reabsorption along the nephron A) Representation of the fraction of calcium reabsorption from different nephron segments, B) Proximal tubular calcium reabsorption. Apical NHE3 reabsorbs calcium from the lumen, either creating the solvent drag or a chemical gradient for calcium to move through the tight junction proteins Claudin-2 and potentially -12. C) Thick ascending limb calcium reabsorption. Sodium reabsorption through the apical membrane transporter NKCC2, drives paracellular calcium flux through a pore generated by claudin-16 and -19. D) Active transcellular calcium reabsorption from the distal convoluted tubule occurs via TRPV5, $Calbindin_{D28K}$ and NCX/PMCA1b.

In humans, increased sodium ingestion leads to stroke, heart and kidney disease (4, 21). One of the main transporters in the renal proximal tubule, maintaining sodium reabsorption and intravascular volume homeostasis, is NHE3. The activity of this transporter is regulated through the renin-angiotensin-aldosterone system (RAAS) (7, 8, 23). Increased sodium ingestion also leads to increased calcium excretion (16, 18). The converse is also true and is used as a treatment for hypercalciuria. However, the mechanism mediating this is not known. Given the link between sodium ingestion and calcium excretion, and the previous work implicating NHE3 in calcium reabsorption we hypothesize that increased sodium ingestion decreases NHE3 activity, by decreasing renin and angiotensin II (AngII), thereby increasing urinary calcium excretion.

To address this hypothesis we fed mice a normal or high salt diet and examined renal sodium and calcium transport pathways. Although renin was decreased in high Na^+ diet, there was no change in expression of sodium or calcium transport proteins. Further studies were carried out in a proximal tubular cell culture model. The addition of AngII increased NHE3 activity and cell surface expression. Together our results support a pathway whereby increased sodium ingestion suppresses AngII expression, NHE3 activity and consequently proximal calcium reabsorption. This in turn leads to hypercalciuria.

4.2. Materials and Methods:

4.2.1. Cell culture studies

Opossum kidney (OK) cells were purchased from ATCC. Cells were grown in DMEM/F12 supplemented with 10% FBS, 100 U/ml penicillin, and 100 µg/ml streptomycin. OK cells were stably transfected with a rat NHE3 construct containing three sequential HA tags (YPYDVPDYAS) in the first extracellular loop ($NHE3_{38HA3}$). Stable cell lines (OK-$NHE3_{38HA3}$) were selected by cloning via limiting dilution in the presence of 750 µg/ml G418 and screened by immunofluorescence of the HA-tagged NHE3 (1).

4.2.2. Animal experiment

Wild-type FVB mice were purchased from Jackson Laboratories (Bar Harbor, ME). Mice were housed in virus-free conditions and maintained on a 12 h light/dark schedule. Mice were fed either a control (0.8% [wt/wt] NaCl) or high salt (8% [wt/wt] NaCl) diet for 7 days with drinking water available ad libitum (n=8 in each group). On the last day they were housed in metabolic cages for 24 h then anesthetized with pentobarbital, and blood was withdrawn by perforating the orbital vessels and used to measure sodium, potassium, ionized calcium, hematocrit, Hb, glucose, pH, pCO_2, pO_2, bicarbonate (with a VetScan i-STAT 1 Analyzer, Abaxis, Union city, CA, USA). Kidneys were then removed and snap frozen in liquid nitrogen. All experiments were performed in compliance with the animal ethics board at the University of Alberta, Health Sciences Section, protocol number 576.

4.2.3. Urinary calcium

Total Ca^{2+} in urine was determined using a colorimetric assay kit (Quantichrom TM Ca^{2+} Assay Kit, BioAssay System, Hayward, CA, USA) as per the manufacturer's protocol. In brief, standards and urine samples were pipetted into a 96-well plate. Working reagent was added and the plate was incubated for 3 mins at room temperature. Absorbance was measured at 570-650 nm using a monochromator-based microplate reader (Synergy Mx, Biotek, USA).

4.2.4. Urinary creatinine

Urinary creatinine was measured using the Creatinine Parameter Assay Kit (R&D Systems Inc., Minneapolis, MN, USA). All samples, standards and controls were prepared as per the manufacturer's protocol. To each well containing the standard, control or sample, alkaline picrate solution was added and then the 96-well plate was incubated for 30 mins at room temperature. The optical density of each well was measured at 490 nm using a monochromator-based microplate reader (Synergy Mx, Biotek, city, state, USA).

4.2.5. RNA isolation

Total mRNA was isolated from half a kidney using TRIzol Reagent (Invitrogen, Carlsbad, CA, USA) as per the manufacturer's instructions. Half a snap frozen kidney was homogenized in ice-cold TriZol and to this chloroform (Invitrogen, Carlsbad, CA, USA) was added. The aqueous phase was separated and then mixed with isopropanol after which it underwent centrifugation at 4 °C, 12000g for 15 mins. The pellet obtained was washed with 70% ethanol and then air-dried. The pellet was next dissolved in RNAse free water and 10X DNase

buffer and DNase added. RNA was precipitated using an ice-cold phenol:chloroform (1:1) mixture. 3M NaAC at pH 5.2 and 100% ethanol were then added to the RNA after which it was incubated overnight at -20 °C, or for 2 h at -80 °C. The solution was centrifuged and the pellet was washed in 70% ethanol before air-drying. The pellet was finally dissolved in RNAse free water and the concentration determined using a spectrophotometer (Nanodrop 2000c, ThermoScientific, Asheville, NC, USA).

4.2.6. Quantitative PCR

Isolated total mRNA was reverse transcribed into cDNA. 1µg of isolated mRNA from whole kidney, 3 µg/µl of random hexamers (Invitrogen, Carlsbad, CA, USA) and RNAse free water was added together and incubated at 70 ºC for 10 mins. Following this 5X buffer provided with SuperScript II (SSII) (Invitrogen, Carlsbad, CA, USA), 0.1 M DTT (Invitrogen, Carlsbad, CA, USA), 25 µM dNTP (Invitrogen, Carlsbad, CA, USA), 40 U/µl RNase Out (Invitrogen, Carlsbad, CA, USA), and 1 µl SSII (Invitrogen, Carlsbad, CA, USA) were added to the mixture and incubated at 40 ^{o}C for 1 h in a C1000 Thermal cycler (BioRad, Mississauga, ON, Canada) to synthesize cDNA.

For quantitative real time PCR, 5 µl (500 ng cDNA) was used as a template to determine the gene expression of NHE3, NKCC2, GAPDH, ENaC, NCC, $Calb_{D28K}$, TRPV5, PMCA1b, SLC8a1, renin, claudin-2, -12, -14, -15, -16 and -19. A mixture consisting of TaqMan universal qPCR master mix (Applied Biosystems Inc, Foster City, CA, USA), primer, probe and RNAse free water was prepared and added to the cDNA in a 96-well plate (Sarstedt Inc, Montreal, QC, Canada). As an

internal control mRNA levels of the housekeeping gene 18S ribosomal RNA were determined. Expression levels were quantified with an ABI Prism 7900 HT Sequence Detection System (Applied Biosystems Inc, Foster City, CA, USA). Primers and probes were made by IDT (Integrated DNA Technologies Inc, San Diego, CA, USA) or ABI (Applied Biosystems Inc, Foster City, CA, USA). The sequences of all primers and probes utilized are listed in Table 4.1 18S was chosen for normalization of RNA as none of the experimental perturbations resulted in a significant change in its expression.

Table 4.1: Real time PCR primers and probes

	Sequence
NHE3	Forward: CTC CCC AAG TAC GGA CAA TAT G Reverse: TCT GTT CCA AGG ACT GCA TG
NKCC2	Forward: TGC TAA TGG AGA TGG GAT GC Reverse: CAG GAG AGG CGA ATG AAG AG
GAPDH	Forward: TTGGCCGTATTGGGCGCCTG Reverse: TCGGCCTTGACTGTGCCGTTG
ENaC	Forward: GCACCCTTAATCCTTACAGATACACTG Reverse: CAAAAAGCGTCTGTTCCGTG
NCC	Forward: TCT CCT TTG CCA ACT ACC TG Reverse: CTA CCA TCA ATG CCT CTC CAG
Calb28K	Forward: AGAACTTGATCCAGGAGCTTC Reverse: CTTCTGTGGGTAAGACGTGAG Probe: AGGCTGGATTGGAGCTATCACCG
TRPV5	Forward: CAGACCCCAGTGAAGGAGCTGGT Reverse: ATCTCGGAACTTGAGGGGGCGG
PMCA1b	Forward: CGCCATCTTCTGCACCATT Reverse: CAGCCATTGCTCTATTGAAAGTTC Probe: CAGCTGAAAGGCTTCCCGCCAAA
SLC8a1 (NCX)	Forward: TGGTCTGAAAGATTCCGTGAC Reverse: AGTGACATTGCCTATAGACGC Probe: CGTAAGAACCAACGGTCTCCCAGG
Claudin 2	Forward: GCATTGTGACGGCGGTTGGC Reverse: GTGGCAAGAGGCTGGGCCTG
Claudin 12	Forward: TGTCGCAGGCCTCTTTGCGG Reverse: CCACAGGCCCGTGTAAATCGTCA
Claudin 14	Forward: TGGCGCTGCCCCGGGATCT Reverse: TGGTAGCTCCGGCCCTGGAC
Claudin 15	Forward: GGCCAAAGCCCCCGGAATTCA Reverse: CTCCAGTAGCTGTTTGAAAGGGTCAA
Claudin 16	Forward: CGTGAAAGACTGGGCACTATCATCCC Reverse: AGTCTGTCCAGGTGGCCACGA
Claudin 19	Forward: CCGCCGCTGTCGCTCCTTTA Reverse: ACACTGAGCGTCGTTATCACACGAA
Renin	Forward: CAGCGACCCGGAGCATTA Reverse: TCAGTCTTGCTGAGGCTCACA

4.2.7. Protein extraction

Total protein was extracted from kidney with RIPA buffer (50 mM Tris, 150 mM NaCl, 1 mM EDTA, 1% Triton X-100, 0.1% SDS, 1% lgepal CA-630, pH 7.4) containing a protease inhibitor cocktail (Calbiochem, Gibbstown, NJ). The tissue was homogenized by mortar and pestle and incubated on ice for 60 min. The extracted protein solution was collected after centrifuging at 14,000 *g* for 15 min at 4 °C. The protein concentration was determined using a spectrophotometer (Nanodrop 2000c, ThermoScientific, Asheville, NC, USA). The samples were stored at −80 °C until used.

4.2.8. Immunoblotting

Equal amounts of total protein were separated by SDS–PAGE and electrotransferred onto Immobilon-P polyvinylidene fluoride membranes (Millipore, Billerica, MA) for 1 h at a constant current of 400 mA. After transfer, membranes were rinsed in TBS (in mM: 150 NaCl, 50 Tris-HCl, pH 7.5) and incubated with TBS-TM (TBS containing 0.1% [vol/vol] Tween-20 and 5% [wt/vol] skim milk) for 1 h at room temperature with gentle rocking to block nonspecific binding. Membranes were then incubated for 16 h at 4 °C with gentle rocking in the presence of either anti-NHE3, NKCC2, ENaC, NCC, or Claudin -2; all at 1:1000 dilution in TBS-TM. After successive washes with TBS-T (TBS containing 0.1% [vol/vol] Tween-20), the membranes were incubated with a 1:5000 dilution of the appropriate HRP-conjugated secondary antibody in TBS-TM for 2 h at 20 °C and then washed further with TBS-T. Proteins were detected using Western Lightning Chemiluminescence Reagent Plus (PerkinElmer, Waltham,

MA) and immunoreactive bands were visualized with a Carestream Advanced Fluorescent Imaging F PRO image station (Carestream Health, Rochester, NY).

4.2.9. Cell surface expression of NHE3

OK cells were stably transfected with a rat NHE3 construct containing three sequential HA tags (YPYDVPDYAS) in the first extracellular loop (NHE3'$_{38HA3}$). Cells were grown on 12 well plates for 24 h in DMEM/F12 supplemented with 10% FBS, 100 U/ml penicillin, and 100 µg/ml streptomycin. For 24 h before the experiment, the cells were incubated with DMEM/F12 with no supplements. The cells were incubated with either vehicle or 100 µM of AngII at 37 ºC 2 h before experiments. After washing the cells with PBS with 1 mM $MgCl_2$ and 1 mM $CaCl_2$ they were fixed with 2% paraformaldehyde on ice for 20 min. After the incubation, cells were quenched with 5% glycine and blocked with 5% PBS milk with or without Triton-X 100. Then a 1:1000 dilution of the primary antibody (mouse anti-HA in PBS milk) was added and incubated for 2 h at 20 ºC. After successive washes with PBS, the cells were incubated with a 1:5000 dilution of the appropriate HRP-conjugated secondary antibody in PBS milk for 1 h at 20 °C and then washed further with PBS. TMB substrate was added to the plate and the optical density of each well was measured at 450 nm using a monochromator-based microplate reader (Synergy Mx, Biotek, city, state, USA).

4.2.10. Measurement of Na^+/H^+ exchanger activity in the absence of CO_2

OK cells stably expressing NHE3$_{38HA3}$ were grown on coverslips in DMEM/F12 media supplemented with 10% FBS, 100 U/ml penicillin, and 100 µg/ml streptomycin. On the day before experiments the media was changed to

DMEM/F12 with no supplements. Cells were incubated with either vehicle or 100 μM of AngII 2 h before the experiment at 37 ºC. At the time of the experiment cells were washed with DMEM/F12 media and loaded with BCECF-AM. Next the cells were rinsed with iso Na^+ buffer (140 mM NaCl, 1 mM $MgCl_2$, 1 mM $CaCl_2$, 3 mM KCl, 10 mM glucose, and 5 mM HEPES, pH 7.4) to remove excess probe and then placed inside a fluorescence cuvette where the coverslip was held immobile with a holder device. pHi was determined with a PTI-Fluorometer (LPS-220B, PTI). The cells were perfused with iso Na^+ buffer, containing 10 mM NH_4Cl for 10 min before acidifying the cells by perfusing them with iso K^+ buffer (140 mM KCl, 1 mM $MgCl_2$, 1 mM $CaCl_2$, 10 mM glucose, and 20 mM HEPES, pH 7.4) for 2 min. The recovery of pH in cells transfected with NHE3 and treated with AngII or in the absence of AngII was then induced by perfusing cells with iso Na^+ buffer. Calibration was performed with a high K^+-containing buffer with 10 mM nigericin for each individual coverslip. NHE3 activity was calculated as the change in pH over the first 30 s after iso Na^+ buffer readdition.

4.2.11. Human diets

A 24 h urine was collected from 12 healthy human volunteers. They then ingested a low sodium diet (less than 500 mg per day) for 7 days. On the last day of the low sodium diet another 24 h urine was collected. The subjects then proceeded to go back on a diet where sodium was not restricted for 7 days. The last day of this diet a 24 h urine was collected. The protocol was approved by the University of Alberta Human ethics committee. Urine creatinine and calcium were determined as above.

4.2.12. Statistical analysis

Data are presented as means ±SE. Paired or unpaired Student's t-tests or ANOVA was carried out to determine statistical significance as appropriate. Tests were performed using Excel software (Microsoft, Santa Monica, CA), and P values <0.05 were considered statistically significant.

4.3 Results

4.3.1. In humans, increased sodium ingestion increases urinary calcium excretion

Healthy human volunteers ingested a diet containing low sodium (less than 500 mg per day) for a week. The day before and on the last day of this diet, 24 h urine was collected. The volunteers then ingested an unrestricted diet and were encouraged to eat sodium for 7 days. On the final day, another 24 h urine was collected. Urinary sodium excretion decreases on a low sodium diet as expected. Further both total urinary calcium excretion and the fractional excretion of calcium decreased on a low sodium diet and then increased on a higher sodium diet (Figure 4.2 B&C). The relationship between urinary sodium and calcium excretion is best appreciated in Figure 4.2 D, where it is apparent that the two processes are somewhat proportional.

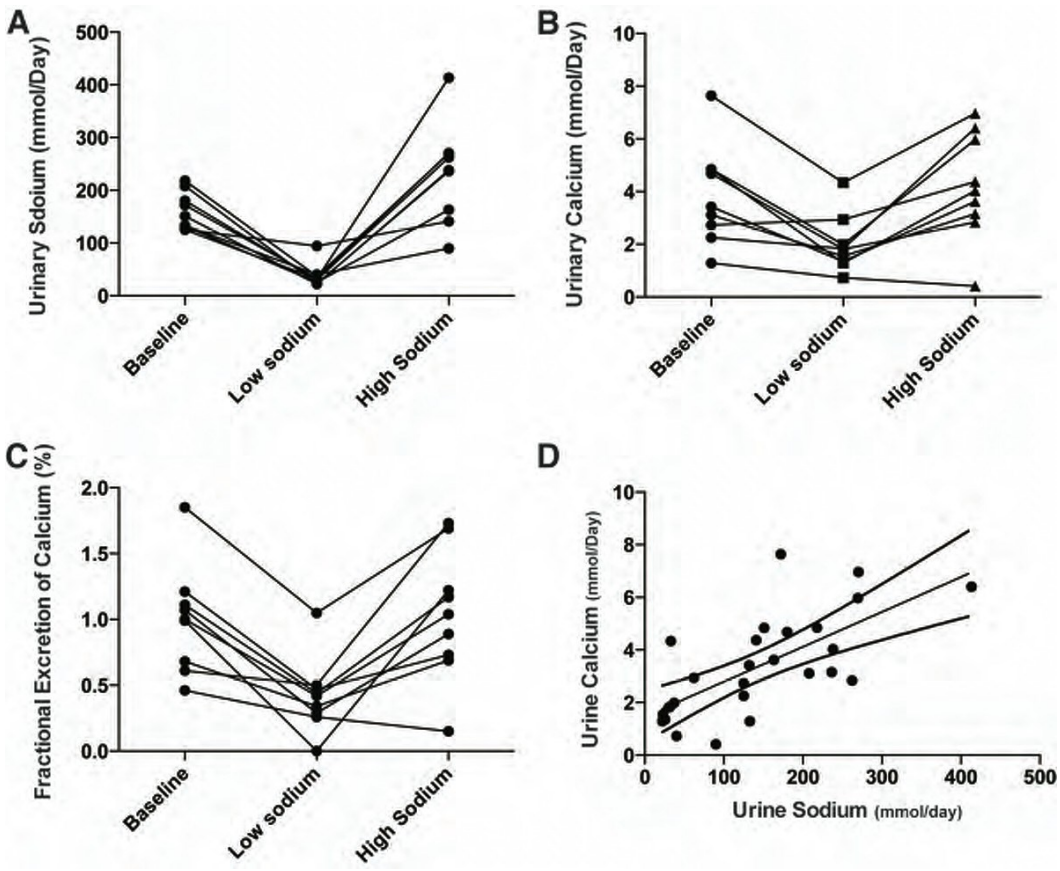

Figure 4.2. In humans, sodium ingestion mirrors urinary calcium excretion. A) Total urinary sodium excretion from volunteers on a normal, low and high sodium diet, B & C) Total urinary calcium excretion and the fractional excretion of calcium decreased on a low sodium diet and then increased on a higher sodium diet. D) The relationship between urinary sodium and calcium excretion. Values are mean ±SE. n=8 in each group.

4.3.2. In mice, a high sodium diet increases calcium excretion in urine

Wildtype FVB mice were placed on a normal (0.8% [wt/wt]), or high (8% [wt/wt]) Na^+ diet for 7 days. The average weight of the animals was the same at the beginning and end of the experimental period. The amount of water consumed was significantly higher in the high salt diet group as was urine volume. There was no difference in food intake between the two groups (Table 4.3). Mice on the high Na^+ diet showed a slight decrease in blood pH at the end of 7 days. There was no difference in HCO_3^- and Hct, however PCO_2 was significantly higher in animals on the high salt diet (Table 4.2). The serum electrolyte sodium was higher in animals on a high salt diet. Urinary sodium excretion was higher in the animals fed a high salt diet. Consistent with the human data, urinary calcium excretion was significantly higher in mice fed a high sodium diet; both total 24 h urine Ca^{2+} excretion and when calcium excretion was normalized to creatinine excretion, to avoid possible changes in glomerular filtration rate between dietary groups. The urinary Ca^{2+} /creatinine ratio increased proportionally to the amount of Na^+ in the diet (Table 4.5). Together these results clearly demonstrate that increased sodium ingestion increases urinary calcium excretion.

Table 4.2: WT: Blood-gas analysis

Diets	pH	P_{CO2}, mm Hg	HCO_3^-, mM	HCT
Control	7.34± 0.01	37.68 ± 2.32	19.93 ± 1.01	0.38 ± 0.006
High Na	7.29± 0.01*	45.14 ± 1.56 *	21.93 ± 0.94	0.39 ± 0.004

Values are mean ±SE. n= 12 in each group. *p <0.05, when compared with control.

Table 4.3: WT: Metabolic cage data

Diets	Weight, g (Day 0)	Weight, g (Day 1)	Δ weight, g	H_2O Drunk, ml/24h	Chow Eaten, g/24 h	Urine Volume, ml/24 h
Control	23.83 ± 0.69	22.43 ± 0.56	-1.40 ± 0.21	5.23 ± 0.54	3.07 ± 0.26	0.46 ± 0.11
High Na	23.39 ± 0.63	21.79 ± 0.66	-1.58 ± 0.38	10.95 ± 1.49 **	3.01 ± 0.44	4.27 ± 0.63 **

Values are mean ±SE. n= 11 in each group. **p <0.005 when compared with control.

Table 4.4: WT: Serum electrolytes

Diets	Na^+, mM	K^+, mM	Ca^{++}, mM
Control	145.7 ± 0.6	4.95 ± 0.17	1.04 ± 0.02
High Na	148 ± 0.6 **	5.05± 0.17	1.09 ± 0.01 *

Values are mean ±SE. n= 12 in each group. *p <0.05, **p <0.005 when compared with control.

Table 4.5: WT: Urine electrolytes

Diets	Ca^{2+}, µmol/24 h	Creatinine, µmol /24 h	Ca^{2+}/Creatinine Ratio (mM/ mM)
Control	1.87 ± 0.5	2.77 ± 0.56	0.72 ± 0.07
High Na	5.99 ± 1.61 *	3.24 ± 0.35	2.01 ± 0.52 *

Values are mean ±SE. n= 8in each group. *p <0.05, **p <0.005 when compared with control.

4.3.3. RNA expression in whole kidney

To examine the molecular mechanism mediating this relationship we first looked at the expression of renal sodium transporting proteins. NHE3 is present both in proximal tubule and thick ascending limb, NKCC2 is in the thick ascending limb and ENaC in the collecting duct. These transporters play a central role in the reabsorption of sodium from these segments. The renal mRNA expression of NHE3, NKCC2, and ENaC was not altered by ingestion of a diet with either normal or high Na^+ content (Figure 4.3). All samples were normalized to the expression of 18S, as we were unable to detect a difference in the expression level of 18S between different diets.

We next examined the expression of sodium and calcium transporting proteins in the DCT. The expression of NCC, Calb28K and NCX (SLC8a1) were significantly higher in animals fed a high salt diet. There was no significant difference in other calcium transporters expressed in this segment including TRPV5 and PMCA1b.

We then turned to examine the expression of TJ proteins implicated in paracellular calcium flux. There was no alteration in renal claudin-2, -12, -14, -16 and -19 expression observed in mice on a high salt diet after 7 days (Figure 4.3). Claudin -2 and -12 have been implicated in calcium reabsorption from the intestine and Claudin -14, -16, -19 are involved in paracellular calcium reabsorption from the TAL.

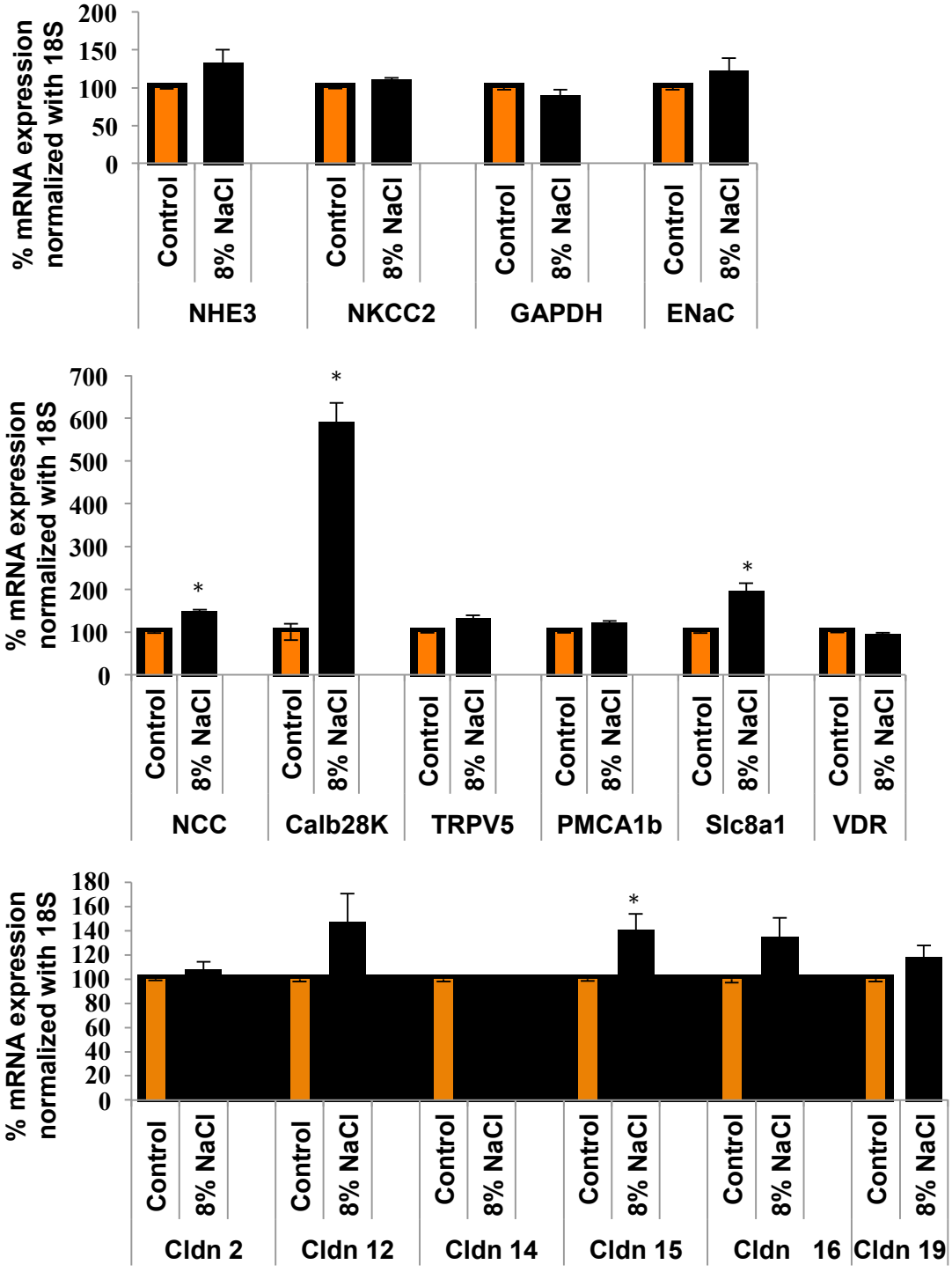

Figure 4.3: mRNA expression in whole kidney from WT mice fed either a normal or high salt diet. The first panel shows the mRNA expression of NHE3, NKCC2, GAPDH, ENaC The second panel is the mRNA expression of NCC, Calb28K, TRPV5, PMCA1b, Slc8a1, VDR. The third panel displays the mRNA expression of claudin -2, -12, -14, -15, -16, -19. Expression is normalized to 18S, values are mean ±SE. n=6-12 per group. *p <0.05 when compared with control.

4.3.4. Protein expression in whole kidney

Although there were only minimal changes in mRNA expression of sodium and calcium transporting genes, not in the direction predicted, there may be alterations in protein expression. We therefore examined the expression of proteins for which antibodies were available by semi-quantitative immunoblotting. Many sodium transporters are involved in sodium reabsorption from the pro-urine. Of those transporters NHE3, NKCC2, NCC and ENaC are the main transporters involved. Semi-quantitative immunoblotting revealed no difference in protein expression between mice fed either a high salt or normal diet (Figure 4.4). As a loading control, membranes were stripped and blotted for β-actin.

A

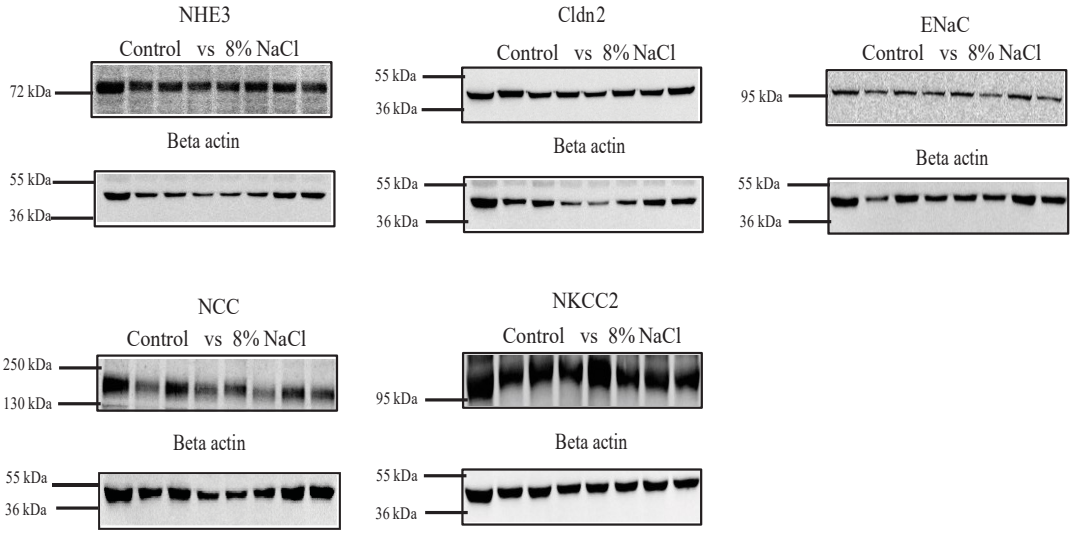

B

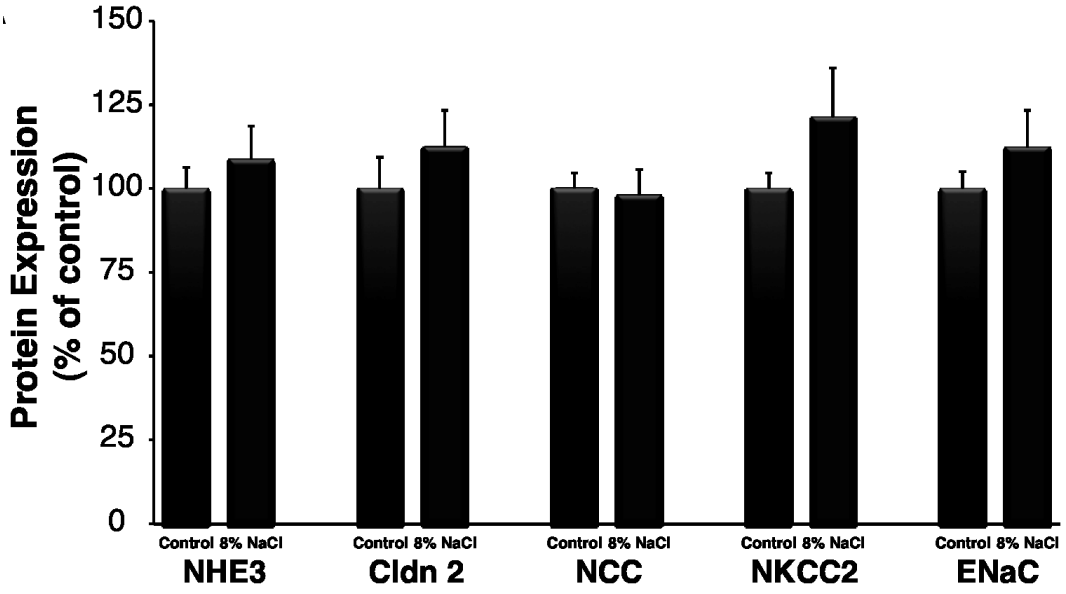

Figure 4.4: Protein expression in whole kidney from mice fed either a normal or high salt diet. A) Representative western blots and B) quantitation of protein expression normalized to β -actin. Values are mean ±SE. n=8 in each group.

4.3.5. Renin mRNA expression in whole kidney

Renin is a hormone, which is synthesized in the juxtraglomerulus apparatus. Renin is involved in the regulation of aldosterone and stimulates AngII levels. These hormones are also involved in the regulation of sodium reabsorption from different segments of the nephron. The mRNA expression of renin from whole kidney was determined using quantitative PCR. We observed that renal mRNA expression of renin is significantly reduced in mice on a high salt diet (Figure 4.5).

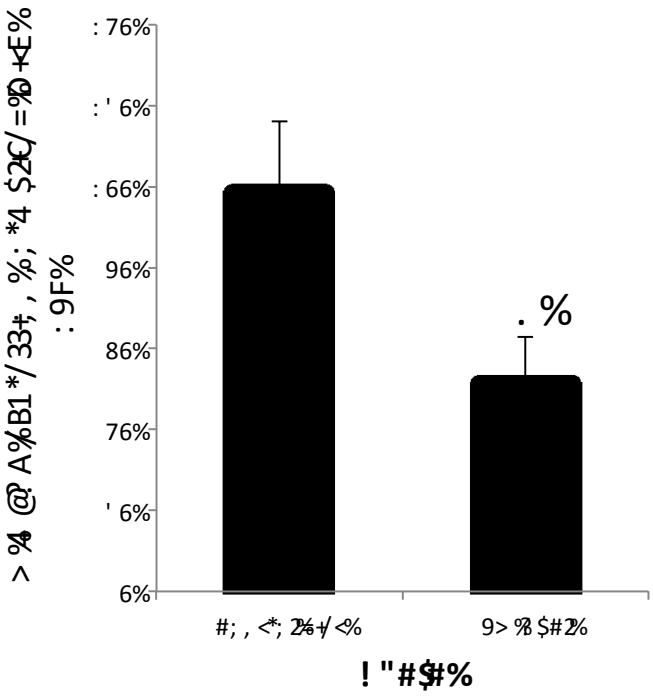

Figure 4.5: mRNA expression of renin in whole kidney from mice fed either a normal or high salt diet normalized to 18S as determined. Values are mean ±SE. n=8-12 in each group. *p <0.05 when compared with control.

4.3.6. Cell surface expression of NHE3 in the presence of AngII

In order to link altered NHE3 activity mediated by AngII to altered proximal tubular calcium flux we turned to a cell culture model. To determine the surface expression of NHE3 in the presence and absence of AngII, OK cells stably expressing NHE3 with a HA tag were treated with vehicle or AngII. The extracellular HA epitope was then used to assess the surface expression of NHE3 via a colorimetric assay. In the presence of AngII surface NHE3 expression is significantly increased. Importantly in parallel, cells were treated with Triton-X 100 before the assay to measure total NHE3 expression (which was not altered by AngII) (Figure 4.6).

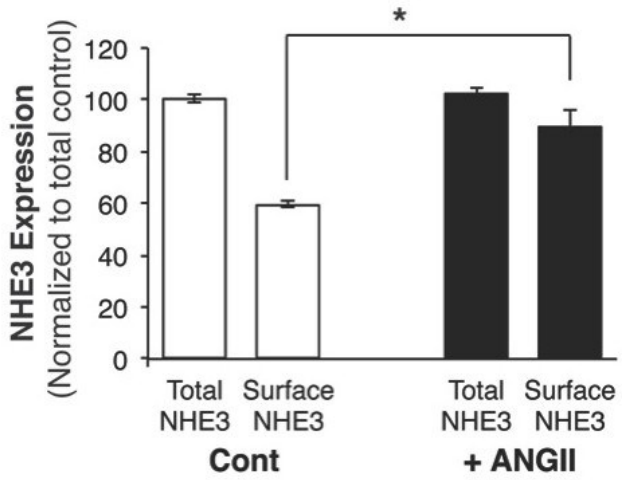

Figure 4.6: Cell surface expression of NHE3 in the presence and absence of AngII. NHE3 with an extracellular HA was transfected into OK cells. The cells were treated with AngII or vehicle (control), 100 nM dose for 2 h. The experiment was performed for total HA (with Triton X100) or surface HA (without Triton X100) with or without the 100 nM AngII incubation for 2 h at 37 °C. Values are mean ±SE. n=6. *$p<0.05$.

4.3.7. AngII increased Na^+/H^+ exchanger activity

To ascertain the effect of AngII on NHE3 activity we performed the assay in the absence of bicarbonate and CO_2, in cells acidified by an ammonium chloride prepulse. Cells stably expressing NHE3 demonstrated a significant increase in recovery from an acid load, when treated with AngII for 2 h before the experiment (Figure 4.7). Taken together, these results demonstrate that AngII increases the surface expression of NHE3 thereby stimulating the exchanger's activity.

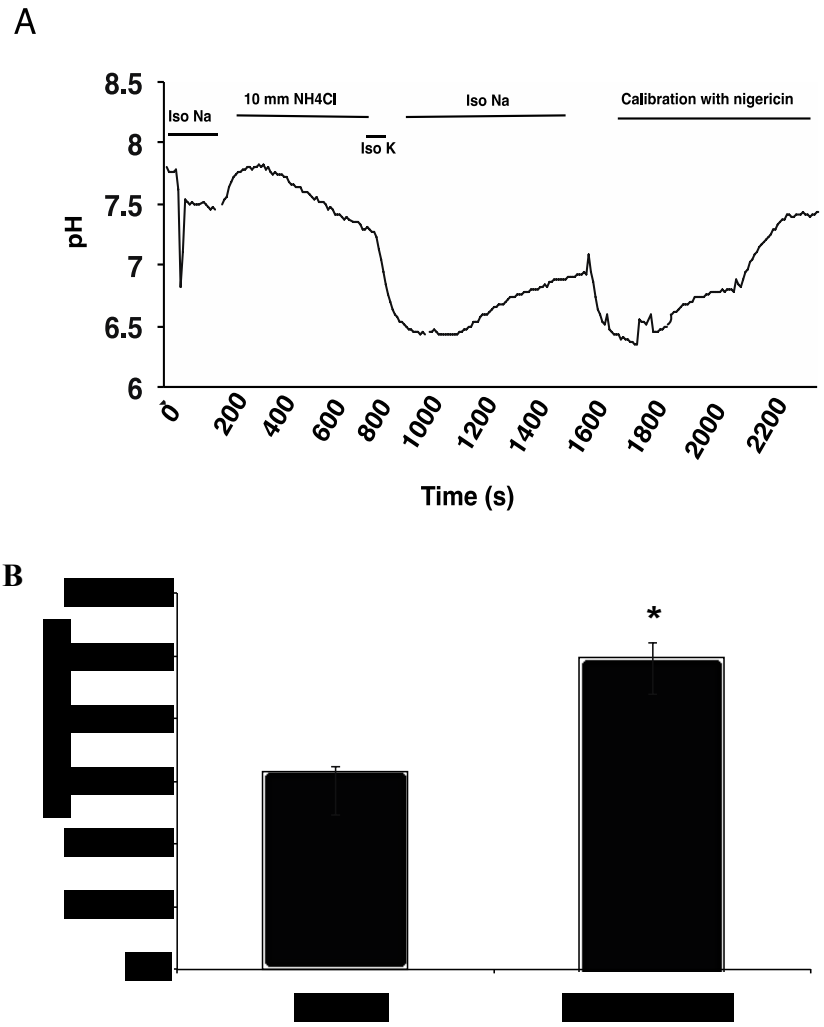

Figure 4.7: AngII increases NHE3 activity. For these studies NHE3 activity was assessed in the absence of CO_2 and HCO_3^-, by pulsing the cells with NH_4Cl. A) Representative traces of the change in intracellular pH of OK cells either stably expressing NHE3 in the presence or absence of 100 nM AngII. B) Quantification of initial NHE3 activity (over the first 100 s) for each condition displayed, n>3 per condition of OK cells expressing NHE3 in the presence and absence of 100 μM AngII.

4.4. Discussion

Evaluation of urinary calcium excretion from humans and mice fed altered sodium containing diets revealed that urinary calcium excretion is proportionate to sodium ingestion. To investigate the mechanism linking these two processes we looked at the renal expression of sodium and calcium absorbing genes/proteins. With the exception of increased NCC, a distal tubular sodium absorbing cotransporter, there were no significant differences. Given involvement of NHE3 in transepithelial calcium flux we speculated that altered NHE3 activity induced by altered sodium ingestion (and consequently volume status) altered proximal calcium reabsorption without changing expression. To assess this we employed a proximal tubular cell culture model. We found that AngII increased NHE3 activity and cell surface expression, a change that would increase calcium absorption, as seen when NHE3 is overexpressed (17). Taken together our data infers that increased sodium ingestion causes volume expansion, decreased RAS activity and consequently decreased proximal tubular calcium absorption and urinary calcium loss.

Consistent with our data, the ingestion of a high salt diet does not alter the expression of NHE3 but leads to its redistribution from the brushborder microvilli to a subapical compartment (7, 23, 24). Further studies have shown a similar effect on NHE3 distribution by manipulating the RAS (13, 24). Perhaps it is not surprising that the expression of NHE3 and other renal sodium transporters are not regulated at the level of expression. This might make sense, as one would hope for rapid dramatically increased NHE3 activity to maintain intravascular status under

circumstances of hypovolemia such as when bleeding, where a delayed response may have serious repercussions.

NHE3 function is regulated by many hormones. Sodium reabsorption along the nephron is commonly regulated via the renin-angiotensin system (RAS). RAS clearly signals in response to changes in volume status as evidenced by Figure 4.5 where mRNA expression of renin in high salt fed animals is significantly suppressed. Further, previous studies demonstrate localization of the angiotensin II 1 receptor (AT1R) and NHE3 to the proximal tubule (24). We provided direct evidence that AngII increases both the membrane expression and activity of NHE3. Thus it is tempting to speculate that AngII indirectly plays a role in altering urinary calcium excretion in animals on altered sodium containing diets. This is because on a high salt diet animals 1) would have reduced AngII levels due to reduced renin production; 2) the decreased AngII would result in the translocation of NHE3 in the proximal tubule from the brush border membrane to a endomembrane compartment at the base of the microvilli; and 3) this in turn would decrease both sodium and consequently calcium reabsorption from the proximal tubule. Ultimately this would result in the loss of calcium from the urine.

These experiments are not complete. To further strengthen this hypothesis we have to perform immunolocalization studies of NHE3 on a normal and high salt diet and show the redistribution of NHE3. Ideally we would show decreased NHE3 activity on perfused tubules and decreased calcium flux. Unfortunately these latter experiments are beyond our current capabilities. To implicate the RAS in sodium induced calcium excretion, we could feed animals or people a low sodium diet and

treat them with an angiotensin converting enzyme inhibitor or angiotensin receptor blocker and measure urinary calcium excretion. If this blocks the hypocalciuria usually induced by a low sodium diet, the RAS would be clearly implicated. Conversely, we could perform a high and control salt diet experiment with mice and intravenously add AngII and measure whether there is a change in urinary calcium excretion between control and high salt diet animals. If the administration of angiotensin to the high salt diet group induced hypocalciuria this would implicate the RAS in this process. To more directly implicate AngII signaling in altered transepithelial calcium flux we will measure calcium flux using radioactive calcium across confluent monolayers of OK cells overexpressing NHE3 treated with AngII or vehicle. Together these studies will strongly support a model whereby sodium ingestion, through altered volume status and consequently AngII signaling, alters NHE3 activity and urinary calcium excretion.

References

1. **Alexander RT, Furuya W, Szaszi K, Orlowski J, and Grinstein S**. Rho GTPases dictate the mobility of the Na/H exchanger NHE3 in epithelia: Role in apical retention and targeting. *Proceedings of the National Academy of Sciences of the United States of America* 102: 12253-12258, 2005.

2. **Alexander RT, Rievaj J, and Dimke H**. Paracellular calcium transport across renal and intestinal epithelia. *Biochemistry and Cell Biology* 92: 467-480, 2014.

3. **Charoenphandhu N, Tudpor K, Pulsook N, and Krishnamra N**. Chronic metabolic acidosis stimulated transcellular and solvent drag-induced calcium transport in the duodenum of female rats. *Am J Physiol*, 291(3) p. G446-G455,2006.

4. **Choi HY, Park HC, and Ha SK**. Salt Sensitivity and Hypertension: A Paradigm Shift from Kidney Malfunction to Vascular Endothelial Dysfunction. *Electrolytes & Blood Pressure : E & BP* 13: 7-16, 2015.

5. **Dimke H, Desai P, Borovac J, Lau A, Pan W, and Alexander RT**. Activation of the Ca^{2+}-sensing receptor increases renal claudin-14 expression and urinary Ca^{2+} excretion. *Am J Physiol*, 304(6) p. F761-F769, 2013.

6. **Dimke H, Hoenderop JGJ, and Bindels RJM**. Molecular basis of epithelial $Ca^{(2+)}$ and $Mg^{(2+)}$ transport: insights from the TRP channel family. *The Journal of Physiology* 589: 1535-1542, 2011.

7. **Dixit MP, Xu L, Xu H, Bai L, Collins JF, and Ghishan FK**. Effect of angiotensin-II on renal Na^+/H^+ exchanger-NHE3 and NHE2. *Biochimica et Biophysica Acta (BBA) - Biomembranes* 1664: 38-44, 2004.

8. **Harris PJ, and Navar LG**. Tubular transport responses to angiotensin. *Am J Physiol* 248: F621-630, 1985.

9. **Hoenderop JGJ, Nilius B, and Bindels RJM**. Calcium Absorption Across Epithelia. *Physiol Rev*, 85 (1) p. 373-422, 2005.

10. **Hou J, Renigunta A, Konrad M, Gomes AS, Schneeberger EE, Paul DL, Waldegger S, and Goodenough DA**. Claudin-16 and claudin-19 interact and form a cation-selective tight junction complex. *The Journal of clinical investigation* 118: 619-628, 2008.

11. **Konrad M, Schaller A, Seelow D, Pandey AV, Waldegger S, Lesslauer A, Vitzthum H, Suzuki Y, Luk JM, Becker C, Schlingmann KP, Schmid M, Rodriguez-Soriano J, Ariceta G, Cano F, Enriquez R, Juppner H, Bakkaloglu SA, Hediger MA, Gallati S, Neuhauss SCF, Nurnberg P, and Weber S**. Mutations in the tight-junction gene claudin 19 (CLDN19) are associated with renal magnesium wasting, renal failure, and severe ocular involvement. *American Journal of Human Genetics* 79: 949-957, 2006.

12. **Lorenz JN, Schultheis PJ, Traynor T, Shull GE, and Schnermann Jr**. Micropuncture analysis of single-nephron function in NHE3-deficient mice. *Am J Physiol*, 277: p. F447-F453, 1999.

13. **McDonough AA**. Mechanisms of proximal tubule sodium transport regulation that link extracellular fluid volume and blood pressure. *Am J Physiol*, 298: p. R851-R861, 2010.

14. **Muto S, Hata M, Taniguchi J, Tsuruoka S, Moriwaki K, Saitou M, Furuse K, Sasaki H, Fujimura A, Imai M, Kusano E, Tsukita S, and Furuse M**. Claudin-2, deficient mice are defective in the leaky and cation-selective paracellular permeability properties of renal proximal tubules. *Proceedings of the National Academy of Sciences of the United States of America* 107: 8011-8016, 2010.

15. **Ng RC, Rouse D, and Suki WN**. Calcium transport in the rabbit superficial proximal convoluted tubule. *The Journal of clinical investigation* 74: 834-842, 1984.

16. **Nordin BEC, Need AG, Morris HA, and Horowitz M**. The Nature and Significance of the Relationship between Urinary Sodium and Urinary Calcium in Women. *The Journal of Nutrition* 123: 1615-1622, 1993.

17. **Pan W, Borovac J, Spicer Z, Hoenderop JG, Bindels RJ, Shull GE, Doschak MR, Cordat E, and Alexander RT**. The epithelial sodium/proton exchanger, NHE3, is necessary for renal and intestinal calcium (re)absorption. *Am J Physiol*, 302: p. F943-F956, 2012.

18. **Park SM, Jee J, Joung JY, Cho YY, Sohn SY, Jin S-M, Hur KY, Kim JH, Kim SW, Chung JH, Lee MK, and Min Y-K**. High dietary sodium intake assessed by 24-hour urine specimen increase urinary calcium excretion and bone resorption marker. *Journal of Bone Metabolism* 21: 189-194, 2014.

19. **Renkema KY, Alexander RT, Bindels RJ, and Hoenderop JG**. Calcium and phosphate homeostasis: Concerted interplay of new regulators. *Annals of Medicine* 40: 82-91, 2008.

20. **Simon DB, Lu Y, Choate KA, Velazquez H, Al-Sabban E, Praga M, Casari G, Bettinelli A, Colussi G, Rodriguez-Soriano J, McCredie D, Milford D, Sanjad S, and Lifton RP**. Paracellin-1, a renal tight junction protein required for paracellular Mg^{2+} resorption. *Science* 285: 103-106, 1999.

21. **Takase H, Sugiura T, Kimura G, Ohte N, and Dohi Y**. Dietary sodium consumption predicts future blood pressure and incident hypertension in the japanese normotensive general population. *Journal of the American Heart Association* 4: 2015.

22. **Worcester EM, Gillen DL, Evan AP, Parks JH, Wright K, Trumbore L, Nakagawa Y, and Coe FL**. Evidence that postprandial reduction of renal calcium reabsorption mediates hypercalciuria of patients with calcium nephrolithiasis. *Am J Physiol*, 292: p. F66-F75, 2007.

23. **Xu L, Dixit MP, Nullmeyer KD, Xu H, Kiela PR, Lynch RM, and Ghishan FK**. Regulation of Na^+/H^+ exchanger-NHE3 by angiotensin-II in OKP cells. *Biochimica et Biophysica Acta (BBA) - Biomembranes* 1758: 519-526, 2006.

24. **Yang LE, Sandberg MB, Can AD, Pihakaski-Maunsbach K, and McDonough AA**. Effects of dietary salt on renal Na^+ transporter subcellular distribution, abundance, and phosphorylation status. *Am J Physiol*, 295: p. F1003-F1016, 2008.

Chapter 5: Discussion

5.1 Summary

The objectives of the thesis were:

a) To determine whether sodium proton exchanger isoform 3 (NHE3) activity is enhanced by a physical and functional interaction with carbonic anhydrase II (CAII)

b) To determine whether carbonic anhydrase II (CAII) enhances aquaporin I (AQP1) activity by a physical and functional interaction

c) To determine whether altered NHE3 activity, via angiotensin II signaling, is the link between altered dietary sodium intake and altered urinary calcium excretion

5.1.1 CAII physically and functionally interacts with NHE3 and enhances its activity

In chapter 2 we performed studies examining a physical and functional interaction between NHE3 and CAII. Both proteins are present in the proximal tubule (3, 8), where NHE3 plays an important role in reabsorbing the majority of sodium from that nephron segment (3). To do so, Opossum kidney cells were used for most of the experiments. We first performed studies to determine if there is a physical interaction between NHE3 and CAII. In these studies, a close association of these two proteins in our proximal tubular cell culture model was confirmed by proximity ligation assay. We also confirmed that these two proteins are in the same complex with each other by performing a co-immunoprecipitation. While we were able to pull down CAII with NHE3, we were unable to successfully Co-IP NHE3 with CAII. This could potentially be due the CAII antibody blocking the

interacting site with NHE3. A microtitre plate assay employing segments of the NHE3 C-terminus fused to GST confirmed a region in the cytosolic C-terminus of NHE3 between amino acids 630-730 that was required for a direct interaction. Importantly, this CAII-NHE3 interaction was augmented at higher pH and physiological ion strength of the buffer used for the assay. Given the role of NHE3 in transtubular sodium and water transport (and not as a house keeping gene) perhaps this helps to maintain NHE3 activity even when the cytosol is alkaline, as may be necessary under some conditions of hypovolemia?

Next we turned to studying whether there was a functional interaction between the two proteins. To this end, we performed studies on the same proximal tubular cell culture model to examine NHE3 mediated changes in intracellular pH using BCECF AM. These studies demonstrate that 1) Co-expression of CAII with NHE3 increases transporter activity, 2) experiments employing the CAII inhibitor acetazolamide and catalytically inactive CAII revealed that CAII activity is necessary to augment NHE3 activity, and 4) a physical interaction with CAII is necessary to increase NHE3 activity, as confirmed by coexpressing NHE3 with CAII containing a putative transporter binding site mutation. Thus we provided evidence that CAII physically and functionally interact with NHE3 to augment its activity. Given the large volume of sodium and consequently osmotically driven water reabsorbed from the proximal tubule (approximately 110 L and 1 kg respectively), such an interaction facilitating increased NHE3 activity may greatly enhance the efficiency of this transport process. NHE3 is also expressed in the TAL and along the intestine. Both these sites see significant transcellular

reabsorption of sodium and water, as in the proximal tubule. Carbonic anhydrase II is also expressed in these locations. We therefore speculate that a carbonic anhydrase II, NHE3 interaction may serve to increase sodium reabsorption from these sites as well.

5.1.2 CAII physically and functionally interacts with AQP1 enhancing its activity

In chapter 3 we performed studies examining a physical and functional interaction between CAII and AQP1. AQP1 is present in both the apical and basolateral membrane of the proximal tubule (1, 9, 10). The majority of water filtered at the glomerulus is reabsorbed along the proximal tubule through AQP1 (1, 9). Immunostaining of mouse kidney sections demonstrate that AQP1 and CAII colocalize in the proximal tubule. A PLA revealed that CAII and AQP1 associate closely in HEK293 cells. Importantly, mutation of the putative binding site in the tail of AQP1 prevented this association. Next we performed measurements of water flux in HEK cells over expressing AQP1 and CAII or mutants lacking either the putative AQP1 binding site or that were functionally inactive. We found that CAII increases water flux through AQP1, an effect attenuated by both mutants.

Red blood cells express copious amounts of AQP1. Moving towards an *in vivo* system we performed measurements of water flux across red blood cell ghost membranes and found that in the presence of CAII water flux increases. To support this result we examined CAII deficient mice and found that they have polyuria, polydipsia and dilute urine relative to their wild-type littermates. CAII deficient mice have increased AQP1 expression, potentially as compensation for decreased water flux through AQP1. Consistent with this, despite the increased expression

level of AQP1 in CAII deficient mice, water flux across renal cortical membrane vesicles derived from CAII deficient mice is greatly reduced when compared to renal cortical membrane vesicles from wild-type mice. These data demonstrate that CAII augments water conductance through the AQP1 pore. To support the possibility that the presence of AQP1 is responsible for this change in water conductance, we performed physical interaction studies between AQP1 and CAII. The PLA assay confirmed that these proteins are in close proximity. A peptide spot assay revealed that there is a physical interaction between CAII and AQP1 and that it required the acidic, LDADD domain. Further, we have shown that binding mutants of CAII failed to increase water flux. These studies demonstrate that binding is necessary to augment AQP1 activity. Together these studies demonstrate that CAII physically and functionally interacts with AQP1, enhancing water conductance.

Given the colocalization of carbonic anhydrase II and aquaporin-1 in the proximal tubule, this interaction likely facilitates the movement of the large volume of water across this segment daily. Aquaporin-1 and carbonic anhydrase II are also abundantly expressed in red blood cells. Consistent with a role for CAII in the augmented water flux through these cells, supplementing of red blood cell ghosts with recombinant aquaporin-1 increased water flux. This interaction may therefore be important for red blood cell and respiratory physiology. Carbon dioxide produced by metabolically active cells in the periphery is partly transported to the lungs as bicarbonate. This requires its conversion in the red blood cell (RBC). Water and carbon dioxide, two substrates of carbonic anhydrase

are transported into the RBC at least in part by aquaporin-1. Perhaps this interaction also increases the efficiency of CO_2 removal. Consistent with this, carbonic anhydrase II null mice also demonstrate a metabolic acidosis (2, 6).

CAII null mice have polydipsia and polyuria as well as dilute urine. We suggest that this may be due to a concentrating defect in these animals. Why might this be the case? In order for mammals to concentrate their urine the distal nephron must be permeable to water, this is achieved by aquaporin-2, which is not altered in expression in the CAII null mice. Further, for water to be absorbed there must be a lumen to medullary interstitium concentration gradient. This is achieved via the separation of water reabsorption from the reabsorption of NaCl in the loop of Henle. Water is reabsorbed from the thin descending limb while sodium and chloride is reabsorbed from the thin and thick ascending limb. The thin descending limb expresses both aquaporin-1 and carbonic anhydrase II. It is therefore tempting to speculate that decreased water flux across the thin descending limb leads to reduced meduallary concentration and therefore a reduced driving force for water reabsorption from the distal nephron, thereby causing polyuria and polydipsia.

5.1.3 The role of angiotensin II in altering urinary calcium excretion in response to altered sodium ingestion

In chapter 4 we performed studies examining the effect of dietary sodium intake on urinary calcium excretion. Data from both humans and mice revealed that increased dietary sodium increases urinary calcium excretion. We speculate that NHE3 is a candidate molecule playing a fundamental role in elevated urinary calcium levels in response to a high salt diet. To assess this possibility we performed mRNA and protein expression studies on sodium transporters along the

nephron including NHE3, NKCC2, NCC and ENaC. We did not find a significant decrease in the expression of these transporters between animals on different diets. Also we performed expression studies on some claudin TJ proteins involved in calcium reabsorption. These studies were performed on claudins-2, -12, -10a, -14, -16 and -19. We found no difference between dietary groups. Many hormones regulate NHE3 function. Commonly sodium reabsorption is regulated by the renin-angiotensin system. We confirmed that renin mRNA expression is significantly reduced on a high salt diet. Previous studies found that the AT1R and NHE3 are expressed in the proximal tubule. Using a cell culture model we provide data demonstrating that angiotensin II increases NHE3 membrane localization and enhances its activity. Thus we postulate that low renin production, might decrease AngII level that in turn translocate NHE3 from the brush border to an endomembrane compartment. This would cause less sodium reabsorption from the proximal tubule thereby increasing calcium excretion in the urine. A similar effect is predicted in people on an ACE inhibitor, they would have reduced AngII signaling decreasing proximal sodium and consequently calcium reabsorption.

5.2 Future directions

We demonstrate a physical and functional interaction between NHE3 and CAII. We have shown a region of the tail of NHE3 that appears to be necessary for this. What remains is to determine which amino acids in this region are responsible for binding to CAII. To do so we could make point mutations in acidic residues (Glutamic acid and Aspartic acid) to neutral charged residue (Alanine) within the putative binding site identified in the tail of NHE3 (^{710}IKEKDLELSDTEE^{722}) (5) and repeat the Co-IP experiments. We speculate that at least one among these acidic acid residues is responsible for binding the amino terminus of CAII, which is rich in positively charged amino acids (eg., histidine) (11). As previous literature reveals that serine phosphorylation in the NHE1 tail is necessary for CAII binding with NHE1 (4) and there are identical residues in the NHE3 tail, we will also ascertain whether this phosphorylation site is essential for CAII binding to NHE3. Examination of the extracellular loops of NHE3 identified putative CAIV binding sites (Figure 5.1). As a future direction we will assess a physical and functional interaction between NHE3 and CAIV via similar methodologies as employed within. We hypothesize that CAIV augments NHE3 activity and is part of a transport metabolon complex with NHE3 and CAII. CAIV is expressed in the proximal tubule and both CAIV and CAII have been shown to bind to the anion exchanger isoform 1, consistent with this possibility (8).

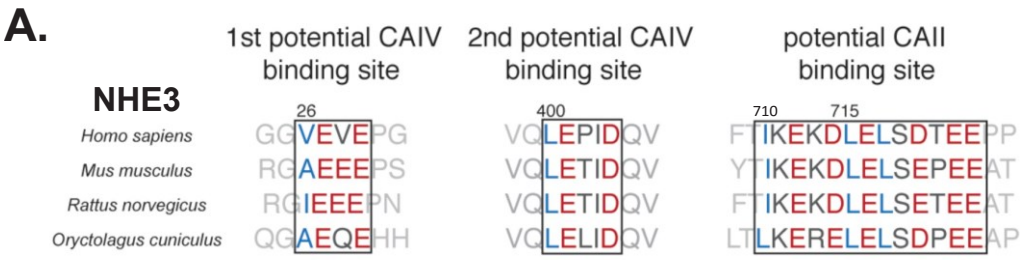

Figure 5.1: Potential CAII and CAIV binding sites in NHE3. A) Represents conserved sequences of two potential CAIV binding sites and a potential CAII binding site from different species.

We also demonstrate an AQP1-CAII physical and functional interaction. Future studies examining this in a more physiological model system would be to examine water flux across the microperfused proximal tubule of carbonic anhydrase II null mice. We could also examine the extracellular loop of AQP1 for putative CAIV binding sites. If one is present then in the future we could look for a physical and functional interaction between AQP1 and CAIV and check whether CAIV augments water flux through AQP1 thereby forming a transport metabolon complex with AQP1 and CAII.

We also wish to follow up on the polyuria and polydipsia in the CAII deficient animals. As described in chapter 3, we predict that this is possibly due to a renal concentration defect. To examine this possibility we need to perform a water deprivation study. We will do so. If the CAII deficient mice fail to concentrate their urine to the same extent as wild-type animals when water is withdrawn and after the administration of ddAVP, we will have confirmed a renal urinary concentration defect. As the expression of aquaporin-2 is not altered in the CAII deficient mice, and the renal expression of aquaporin-1 and CAII is such that it may affect the counter-current multiplier mechanism, via preventing the concentration of the medullary interstitium, we will measure this. We predict that the carbonic anhydrase II null mice will have a dilute medullary interstitium, preventing them from maximally concentrating their urine.

We also plan to generate knock in mouse models with the point mutations employed for these studies, the V143Y catalytically inactive mutation and the HEX

mutation that prevents binding to the transporters. We will explore NHE3 and AQP1 function in these knock-in mice. We speculate that the V143Y knock in mice would have polyuria and metabolic acidosis similar to the CAII null mice. We also hypothesize a similar, but perhaps milder phenotype in the HEX mutant. By employing microperfusion studies to these models, we predict decreased sodium, water, bicarbonate and calcium reabsorption across the proximal tubule of the knock-in animals compared to wild-type mice.

Finally we provide evidence implying a role for angiotensin II in altering urinary calcium excretion in response to altered sodium ingestion. In the future, we will examine the expression of the angiotensin II receptor I (AT1R) mRNA levels in animals on a high salt and control diet. Further, the renal immunolocalization of NHE3 will be determined in mice fed the two different diets. We predict a high salt diet will cause redistribution to the sub-apical endomembrane compartment. To more definitively invoke the RAS we will give mice AngII intravenously on either a high or control salt diet. We predict the increase in urinary calcium excretion mediated by a high salt diet will be attenuated by the administration of AngII. Also we will perform microperfusion studies on proximal tubules to determine the difference in calcium flux across the proximal tubule of mice on both diets. Using OK cells stably transfected with NHE3, in the presence and absence of AngII we will perform functional studies using the radioisotope $^{45}Ca^{2+}$ to examine whether there is an alteration in calcium flux induced by AngII (7). Together these proposed studies with the data in chapter 4 may clearly implicate NHE3 and RAS signaling in mediating increased urinary calcium excretion in response to a high salt diet.

References

1. **Bondy C, Chin E, Smith BL, Preston GM, and Agre P**. Developmental gene expression and tissue distribution of the CHIP28 water-channel protein. *Proceedings of the National Academy of Sciences* 90: 4500-4504, 1993.

2. **Brown BF, Quon A, Dyck JRB, and Casey JR**. Carbonic anhydrase II promotes cardiomyocyte hypertrophy. *Canadian Journal of Physiology and Pharmacology* 90: 1599-1610, 2012.

3. **Krishnan D, Liu L, Wiebe SA, Casey JR, Cordat E, and Alexander RT**. Carbonic anhydrase II binds to and increases the activity of the epithelial sodium-proton exchanger, NHE3. *Am J Physiol*, 309: p. F383-F392, 2015.

4. **Li X, Alvarez B, Casey JR, Reithmeier RAF, and Fliegel L**. Carbonic Anhydrase II Binds to and Enhances Activity of the Na^+/H^+ Exchanger. *Journal of Biological Chemistry* 277: 36085-36091, 2002.

5. **Li X, Liu Y, Alvarez BV, Casey JR, and Fliegel L**. A Novel Carbonic Anhydrase II Binding Site Regulates NHE1 Activity,. *Biochemistry* 45: 2414-2424, 2006.

6. **Lien Y-HH, and Lai L-W**. Respiratory acidosis in carbonic anhydrase II-deficient mice. *Am J Physiol*, 274: p. L301-L304, 1998.

7. **Pan W, Borovac J, Spicer Z, Hoenderop JG, Bindels RJ, Shull GE, Doschak MR, Cordat E, and Alexander RT**. The epithelial sodium/proton exchanger, NHE3, is necessary for renal and intestinal calcium (re)absorption. *Am J Physiol*, 302: p. F943-F956, 2012.

8. **Purkerson JM, and Schwartz GJ**. The role of carbonic anhydrases in renal physiology. *Kidney Int* 71: 103-115, 2006.

9. **Schnermann J, Chou C-L, Ma T, Traynor T, Knepper MA, and Verkman AS**. Defective proximal tubular fluid reabsorption in transgenic aquaporin-1 null mice. *Proceedings of the National Academy of Sciences* 95: 9660-9664, 1998.

10. **Vilas G, Krishnan D, Loganathan SK, Malhotra D, Liu L, Beggs MR, Gena P, Calamita G, Jung M, Zimmermann R, Tamma G, Casey JR, and Alexander RT**. Increased water flux induced by an aquaporin-1/carbonic anhydrase II interaction. *Molecular Biology of the Cell* 26: 1106-1118, 2015.

11. **Vince JW, and Reithmeier RAF**. Carbonic anhydrase II binds to the carboxyl terminus of human band 3, the erythrocyte Cl^-/HCO_3^- exchanger. *Journal of Biological Chemistry* 273: 28430-28437, 1998.

Bibliography

Alexander RS, Nair SK, and Christianson DW. Engineering the hydrophobic pocket of carbonic anhydrase II. *Biochemistry* 30: 11064-11072, 1991.

Alexander RT, Furuya W, Szaszi K, Orlowski J, and Grinstein S. Rho GTPases dictate the mobility of the Na/H exchanger NHE3 in epithelia: Role in apical retention and targeting. *Proceedings of the National Academy of Sciences of the United States of America* 102: 12253-12258, 2005.

Alexander RT, and Grinstein S. Na^+/H^+ exchangers and the regulation of volume. *Acta Physiologica* 187: 159-167, 2006.

Alexander RT, and Grinstein S. Tethering, recycling and activation of the epithelial sodium/proton exchanger, NHE3. *Journal of Experimental Biology* 212: 1630-1637, 2009.

Alexander RT, Malevanets A, Durkan AM, Kocinsky HS, AronsonPS, Orlowski J, Grinstein S. Membrane curvature alters the activation kinetics of the epithelial Na^+/H^+ exchanger, NHE3. *J Biol Chem* 282:7376–7384, 2007.

Alexander RT, Rievaj J, and Dimke H. Paracellular calcium transport across renal and intestinal epithelia. *Biochemistry and Cell Biology* 92: 467-480, 2014.

Almomani EY, King JC, Netsawang J, Yenchitsomanus PT, Malasit P, Limjindaporn T, Alexander RT, Cordat E. Adaptor protein 1complexes regulate intracellular trafficking of the kidney anion exchanger1 in epithelial cells. *Am J Physiol Cell Physiol* 303: C554–C566, 2012.

Al-Samir S, Papadopoulos S, Scheibe RJ, Meissner JD, Cartron JP, Sly WS, Alper SL, Gros G, Endeward V. Activity and distribution of intracellular carbonic anhydrase II and their effects on the transport activity of anion exchanger

AE1/SLC4A1. *J Physiol* 591: 4963–4982, 2013.

Alvarez BV, Loiselle FB, Supuran CT, Schwartz GJ, and Casey JR. Direct Extracellular Interaction between Carbonic Anhydrase IV and the Human NBC1 Sodium/Bicarbonate Co-Transporter. *Biochemistry* 42: 12321-12329, 2003.

Alvarez BV, Vilas GL, and Casey JR. Metabolon disruption: a mechanism that regulates bicarbonate transport. *EMOB J*, 24: p. 2499-2511, 2005.

Alvarez BV, Vithana EN, Yang Z, Koh AH, Yeung K, Yong V, Shandro HJ, Chen Y, Kolatkar P, Palasingam P, Zhang K, Aung T, Casey JR. Identification and characterization of a novel mutation in the carbonic anhydrase IV gene that causes retinitis pigmentosa. *Invest Ophthalmol Vis Sci* 48: 3459–3468, 2007.

Anstee DJ. The functional importance of blood group-active molecules in human red blood cells. *Vox Sang* 100: 140-149, 2011.

Azarani A, Goltzman D, and Orlowski J. Structurally Diverse N-terminal Peptides of Parathyroid Hormone (PTH) and PTH-related Peptide (PTHRP) Inhibit the Na^+/H^+ Exchanger NHE3 Isoform by Binding to the PTH/PTHRP Receptor Type I and Activating Distinct Signaling Pathways. *Journal of Biological Chemistry* 271: 14931-14936, 1996.

Babich V, and Di Sole F. The Na^+/H^+ Exchanger-3 (NHE3) Activity Requires Ezrin Binding to Phosphoinositide and Its Phosphorylation. *PLoS ONE* 10: e0129306, 2015.

Bartsch P, and Swenson ER. Clinical practice: Acute high-altitude illnesses. *N Engl J Med* 368: 2294-2302, 2013.

Becker HM, Deitmer JW. Carbonic anhydrase II increases the activity of the

human electrogenic Na^+/cotransporter. *J Biol Chem* 282: 13508–13521, 2007.

Becker H, Klier M, and Deitmer J. Nonenzymatic Augmentation of Lactate Transport via Monocarboxylate Transporter Isoform 4 by Carbonic Anhydrase II. *J Membrane Biol* 234: 125-135, 2010.

Becker HM, and Deitmer JW. Nonenzymatic Proton Handling by Carbonic Anhydrase II during H^+-Lactate Cotransport via Monocarboxylate Transporter 1. *Journal of Biological Chemistry* 283: 21655-21667, 2008.

Becker HM, Hirnet D, Fecher-Trost C, Sultemeyer D, and Deitmer JW. Transport activity of MCT1 expressed in Xenopus oocytes is increased by interaction with carbonic anhydrase. *Journal of Biological Chemistry* 280: 39882-39889, 2005.

Becker HM, Klier M, Schuler C, McKenna R, and Deitmer JW. Intramolecular proton shuttle supports not only catalytic but also noncatalytic function of carbonic anhydrase II. *Proceedings of the National Academy of Sciences* 108: 3071-3076, 2011.

Biemesderfer D, Rutherford PA, Nagy T, Pizzonia JH, Abu-Alfa AK, Aronson PS. Monoclonal antibodies for high-resolution localization of NHE3 in adult and neonatal rat kidney. *Am J Physiol Renal Physiol* 273:F289–F299, 1997.

Binswanger U, Helmle-Kolb C, Forgo J, Mrkic B, and Murer H. Rapid stimulation of Na^+/H^+ exchange by 1,25-dihydroxyvitamin D3; interaction with parathyroid-hormone-dependent inhibition. *Pflugers Arch* 424: 391-397, 1993.

Boassa D, and Yool AJ. A fascinating tail: cGMP activation of aquaporin-1 ion channels. *Trends Pharmacol Sci* 23: 558-562, 2002.

Bobulescu IA, Dubree M, Zhang J, McLeroy P, Moe OW. Effect of renal lipid accumulation on proximal tubule Na^+/H^+ exchange and ammonium secretion. *Am J Physiol Renal Physiol* 294: F1315–F1322,2008.

Bobulescu IA, Quinones H, Gisler SM, Di Sole F, Hu M-C, Shi M, Zhang J, Fuster DG, Wright N, Mumby M, and Moe OW. Acute regulation of renal Na^+/H^+ exchanger NHE3 by dopamine: role of protein phosphatase 2A. *American Journal of Physiology:*298(5), p. F1205-F1213,2010.

Bondy C, Chin E, Smith BL, Preston GM, and Agre P. Developmental gene expression and tissue distribution of the CHIP28 water-channel protein. *Proceedings of the National Academy of Sciences of the United States of America* 90: 4500-4504, 1993.

Brown BF, Quon A, Dyck JR, and Casey JR. Carbonic anhydrase II promotes cardiomyocyte hypertrophy. *Can J Physiol Pharmacol* 90: 1599-1610, 2012.

Calamita G, Ferri D, Gena P, Carreras FI, Liquori GE, Portincasa P, Marinelli RA, and Svelto M. Altered expression and distribution of aquaporin-9 in the liver of rat with obstructive extrahepatic cholestasis. *Am J Physiol Gastrointest Liver Physiol* 295: G682-690, 2008.

Cappuccio FP, Kalaitzidis R, Duneclift S, and Eastwood JB. Unravelling the links between calcium excretion, salt intake, hypertension, kidney stones and bone metabolism. *J Nephrol* 13: 169-177, 2000.

Carey RM. The Intrarenal Renin-Angiotensin System in Hypertension. *Advances in Chronic Kidney Disease* 22: 204-210, 2015.

Castrop H, and Schießül IM. Physiology and pathophysiology of the renal Na-K-2Cl cotransporter (NKCC2). *American journal of physiology:*307, p. F991- F1002, 2014.

Calinescu O, Paulino C, Kuhlbrandt W, and Fendler K. Keeping It Simple, Transport Mechanism and pH Regulation in Na^+/H^+ Exchangers. *Journal of Biological Chemistry* 289: 13168-13176, 2014.

Cha B, Tse M, Yun C, Kovbasnjuk O, Mohan S, Hubbard A, Arpin M, and Donowitz M. The NHE3 Juxtamembrane Cytoplasmic Domain Directly Binds Ezrin: Dual Role in NHE3 Trafficking and Mobility in the Brush Border. *Molecular Biology of the Cell* 17: 2661-2673, 2006.

Charoenphandhu N, Tudpor K, Pulsook N, and Krishnamra N. Chronic metabolic acidosis stimulated transcellular and solvent drag-induced calcium transport in the duodenum of female rats. *Am J Physiol*, 291: p. G446-G455, 2006.

Chen T, Kocinsky HS, Cha B, Murtazina R, Yang J, Tse CM, Singh V, Cole R, Aronson PS, de Jonge H, Sarker R, and Donowitz M. Cyclic GMP Kinase II (cGKII) Inhibits NHE3 by Altering Its Trafficking and Phosphorylating NHE3 at Three Required Sites: Identification of a multifunctional phosphorylation site. *Journal of Biological Chemistry* 290: 1952-1965, 2015.

Choi HY, Park HC, and Ha SK. Salt Sensitivity and Hypertension: A Paradigm Shift from Kidney Malfunction to Vascular Endothelial Dysfunction. *Electrolytes & Blood Pressure : E & BP* 13: 7-16, 2015.

Chou CL, Knepper MA, Hoek AN, Brown D, Yang B, Ma T, and Verkman AS. Reduced water permeability and altered ultrastructure in thin descending limb of Henle in aquaporin-1 null mice. *J Clin Invest* 103: 491-496, 1999.

Chow C-W, Khurana S, Woodside M, Grinstein S, and Orlowski J. The Epithelial Na^+/H^+ Exchanger, NHE3, Is Internalized through a Clathrin-mediated Pathway. *Journal of Biological Chemistry* 274: 37551-37558, 1999.

Chu TS, Peng Y, Cano A, Yanagisawa M, and Alpern RJ. Endothelin(B) receptor activates NHE-3 by a Ca^{2+}-dependent pathway in OKP cells. *Journal of Clinical Investigation* 97: 1454-1462, 1996.

Conner MT, Conner AC, Bland CE, Taylor LH, Brown JE, Parri HR, and Bill RM. Rapid aquaporin translocation regulates cellular water flow: mechanism of hypotonicity-induced subcellular localization of aquaporin 1 water channel. *J Biol Chem* 287: 11516-11525, 2012.

Counillon L, Franchi A, and Pouyssegur J. A point mutation of the Na^+/H^+ exchanger gene (NHE1) and amplification of the mutated allele confer amiloride resistance upon chronic acidosis. *Proceedings of the National Academy of Sciences* 90: 4508-4512, 1993.

Del Fattore A, Cappariello A, and Teti A. Genetics, pathogenesis and complications of osteopetrosis. *Bone* 42: 19-29.

Di Sole F, Babich V, and Moe OW. The Calcineurin Homologous Protein-1 Increases Na^+/H^+ Exchanger 3 Trafficking via Ezrin Phosphorylation. *Journal of the American Society of Nephrology* 20: 1776-1786, 2009.

Di Sole F, Cerull R, Casavola V, Moe OW, Burckhardt G, and Helmle-Kolb C. Molecular aspects of acute inhibition of Na^+/H^+ exchanger NHE3 by A2-adenosine receptor agonists. *The Journal of Physiology* 541: 529-543, 2002.

Dimke H, Desai P, Borovac J, Lau A, Pan W, and Alexander RT. Activation of the Ca^{2+}sensing receptor increases renal claudin-14 expression and urinary Ca^{2+} excretion. *Am J Physiol Renal Physiol* 304, p. F 761-F769, 2013.

Dimke H, Hoenderop JG, and Bindels RJ. Hereditary tubular transport disorders: implications for renal handling of Ca^{2+} and Mg^{2+}. *Clin Science (London)*, 118-1 p. 1-18, 2010.

Dirks JH, Cirksena WJ, Berliner RW. Micropuncture study of the effect of various diuretics on sodium reabsorption by the proximal tubules of the dog. *J Clin Invest* 45: 1875–1885, 1966.

Dixit MP, Xu L, Xu H, Bai L, Collins JF, and Ghishan FK. Effect of angiotensin-II on renal Na^+/H^+ exchanger-NHE3 and NHE2. *Biochimica et Biophysica Acta (BBA) - Biomembranes* 1664: 38-44, 2004.

Donowitz M, and Li X. Regulatory Binding Partners and Complexes of NHE3. *Physiol Rev*, 87 (3) p. 825-872, 2007.

Donowitz M, Ming Tse C, and Fuster D. SLC9/NHE gene family, a plasma membrane and organellar family of Na^+/H^+ exchangers. *Molecular Aspects of Medicine* 34: 236-251, 2013.

Donowitz M, Mohan S, Zhu CX, Chen T-E, Lin R, Cha B, Zachos NC, Murtazina R, Sarker R, and Li X. NHE3 regulatory complexes. *Journal of Experimental Biology* 212: 1638-1646, 2009.

Endeward V, Musa-Aziz R, Cooper GJ, Chen L-M, Pelletier MF, Virkki LV, Supuran CT, King LS, Boron WF, and Gros G. Evidence that aquaporin 1 is a major pathway for CO_2 transport across the human erythrocyte membrane. *The FASEB Journal* 20: 1974-1981, 2006.

Ellison DH. Through a glass darkly: salt transport by the distal tubule. *Kidney Int* 79: 5-8, 2011.

Fang X, Yang B, Matthay MA, and Verkman AS. Evidence against aquaporin-1-dependent CO_2 permeability in lung and kidney. *J Physiol* 542: 63-69, 2002.

Faraggiana T, Malchiodi F, Prado A, and Churg J. Lectin-peroxidase conjugate reactivity in normal human kidney. *J Histochem Cytochem* 30: 451-458, 1982.

Fierke CA, Calderone TL, and Krebs JF. Functional consequences of engineering the hydrophobic pocket of carbonic anhydrase II. *Biochemistry* 30: 11054-11063, 1991.

Fisher Z, Boone CD, Biswas SM, Venkatakrishnan B, Aggarwal M, Tu C, Agbandje-McKenna M, Silverman D, and McKenna R. Kinetic and structural characterization of thermostabilized mutants of human carbonic anhydrase II. *Protein Eng Des Sel* 25: 347-355, 2012.

Fliegel L. The Na^+/H^+ exchanger isoform 1. *The International Journal of Biochemistry & Cell Biology* 37: 33-37, 2005.

Fujita H, Sugimoto K, Inatomi S, Maeda T, Osanai M, Uchiyama Y, Yamamoto Y, Wada T, Kojima T, Yokozaki H, Yamashita T, Kato S, Sawada N, and Chiba H. Tight junction proteins claudin-2 and -12 are critical for vitamin

d-dependent Ca^{2+} absorption between enterocytes. *Molecular Biology of the Cell* 19: 1912-1921, 2008.

Fujiwara Y, Tanoue A, Tsujimoto G, and Koshimizu T-a. The roles of V1a vasopressin receptors in blood pressure homeostasis: a review of studies on V1a receptor knockout mice. *Clin Exp Nephrol* 16: 30-34, 2012.

Fuster D, and Alexander RT. Traditional and emerging roles for the SLC9 Na^+/H^+ exchangers. *Pflugers Arch - Eur J Physiol* 466: 61-76, 2014.

Fuster DG, Bobulescu IA, Zhang J, Wade J, and Moe OW. Characterization of the regulation of renal Na^+/H^+ exchanger NHE3 by insulin. *American journal of physiology*, 292 (2) p. F577-F585, 2007.

Gao J, Wang X, Chang Y, Zhang J, Song Q, Yu H, and Li X. Acetazolamide inhibits osmotic water permeability by interaction with aquaporin-1. *Anal Biochem* 350: 165-170, 2006.

Gawenis LR, Stien X, Shull GE, Schultheis PJ, Woo AL, Walker NM, Clarke LL. Intestinal NaCl transport in NHE2 and NHE3 knockout mice. *Am J Physiol Gastrointest Liver Physiol* 282: G776–G784, 2002.

Geyer RR, Musa-Aziz R, Qin X, and Boron WF. Relative CO_2/NH_3 selectivities of mammalian aquaporins 0-9. *American Journal of Physiology* 304 (3), p. C985-C994, 2013.

Gong Y, Renigunta V, Himmerkus N, Zhang J, Renigunta A, Bleich M, and Hou J. Claudin-14 regulates renal $Ca^{(++)}$ transport in response to CaSR signalling via a novel microRNA pathway. *The EMBO Journal* 31: 1999-2012, 2012.

Good DW, and Watts BA. Functional roles of apical membrane Na^+/H^+ exchange in rat medullary thick ascending limb. *American Journal of Physiology*, 270 p. F691-F699, 1996.

Goodenough DA. Plugging the leaks. *Proceedings of the National Academy of Sciences* 96: 319-321, 1999.

Greger R, Bleich M, and Schlatter E. Ion channels in the thick ascending limb of henle loop. *Renal Physiol Biochem* 13: 37-50, 1990.

Gross E, Pushkin A, Abuladze N, Fedotoff O, and Kurtz I. Regulation of the sodium bicarbonate cotransporter knbc1 function: role of Asp986, Asp988 and kNBC1-carbonic anhydrase II binding. *The Journal of Physiology* 544: 679-685, 2002.

Harris PJ, and Navar LG. Tubular transport responses to angiotensin. *Am J Physiol* 248: F621-630, 1985.

He P, Klein J, and Yun CC. Activation of Na^+/H^+ Exchanger NHE3 by Angiotensin II Is Mediated by Inositol 1,4,5-Triphosphate (IP3) Receptor-binding Protein Released with IP3 (IRBIT) and Ca^{2+}/Calmodulin-dependent Protein Kinase II. *Journal of Biological Chemistry* 285: 27869-27878, 2010.

Hilpert K, Winkler DF, and Hancock RE. Peptide arrays on cellulose support: SPOT synthesis, a time and cost efficient method for synthesis of large numbers of peptides in a parallel and addressable fashion. *Nat Protoc* 2: 1333-1349, 2007.

Hoenderop JGJ, Nilius B, and Bindels RJM. Calcium Absorption Across Epithelia. *Physiol Rev*, 85 p. 373-422, 2005.

Hoenderop JGJ, van Leeuwen JPTM, van der Eerden BCJ, Kersten FFJ, van derKemp AWCM, Merillat A-M, Waarsing JH, Rossier BC, Vallon V, Hummler E, and Bindels RJM. Renal Ca^{2+} wasting, hyperabsorption, and reduced bone thickness in mice lacking TRPV5. *Journal of Clinical Investigation* 112: 1906-1914, 2003.

Hou J, Rajagopal M, and Yu ASL. Claudins and the Kidney Volume 75: Annual Review of Physiology. *Annual Review of Physiology* 75: 479-501, 2013.

Hou J, Renigunta A, Konrad M, Gomes AS, Schneeberger EE, Paul DL, Waldegger S, and Goodenough DA. Claudin-16 and claudin-19 interact and form a cation-selective tight junction complex. *The Journal of Clinical Investigation* 118: 619-628, 2008.

Ismail EAR, Abul Saad S, and Sabry MA. Nephrocalcinosis and urolithiasis in carbonic anhydrase II deficiency syndrome. *Eur J Pediatr* 156: 957-962, 1997.

Itoh M, Furuse M, Morita K, Kubota K, Saitou M, and Tsukita S. Direct Binding of Three Tight Junction-Associated Maguks, Zo-1, Zo-2, and Zo-3, with the COOH Termini of Claudins. *The Journal of Cell Biology* 147: 1351-1363, 1999. **Kawaguchi Y, Hasegawa T, Nakayama M, Kubo H, and Shigematu T**. Issues affecting the longevity of the continuous peritoneal dialysis therapy. *Kidney Int Suppl* 62: S105-107, 1997.

King LS, Choi M, Fernandez PC, Cartron J-P, and Agre P. Defective Urinary Concentrating Ability Due to a Complete Deficiency of Aquaporin-1. *New England Journal of Medicine* 345: 175-179, 2001.

Kinsella JL, and Aronson PS. Interaction of NH_4^+ and Li^+ with the renal microvillus membrane Na^+/H^+ exchanger. *Am J Physiol* 241: C220-226, 1981.

Klier M, Schuler C, Halestrap AP, Sly WS, Deitmer JW, and Becker HM. Transport Activity of the High-affinity Monocarboxylate Transporter MCT2 Is Enhanced by Extracellular Carbonic Anhydrase IV but Not by Intracellular Carbonic Anhydrase II. *Journal of Biological Chemistry* 286: 27781-27791, 2011.

Krishnan D, Liu L, Wiebe SA, Casey JR, Cordat E, and Alexander RT. Carbonic anhydrase II binds to and increases the activity of the epithelial sodium proton exchanger, NHE3. *American Journal of Physiol,* 309 (4), F383-92, 2015.

Konrad M, Schaller A, Seelow D, Pandey AV, Waldegger S, Lesslauer A, Vitzthum H, Suzuki Y, Luk JM, Becker C, Schlingmann KP, Schmid M, Rodriguez-Soriano J, Ariceta G, Cano F, Enriquez R, Juppner H, Bakkaloglu SA, Hediger MA, Gallati S, Neuhauss SCF, Nurnberg P, and Weber S. Mutations in the tight-junction gene claudin 19 (CLDN19) are associated with renal magnesium wasting, renal failure, and severe ocular involvement. *American Journal of Human Genetics* 79: 949-957, 2006.

Kurashima K, Yu FH, Cabado AG, Szabo EdZ, Grinstein S, and Orlowski J. Identification of sites required for down-regulation of Na^+/H^+ Exchanger NHE3 activity by cAMP-dependent protein kinase: phosphorylation-dependent and -independent mechanisms. *Journal of Biological Chemistry* 272: 28672-28679, 1997.

Lambers TT, Bindels RJM, and Hoenderop JGJ. Coordinated control of renal Ca^{2+} handling. *Kidney Int* 69: 650-654, 2006.

Lee-Kwon W, Kim JH, Choi JW, Kawano K, Cha B, Dartt DA, Zoukhri D, and Donowitz M. Ca^{2+}-dependent inhibition of NHE3 requires PKCŒ± which binds to E3KARP to decrease surface NHE3 containing plasma membrane complexes. *American Journal of Physiol,* 285(6), p. C1527-C1536,2003.

Lewis SE, Erickson RP, Barnett LB, Venta PJ, and Tashian RE. N-ethyl-N-nitrosourea-induced null mutation at the mouse Car-2 locus: an animal model for human carbonic anhydrase II deficiency syndrome. *Proc Natl Acad Sci U S A* 85: 1962-1966, 1988.

Li X, Alvarez B, Casey JR, Reithmeier RAF, and Fliegel L. Carbonic Anhydrase II Binds to and Enhances Activity of the Na^+/H^+ Exchanger. *Journal of Biological Chemistry* 277: 36085-36091, 2002.

Li X, Liu Y, Alvarez BV, Casey JR, and Fliegel L. A Novel Carbonic Anhydrase II Binding Site Regulates NHE1 Activity, *Biochemistry* 45: 2414-2424, 2006.

Lien Y-HH, and Lai L-W. Respiratory acidosis in carbonic anhydrase II-deficient mice. 1998, p. L301-L304.

Loiselle FB, Morgan PE, Alvarez BV, and Casey JR. Regulation of the human NBC3 Na^+/HCO_3^- cotransporter by carbonic anhydrase II and PKA. *Am J Physiol*, 286: p. C1423-C1433, 2004.

Lorenz JN, Schultheis PJ, Traynor T, Shull GE, and Schnermann Jr. Micropuncture analysis of single-nephron function in NHE3-deficient mice. *Am J Physiol*, 277: p. F447-F453, 1999.

Low EV, Avery AJ, Gupta V, Schedlbauer A, and Grocott MP. Identifying the lowest effective dose of acetazolamide for the prophylaxis of acute mountain sickness: systematic review and meta-analysis. *British Medical Journal* 345: e6779, 2012.

Ma B, Xiang Y, Mu SM, Li T, Yu HM, and Li XJ. Effects of acetazolamide and anordiol on osmotic water permeability in AQP1-cRNA injected Xenopus oocyte. *Acta Pharmacol Sin* 25: 90-97, 2004.

Ma T, Yang B, Gillespie A, Carlson EJ, Epstein CJ, and Verkman AS. Severely impaired urinary concentrating ability in transgenic mice lacking aquaporin-1 water channels. *Journal of Biological Chemistry* 273: 4296-4299, 1998.

Margolis DS, Szivek JA, Lai LW, and Lien YH. Phenotypic characteristics of bone in carbonic anhydrase II-deficient mice. *Calcif Tissue Int* 82: 66-76, 2008.

McDonough AA. Mechanisms of proximal tubule sodium transport regulation that link extracellular fluid volume and blood pressure. *Am J Physiol* 2010, p. R851-R861.

McMurtrie HL, Cleary HJ, Alvarez BV, Loiselle FB, Sterling D, Morgan PE, Johnson DE, and Casey JR. Journal of Enzyme Inhibition and *Medicinal Chemistry* 19: 231-236, 2004.

Miles EW, Rhee S, and Davies DR. The Molecular Basis of Substrate Channeling. *Journal of Biological Chemistry* 274: 12193-12196, 1999.

Musa-Aziz R, Chen LM, Pelletier MF, and Boron WF. Relative CO_2/NH_3 selectivities of AQP1, AQP4, AQP5, AmtB, and RhAG. *Proc Natl Acad Sci U S A*

106: 5406-5411, 2009.

Muto S, Hata M, Taniguchi J, Tsuruoka S, Moriwaki K, Saitou M, Furuse K, Sasaki H, Fujimura A, Imai M, Kusano E, Tsukita S, and Furuse M. Claudin-2 deficient mice are defective in the leaky and cation-selective paracellular permeability properties of renal proximal tubules. *Proceedings of the National Academy of Sciences of the United States of America* 107: 8011-8016, 2010.

Nagami GT. Role of angiotensin II in the enhancement of ammonia production and secretion by the proximal tubule in metabolic acidosis. *Am J Physiol, 294*, p. F874-F880, 2008.

Nakamura N, Tanaka S, Teko Y, Mitsui K, and Kanazawa H. Four Na^+/H^+ Exchanger Isoforms Are Distributed to Golgi and Post-Golgi Compartments and Are Involved in Organelle pH Regulation. *Journal of Biological Chemistry* 280: 1561-1572, 2005.

Nakhoul NL, Davis BA, Romero MF, and Boron WF. Effect of expressing the water channel aquaporin-1 on the CO_2 permeability of Xenopus oocytes. *Am J Physiol* 274: C543-548, 1998.

Nesterov V, Dahlmann A, Krueger B, Bertog M, Loffing J, and Korbmacher C. Aldosterone-dependent and -independent regulation of the epithelial sodium channel (ENaC) in mouse distal nephron. *Am J Physiol*, 303 p. F1289-F1299, 2012.

Ng RC, Rouse D, and Suki WN. Calcium transport in the rabbit superficial proximal convoluted tubule. *Journal of Clinical Investigation* 74: 834-842, 1984.

Nordin BEC, Need AG, Morris HA, and Horowitz M. The Nature and Significance of the Relationship between Urinary Sodium and Urinary Calcium in Women. *The Journal of Nutrition* 123: 1615-1622, 1993.

Okamoto K, Hanazaki K, Akimori T, Okabayashi T, Okada T, Kobayashi M, Ogata T. Immunohistochemical and electron microscopic characterization of brush cells of the rat cecum. *Med Mol Morphol* 41: 145–150, 2008.

Orlowski J, and Grinstein S. Diversity of the mammalian sodium/proton exchanger SLC9 gene family. *Pflugers Arch* 447: 549-565, 2004.

Orlowski J, Kandasamy RA, Shull GE. Molecular cloning of putative members of the Na/H exchanger gene family. cDNA cloning, deduced amino acid sequence, and mRNA tissue expression of the rat Na/H exchanger NHE-1 and two structurally related proteins. *J Biol Chem* 267:9331–9339, 1992.

Pan W, Borovac J, Spicer Z, Hoenderop JG, Bindels RJ, Shull GE, Doschak MR, Cordat E, and Alexander RT. The epithelial sodium/proton exchanger, NHE3, is necessary for renal and intestinal calcium (re)absorption. *Am J Physiol*, 302 p. F943-F956, 2012.

Pang T, Su X, Wakabayashi S, and Shigekawa M. Calcineurin Homologous Protein as an Essential Cofactor for Na^+/H^+ Exchangers. *Journal of Biological Chemistry* 276: 17367-17372, 2001.

Pao AC, Bhargava A, Sole FD, Quigley R, Shao X, Wang J, Thomas S, Zhang J, Shi M, Funder JW, Moe OW, and Pearce D. Expression and role of serum and glucocorticoid-regulated kinase 2 in the regulation of Na^+/H^+ exchanger 3 in the mammalian kidney. *Am J Physiol Renal Physiol.* 2010, p. F1496-F1506.

Park SM, Jee J, Joung JY, Cho YY, Sohn SY, Jin S-M, Hur KY, Kim JH, Kim SW, Chung JH, Lee MK, and Min Y-K. High dietary sodium intake assessed by 24-hour urine specimen increase urinary calcium excretion and bone resorption marker. *Journal of Bone Metabolism* 21: 189-194, 2014.

Parkkila S. Distribution of the carbonic anhydrase isoenzyme I, II, and VI in the human alimentary tract. *Gut* 35: 646–650, 1994.

Piermarini PM, Kim EY, Boron WF. Evidence against a direct interaction between intracellular carbonic anhydrase II and pure C-terminal domains of SLC4 bicarbonate transporters. *J Biol Chem* 282: 1409–1421, 2007.

Piontek Jr, Winkler L, Wolburg H, Muller SL, Zuleger N, Piehl C, Wiesner B, Krause G, and Blasig IE. Formation of tight junction: determinants of homophilic interaction between classic claudins. *The FASEB Journal* 22: 146-158, 2008.

Prasad GVR, Coury LA, Finn F, and Zeidel ML. Reconstituted Aquaporin 1 Water Channels Transport CO_2 across Membranes. *Journal of Biological Chemistry* 273: 33123-33126, 1998.

Preston G, Smith B, Zeidel M, Moulds J, and Agre P. Mutations in aquaporin-1 in phenotypically normal humans without functional CHIP water channels. *Science* 265: 1585-1587, 1994.

Preston GM, and Agre P. Isolation of the cDNA for erythrocyte integral membrane protein of 28 kilodaltons: member of an ancient channel family. *Proceedings of the National Academy of Sciences of the United States of America* 88: 11110-11114, 1991.

Preston GM, Carroll TP, Guggino WB, and Agre P. Appearance of Water Channels in Xenopus Oocytes Expressing Red Cell CHIP28 Protein. *Science* 256: 385-387, 1992.

Purkerson JM, and Schwartz GJ. The role of carbonic anhydrases in renal physiology. *Kidney Int* 71: 103-115, 2006.

Pushkin A, Abuladze N, Gross E, Newman D, Tatishchev S, Lee I, Fedotoff O, Bondar G, Azimov R, Ngyuen M, Kurtz I. Molecular mechanism of kNBC1, carbonic anhydrase II interaction in proximal tubule cells. *J Physiol* 559: 55–65, 2004.

Reithmeier RAF. A Membrane Metabolon Linking Carbonic Anhydrase with Chloride/Bicarbonate Anion Exchangers. *Blood Cells, Molecules, and Diseases* 27: 85-89, 2001.

Renkema KY, Alexander RT, Bindels RJ, and Hoenderop JG. Calcium and phosphate homeostasis: Concerted interplay of new regulators. *Annals of Medicine* 40: 82-91, 2008.

Rievaj J, Pan W, Cordat E, Alexander RT. The Na^+/H^+ exchanger isoform 3 is required for active paracellular and transcellular Ca^{2+} transport across murine cecum. *Am J Physiol Gastrointest Liver Physiol* 305: G303–G313, 2013.

Rubio CR, de Mello GB, Mangili OC, Malnic G. H^+ ion secretion in proximal tubule of low-CO_2/HCO_3^- perfused isolated rat kidney. *Pflügers Arch* 393: 63–70, 1982.

Ruetz S LA, Kopito RR. Function and biosynthesis of erythroid and nonerythroid anion exchangers. *Soc Gen Physiol Ser* 48: 193-200, 1993.

Sabolic I, Valenti G, Verbavatz JM, Van Hoek AN, Verkman AS, Ausiello DA, and Brown D. Localization of the CHIP28 water channel in rat kidney. *Am J Physiol* 263: C1225-1233, 1992.

Sarker R, Gronborg M, Cha B, Mohan S, Chen Y, Pandey A, Litchfield D, Donowitz M, and Li X. Casein Kinase 2 Binds to the C Terminus of Na^+/H^+ exchanger 3 (NHE3) and Stimulates NHE3 Basal Activity by Phosphorylating a Separate Site in NHE3. *Molecular Biology of the Cell* 19: 3859-3870, 2008.

Schnermann J, Chou C-L, Ma T, Traynor T, Knepper MA, and Verkman AS. Defective proximal tubular fluid reabsorption in transgenic aquaporin-1 null mice. *Proceedings of the National Academy of Sciences* 95: 9660-9664, 1998.

Schultheis PJ, Clarke LL, Meneton P, Miller ML, Soleimani M, Gawenis LR, Riddle TM, Duffy JJ, Doetschman T, Wang T, Giebisch G, Aronson PS, Lorenz JN, and Shull GE. Renal and intestinal absorptive defects in mice lacking the NHE3 Na^+/H^+ exchanger. *Nat Genet* 19: 282-285, 1998.

Simon DB, Lu Y, Choate KA, Velazquez H, Al-Sabban E, Praga M, Casari G, Bettinelli A, Colussi G, Rodriguez-Soriano J, McCredie D, Milford D, Sanjad S, and Lifton RP. Paracellin-1, a Renal Tight Junction Protein Required for Paracellular Mg^{2+} Resorption. *Science* 285: 103-106, 1999.

Simon EE, Merli C, Herndon J, Cragoe EJ, and Hamm LL. Effects of barium and 5-(N-ethyl-N-isopropyl)-amiloride on proximal tubule ammonia transport. *Am J Physiol*, 262(1 Pt 2) p. F36-F39, 1992.

Sjöblom M, Singh AK, Zheng W, Wang J, Tuo Bg Krabbenhöft A, Riederer B, Gros G, Seidler U. Duodenal acidity sensing, but not epithelial HCO_3^-, supply

is critically dependent on carbonic anhydrase II expression. *Proc Natl Acad Sci* USA 106: 13094–13099, 2009.

Sly WS, Hewett-Emmett D, Whyte MP, Yu YS, and Tashian RE. Carbonic anhydrase II deficiency identified as the primary defect in the autosomal recessive syndrome of osteopetrosis with renal tubular acidosis and cerebral calcification. *Proceedings of the National Academy of Sciences of the United States of America* 80: 2752-2756, 1983.

Soderberg O, Gullberg M, Jarvius M, Ridderstrale K, Leuchowius KJ, Jarvius J, Wester K, Hydbring P, Bahram F, Larsson LG, Landegren U. Direct observation of individual endogenous protein complexes in situ by proximity ligation. *Nat Methods* 3: 995–1000, 2006.

Sowah D, and Casey JR. An intramolecular transport metabolon: fusion of carbonic anhydrase II to the COOH terminus of the Cl^-/HCO_3^- exchanger, AE1. *Am J Physiol*, 301: p. C336-C346, 2011.

Srere PA, Sumegi B, Sherry AD. Organizational aspects of the citric acid cycle. *Biochem Soc Symp* 54: 173–178, 1987.

Spicer SS, Lewis SE, Tashian RE, and Schulte BA. Mice carrying a CAR-2 null allele lack carbonic anhydrase II immunohistochemically and show vascular calcification. *The American Journal of Pathology* 134: 947-954, 1989.

Sterling D, Alvarez BV, and Casey JR. The Extracellular Component of a Transport Metabolon: extracellular loop 4 of the human AE1 Cl^-/HCO_3^- exchanger binds carbonic anhydrase IV. *Journal of Biological Chemistry* 277: 25239-25246, 2002.

Sterling D, Reithmeier RAF, and Casey JR. A transport metabolon: Functional interaction of carbonic anhydrase II and chloride/bicarbonate exchangers. *Journal of Biological Chemistry* 2001.

Sun X, Soleimani M, and Petrovic S. Decreased Expression of Slc26a4 (Pendrin) and Slc26a7 in the Kidneys of Carbonic Anhydrase II-Deficient Mice. *Cellular Physiology and Biochemistry* 21: 095-108, 2008.

Takase H, Sugiura T, Kimura G, Ohte N, and Dohi Y. Dietary Sodium Consumption Predicts Future Blood Pressure and Incident Hypertension in the Japanese Normotensive General Population. *Journal of the American Heart Association* 4: 2015.

Tani K, and Fujiyoshi Y. Water channel structures analysed by electron crystallography. *Biochimica et Biophysica Acta (BBA) - General Subjects* 1840: 1605-1613, 2014.

Tashian RE CN. Biochemical genetics of carbonic anhydrase. *Adv Hum Genet* 7: 1-56, 1976.

Theilig F, and Wu Q. ANP-induced signaling cascade and its implications in renal pathophysiology. *Am J Physiol*, 308 (10) p. F1047-F1055, 2015.

Thomas JA, Buchsbaum RN, Zimniak A, Racker E. Intracellular pH measurements in Ehrlich ascites tumor cells utilizing spectroscopic probes generated in situ. *Biochemistry* 18: 2210–2218, 1979.

Tse CM, Levine SA, Yun CH, Brant SR, Pouyssegur J, Montrose MH, Donowitz M. Functional characteristics of a cloned epithelial Na^+/H^+exchanger (NHE3): resistance to amiloride and inhibition by protein kinase C. *Proc NatlAcad*

Sci USA 90: 9110–9114, 1993.

van Heeswijk MPE, and van Os CH. Osmotic water permeabilities of brush border and basolateral membrane vesicles from rat renal cortex and small intestine. *J Membrane Biol* 92: 183-193, 1986.

Vilas G, Krishnan D, Loganathan SK, Malhotra D, Liu L, Beggs MR, Gena P, Calamita G, Jung M, Zimmermann R, Tamma G, Casey JR, and Alexander RT. Increased water flux induced by an aquaporin-1/carbonic anhydrase II interaction. *Molecular Biology of the Cell* 26: 1106-1118, 2015.

Vilas GL, Loganathan SK, Liu J, Riau AK, Young JD, Mehta JS, Vithana EN, and Casey JR. Transmembrane water-flux through SLC4A11: a route defective in genetic corneal diseases. *Human Molecular Genetics* 22: 4579-4590, 2013.

Vince JW, Carlsson U, and Reithmeier RAF. Localization of the Cl^-/HCO_3^- Anion Exchanger Binding Site to the Amino-Terminal Region of Carbonic Anhydrase II, *Biochemistry* 39: 13344-13349, 2000.

Vince JW, and Reithmeier RAF. Carbonic Anhydrase II Binds to the Carboxyl Terminus of Human Band 3, the Erythrocyte Cl^-/HCO_3^- Exchanger. *Journal of Biological Chemistry* 273: 28430-28437, 1998.

Vince JW, and Reithmeier RAF. Identification of the Carbonic Anhydrase II Binding Site in the Cl^-/HCO_3^- Anion Exchanger AE1, *Biochemistry* 39: 5527-5533, 2000.

Waheed A, Zhu XL, Sly WS, Wetzel P, and Gros G. Rat skeletal muscle membrane associated carbonic anhydrase is 39-kDa, glycosylated, GPI-anchored CA IV. *Archives of Biochemistry and Biophysics* 294: 550-556, 1992.

Weiner ID, and Verlander JW. Role of NH_3 and NH_4^+ transporters in renal acid-base transport. *Am J Physiol*, 300 p. F11-F23, 2011.

Weinman EJ, Wang Y, Wang F, Greer C, Steplock D, and Shenolikar S. A C-Terminal PDZ Motif in NHE3 Binds NHERF-1 and Enhances cAMP Inhibition of Sodium,àíHydrogen Exchange, *Biochemistry* 42: 12662-12668, 2003.

Weise A, Becker HM, and Deitmer JW. Enzymatic suppression of the membrane conductance associated with the glutamine transporter SNAT3 expressed in Xenopus oocytes by carbonic anhydrase II. *The Journal of General Physiology* 130: 203-215, 2007.

Wiederkehr MR, Zhao H, and Moe OW. Acute regulation of Na^+/H^+ exchanger NHE3 activity by protein kinase C: role of NHE3 phosphorylation. *Am J Physiol*, 276 (5 Pt 1) p. C1205-C1217,1999.

Worcester EM, Gillen DL, Evan AP, Parks JH, Wright K, Trumbore L, Nakagawa Y, and Coe FL. Evidence that postprandial reduction of renal calcium reabsorption mediates hypercalciuria of patients with calcium nephrolithiasis. *Am J Physiol*, 292: p. F66-F75, 2007.

Xu L, Dixit MP, Nullmeyer KD, Xu H, Kiela PR, Lynch RM, and Ghishan FK. Regulation of Na^+/H^+ exchanger-NHE3 by angiotensin-II in OKP cells. *Biochimica et Biophysica Acta - Biomembranes* 1758: 519-526, 2006.

Yang LE, Sandberg MB, Can AD, Pihakaski-Maunsbach K, and McDonough AA. Effects of dietary salt on renal Na^+ transporter subcellular distribution, abundance, and phosphorylation status. *Am J Physiol*, 295: p. F1003-F1016, 2008.

Yool AJ, Morelle J, Cnops Y, Verbavatz J-M, Campbell EM, Beckett EAH, Booker GW, Flynn G, and Devuyst O. AqF026 Is a Pharmacologic Agonist of the Water Channel Aquaporin-1. *Journal of the American Society of Nephrology* 24: 1045-1052, 2013.

Zaun HC, Shrier A, and Orlowski J. Calcineurin B Homologous Protein 3 Promotes the Biosynthetic Maturation, Cell Surface Stability, and Optimal Transport of the Na^+/H^+ Exchanger NHE1 Isoform. *The Journal of Biological Chemistry* 283: 12456-12467, 2008.

Zhang R, Skach W, Hasegawa H, van Hoek AN, and Verkman AS. Cloning, functional analysis and cell localization of a kidney proximal tubule water transporter homologous to CHIP28. *The Journal of Cell Biology* 120: 359-369, 1993.

Zhang J, Tackaberry T, Ritzel MW, Raborn T, Barron G, Baldwin SA, Young JD, Cass CE. Cysteine-accessibility analysis of transmembrane domains 11–13 of human concentrative nucleoside transporter 3. *Biochem J* 394: 389–398, 2006.

Zhang W, Zitron E, Homme M, Kihm L, Morath C, Scherer D, Hegge S, Thomas D, Schmitt CP, Zeier M, Katus H, Karle C, and Schwenger V. Aquaporin-1 channel function is positively regulated by protein kinase C. *Journal of Biological Chemistry* 282: 20933-20940, 2007.

Zhu XC, Sarker R, Horton JR, Chakraborty M, Chen T-E, Tse CM, Cha B, and Donowitz M. Nonsynonymous single nucleotide polymorphisms of NHE3 differentially decrease NHE3 transporter activity. *Am J Physiol*, 308 p. C758-C766, 2015.

Zizak M, Chen T, Bartonicek D, Sarker R, Zachos NC, Cha B, Kovbasnjuk O, Korac J, Mohan S, Cole R, Chen Y, Tse CM, and Donowitz M. Calmodulin Kinase II constitutively binds, phosphorylates, and inhibits brush border Na^+/H^+ exchanger 3 (NHE3) by a NHERF2 protein-dependent process. *Journal of Biological Chemistry* 287: 13442-13456, 2012.